Characteristics of the ceramics GEMs

by

Amir Tosson

A thesis submitted in partial fulfillment for the degree of
Master of physics

in the
Faculty Number 4
Department of Physics

August 2015

Declaration of Authorship

I, Amir Tosson, declare that this thesis titled, 'Characteristics of the ceramics GEMs' and the work presented in it are my own. I confirm that:

- This work was done wholly or mainly while in candidature for a research degree at this University.

- Where any part of this thesis has previously been submitted for a degree or any other qualification at this University or any other institution, this has been clearly stated.

- Where I have consulted the published work of others, this is always clearly attributed.

- Where I have quoted from the work of others, the source is always given. With the exception of such quotations, this thesis is entirely my own work.

- I have acknowledged all main sources of help.

- Where the thesis is based on work done by myself jointly with others, I have made clear exactly what was done by others and what I have contributed myself.

Signed:

_____

Date:

_____

"No one undertakes research in physics with the intention of winning a prize. It is the joy of discovering something no one knew before."

- Stephen Hawking

"With particle physics, we can fill the ID of our universe"

- Amir Tosson

Abstract

The Gas Electron Multiplier (GEM) has been proven to fulfill the demands of high energy physics experiments. The effective gas gain , the resistance to the electrical sparks and the energy resolution are significant issues to be investigated.

A new type of GEM, made out of the ceramic as insulator and gold and silver as conductor, has been produced and results from measurements with this ceramic GEM are presented. The advantages of the ceramic material are its stability versus change in temperature and its electrical properties.

Using Ar-CO_2($80 - 20\%$) gas mixture and a X-rays source compiled with pads readout system, the gain of the ceramic GEMs was measured and compared with the one for CERN GEMs. The measurements included the energy resolution and the open area for both types of GEM. These results assure the possibility of using the ceramic GEMs for high-luminosity experiments.

Acknowledgements

Contents

List of Figures

List of Tables

Abbreviations

SM	**S**tandard **M**odel
LEP	**L**arge **E**lectron **P**ositron collider
LHC	**L**arge **H**adron **C**ollider
ILC	**I**nternational **L**inear **C**ollider
CT	**C**athode **T**ube
IC	**I**onization **C**hamber
PC	**P**roportional **C**ounter
GMT	**G**eiger **M**ueller **T**ube
TPC	**T**ime **P**rojection **C**hamber
ILD	**I**nternational **L**arge **D**etector
SiD	**Si**licon **D**etector
GEM	**G**as**E**lectron **M**ultiplier
HVS	**H**igh**V**oltage **S**ystem
MCA	**M**ulti**C**hannel **A**nalyzer

Chapter 1

Introduction

For over three thousands years, humans have tried to understand the nature of the universe. 624-547 B.C., Thalws of Miletus, Greek philosopher gave the first hypothesis about the matter. He assumed that water is the fundamental constituent of the matter. As time went by, physicists developed the classical mechanics and discovered the atom which is considered to be a scientific revolution. Then, quantum mechanics entered the game and changed our idea about the Universe. "Knowledge has to be improved, challenged, and increased constantly, or it vanishes"- [Peter Druker], for this reason physicists try to take a turn to the better. On 4th July 2012, a new particle -known as Higgs boson- was announced to be the starting point for a new physics. Nowadays Higgs field, Supersymmetry theory and beyond the Standard model are the most important enigmas for the particle physics community to deal with.

1.1 Particle physics in a few lines

Particle physics is a section of science which demonstrates the inwardness of the particles and their interactions with matter. The Standard Model (SM) is the sorting of the elementary particles and the interaction forces [Gri08]. In particular, the fundamental forces which govern the universe -as far as we know- are the gravitational force, the weak interaction, the electromagnetic force and the strong interaction. Table 1.1 summarizes the fundamental properties of these forces according to the Standard Model. So far so good, but this is not the end of the story. There are many question marks that the SM failed to answer. Such as, what is the origin of the mass for the particles?, why is there an imbalance (asymmetry) between the matter and the antimatter? and what is the dark matter?. All these questions are the motivation which forced the scientific community to go deeply in this mystery. Therefore, many colliders were built and will

be built in order to help us to travel inside the atom and discover the subatomic level particles. In next section we discuss three of the particle colliders, i.e. Large Electron-Positron collider (LEP), Large Hadron Collider (LHC) and International Linear Collider (ILC).

—	Gravity	Weak interaction	Electromagnetic	Strong interaction
Discovery	1687, by Newton	1933, by E.Fermi	1821, by M.Faraday	around 1970
Relative strength	10^{-42}	10^{-11}	10^{-2}	10
Dealing with	Energy-Mass	Flavor	Electric charge	Color charge
Range (mm)	Infinite	10^{-15}	Infinite	10^{-12}
Mediator	Graviton	W^+, W^- , Z^0	Photon	Gluon
Theory	General Relativity	Electroweak	Electrodynamics	Chromodynamics

TABLE 1.1: Properties of the fundamental forces according to the SM

1.2 Particles colliders

In fact, if you have a look around yourself, you can find that you are surrounded by many particles colliders (particles accelerators). For instance, your computer monitor (with the cathode tube) is a small particle accelerator. Accordingly, the cathode tube (CT) speeds the electrons up and then collides them with the target, the CT can control the fields direction of the particles by the electromagnetic. Then, these accelerated particles hit the target (the screen) which gives you a picture.

Comparatively, particle colliders -for a real particle experiments- work the same manner, but the size is much bigger and the energy is much higher. In recent accelerators, particles reach almost the speed of light and an energy around a few thousands of GeV. These high energetic particles are very useful for many researches as their energy can be use to produce new particles according to the Einstein relation $E = mc^2$.

There are two types of experiments, the fixed-target and the accelerated-target. In the first one, the particle is shot against a target at rest. The disadvantage of this technique is the losing of kinetic energy of the accelerated particle as a recoil energy. For this reason, the second type was developed. The collision happens between two accelerated particles moving in opposite direction to each other that insures 100% of the kinetic energy is used for new particles production.

Additionally, the accelerated-target is categorized into two other basic types of the colliders. Namely, **the circular accelerator** in which the particles are accelerated in a circle (Figure 1.1) and **the linear accelerator** in which the particles are accelerated in a line (Figure 1.2)

The circular acceleration means that the particles can go around many times and their energy is increased each round. Moreover, large magnets are needed in order to keep the particles going in a circle.

On the other hand, the linear colliders are much easier to build because there is no need for large magnets.
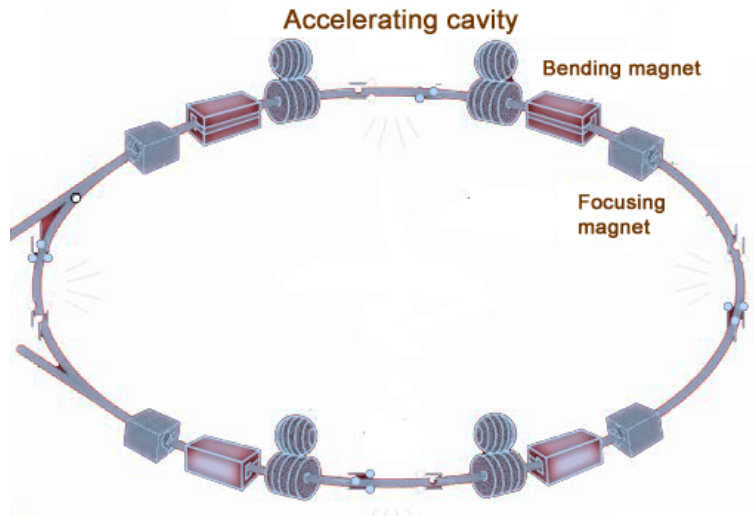
FIGURE 1.1: Circular accelerator [XV].
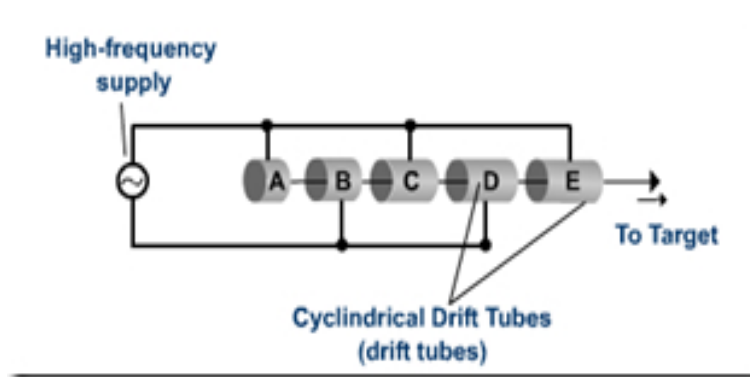
FIGURE 1.2: Linear accelerator [Eme].

1.2.1 The Large Electron-Positron collider (LEP)

The Large Electron-Positron collider (LEP) is a circular collider (circumference = 27 km), was operated at CERN between 1989-2000, shown in Figure 1.3. It was used to accelerate the leptons (electrons, positrons) with center mass energy ($\sqrt{s}$) around 91 Gev . It contained four detectors ALEPH, OPAL, DELPHI and L3. LEP enabled us to measure the Z and W bosons masses with high precision.
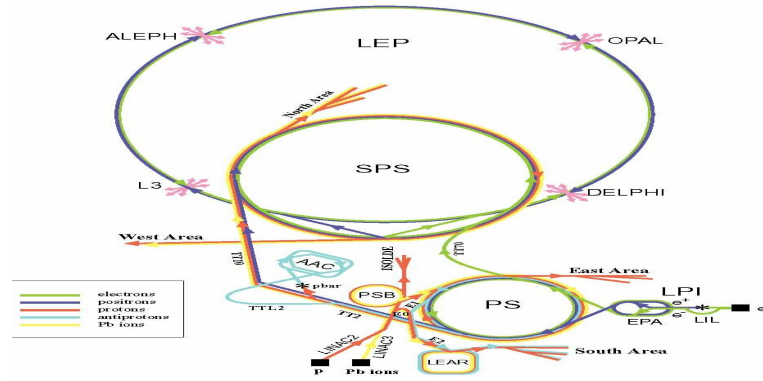
FIGURE 1.3: The Large Electron-Positron collider (LEP) [Cel].

1.2.2 The Large Hadron Collider (LHC)

The first starting up was on 10 September 2008, at CERN (Figure 1.4). It accelerates the hadrons (protons) to 3500 GeV with collision energy 7000 GeV [CERa]. The LEP tunnel was used for the LHC collider. There are four detectors for this collider ATLAS, CMS, ALICE and LHCb, see Figure 1.5. The most magnificent achievement was on 4th July 2012, when the ATLAS and CMS discovered the Higgs boson with a mass of about 125 GeV. The Nobel prize was given to F. Englert and P. Higgs for this discovery in October 2013.
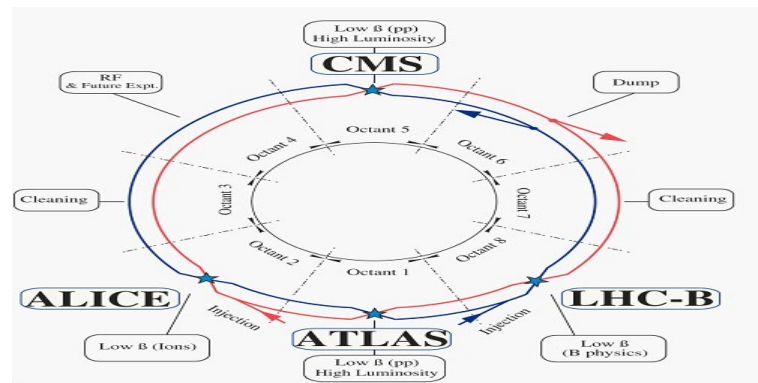
FIGURE 1.4: The Large Hadron Collider (LHC) [Chu].

1.2.3 The International Linear Collider (ILC)

Physicists believe that the ILC is a new gate to discover the physics beyond the range of today's colliders. The collision energy is designed to be at the Tera-scale. It consists of two linear accelerators facing each other (both 11 km long) with two damping rings in the center -Figure 1.6. It is designed to reach a peak luminosity of around $2x10^{34} \frac{1}{cm^2 s}$ and a resolution 10 times better than the one at LEP [Att09]. It accelerates the electrons and their anti-particles (positrons) to -nearly- the speed of light. Two detectors will serve
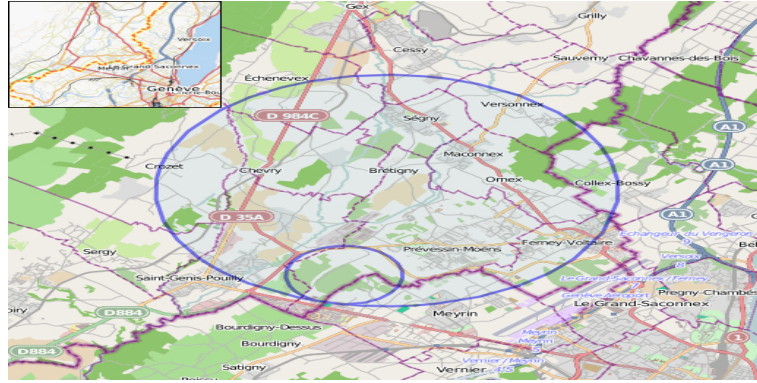
FIGURE 1.5: Map of the Large Hadron Collider (LHC) at CERN [Wik].

the ILC namely, the International Large Detector (ILD) and the Silicon Detector (SiD) [Gro12]. Scientists and engineers admit that ILC will bring many new technological benefits for many areas. For example, medicine, computing and environment will touch a huge progress thanks to the ILC technology [Gra].
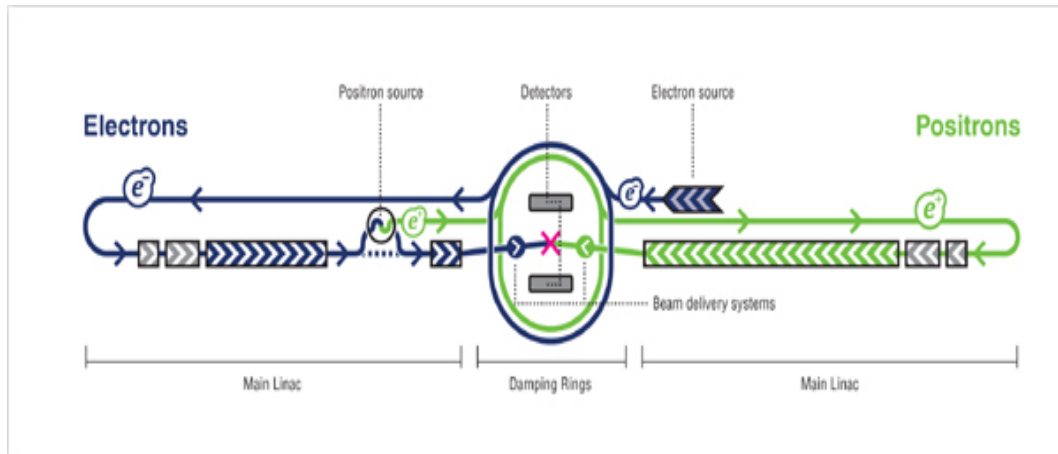
FIGURE 1.6: The International Linear Collider [Pet].

Chapter 2

Detection phenomena

The goal of this chapter is to give the reader an idea about the interaction between the particles and the matter.

2.1 Particles and Matter

2.1.1 The cross section and the mean free path

When a charged particle passes through a slice of a material, the probability to interact with the nuclei or the electrons in this material is proportional to the thickness of this slice and the density of it [Tav10]. Equation 2.1 gives the relation of the interaction probability (dW).

$$\mathrm{dW} = \mathrm{dx}\ \mathrm{N}\ \sigma \tag{2.1}$$

where dx is the thickness of the material, N is the number of particle per unit volume and σ is the cross section. In particular, the concept of cross section is used to express the effective area for the interaction.

The average distance between two successive collisions is known as the mean free path(λ). Equation 2.2 is the relation between the mean free path and the cross section.

$$\lambda = \frac{1}{N\sigma} \tag{2.2}$$

2.1.2 The energy loss of charged particles

If a charged particle passes through matter, it will perform inelastic or elastic collisions. Consequently, it suffers energy loss and deviation in the traveling direction. The charged particles are classified according to their mass. In other words, there are low mass particles (e.g. electrons and positrons) and high mass particles (e.g. muons, pions and protons). Equations 2.3 shows the Bloch formula of the energy loss ($\frac{dE}{dx}$) [Kle98][Fer86] .

$$-\frac{dE}{dx} = \rho K z^2 \frac{Z}{A} \frac{1}{\beta^2} [\ln \frac{2m_e c^2 \gamma^2 \beta^2}{I} - \beta^2]$$ (2.3)

where

ρ is the density of the material,

Z is the atomic number ot the material,

A is the mass number ot the material,

N_A is the Avogadro number,

m_e is the electron mass,

c is the speed of light,

β equals $\frac{v}{c}$,

γ is the Lorentz factor,

I is the ionization constant,

z is the atomic number of the incident particle ($z = 1$ for e^- and e^+),

$\frac{K}{A} = 4\pi N_A r_0^2 m_e c^2 / A = 0.307075$ MeV $g^{-1} cm^2$

2.2 Important Definitions

2.2.1 Drift velocity

The average velocity with which the charged particles (e.g. electrons, ions) drift when an electric field is applied to a gaseous medium is known as the drift velocity [WB08]. It depends on the mass of the drifted particle. For this reason, the behavior of the electrons differs from that for ions as a result of the mass difference between them. To clarify, let us consider an electron with mass m_e passing through an electric field in a volume fills with a gas. The drift velocity v_d of this electron is proportional to the strength of the applied electric field E, equation 2.4 [WBR08].

$$v_d = \frac{eE}{m_e}\tau$$ (2.4)

where e is the charge of the electron and τ is the average time between two collisions. Figure 2.1 displays the relation between the electron drift velocity and the applied electric

field for Argon Carbon-dioxide gas mixture with $(85-15\%)$ concentration. Also, is shown the changing in the drift velocity when an amount of Nitrogen is added to the mixture [AAT04].
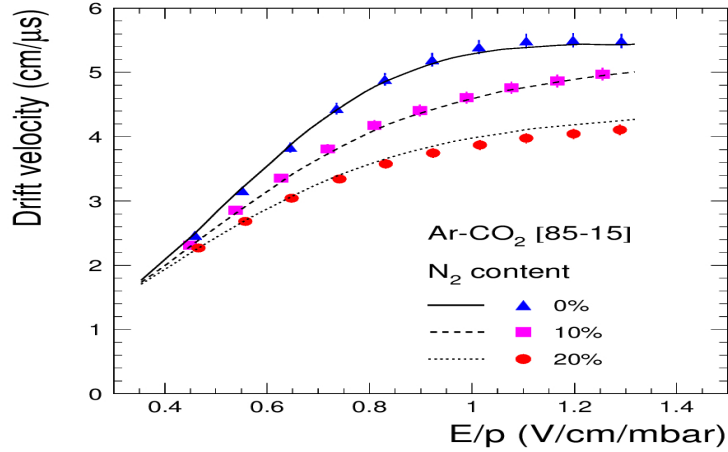
FIGURE 2.1: The drift velocity vs the electric field for $Ar - CO_2$ mixture with N_2 in addition

2.2.2 Diffusion

Generally, The diffusion is the tendency of the particles to redistribute their position, randomly, after the collision and in the absence of the external fields. Thus, the momenta of the electrons will have components in all directions [Sha14].

Equation 2.5 shows the diffusion equation according to the classical kinetic theory of gases.

$$\frac{dN(x)}{dx} = \frac{N_0}{\sqrt{4\pi D_e t}} exp(-\frac{x^2}{4D_e t}) \tag{2.5}$$

where $\frac{dN(x)}{dx}$ is the change of the electrons number per unit distance,N_0 the initial electrons, number D_e is the diffusion coefficient for electrons and t is the time [WBR08].

For diffusion time t the electrons will spread with Gaussian distribution with deviation $\sigma(r)$;

$$\sigma(r) = \sqrt{6D_e t} \tag{2.6}$$

2.2.3 Gas gain

Gas gain or gas amplification measures the efficiency of the gas filled detectors. Furthermore, when an electron passes through the gas medium inside the detector, it interacts with one atom of the gas. If this primary electron has enough energy (higher than the excitation energy of the gas atoms) a secondary electron will be freed which in its turns

produces another one and so on. Finally, one primary electron produces an avalanche of electrons along its track. The ratio between the number of primary electrons and the number of secondary electrons is defined as the gas amplification of the detector. For more details see chapter 4.

2.3 Types of detectors

2.3.1 Ionization chamber (IC)

An ionization chamber is a radiation detector which determines the intensity of the incident radiation beam or counts the charged particles. It consists of a chamber filled by gas and two electrodes to apply an external voltage difference (Figure 2.2). As a fast charged particle passes through, it creates positive ions and free electrons (electron-ion pairs). It is considered to be the fundamental electrical signal developed by the ionization chamber [Kno89]. The magnitude of the applied voltage difference specifies the type of the gas-filled detector. Figure 2.3 represents the different types of gas-filled detectors and their region with respect to the external applied voltage.
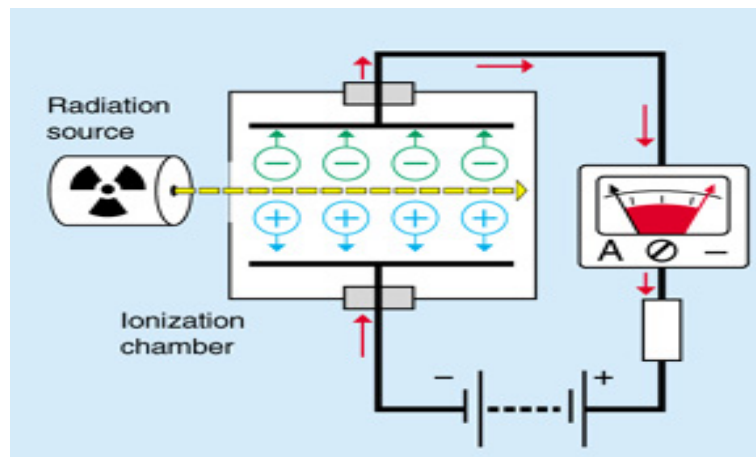
FIGURE 2.2: The ionization chamber [Ens].

2.3.2 Proportional counter (PC)

The Proportional Counter (P.C.) is another type of gaseous detectors developed in 1940. In an ionization chamber there is no gas gain, in other words, the primary charge which is created by a primary particle is not multiplied [Gru96]. In this case, the elementary charge created by the incident radiation is collimated on the two electrodes when an external voltage is applied. Thus, the collected charge is proportional to the applied voltage (see Figure 2.3).
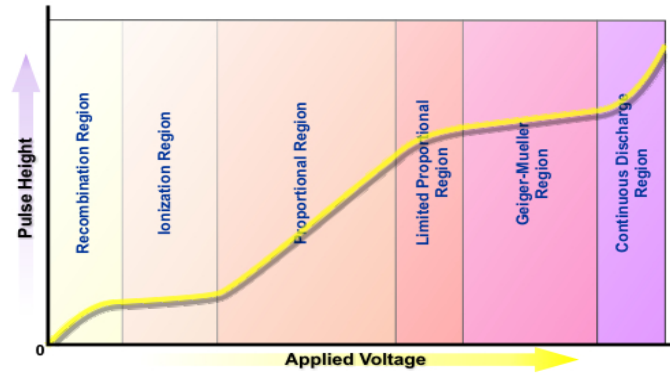
FIGURE 2.3: The gas-filled detectors curve [gro].

2.3.3 Geiger-Mueller tube (GMT)

A Geiger-Mueller tube (GMT) was introduced in 1928 by Geiger and Mueller. It is a gas-filled detector with the shape of a cylindrical outer layer as cathode and the sealed gas-filled space with a thin wire as anode. The common used gas is Argon (Ar) with a quencher which function is to prevent the discharge.

It reckons on the gas gain or gas amplification phenomena- see section 2.2.3. Therefore, the applied voltage has to be higher than the one for the proportional counter. The lower value of the applied voltage for GM region (Figure 2.3) is known as the threshold voltage at which the incident particle is able to create an avalanche [Kno89]. Increasing the applied voltage (the electric field) increases - in turn - the probability of producing more avalanches [Gru96]. Overall, the primary charge creates clusters of secondary charges on its track which are collected by the electrodes.

2.3.4 Drift chamber

A drift chamber is a multiwire chamber in which the spatial coordinates of ionization particle are calculated. That can be achieved by measuring the drift time of ionization electrons. Particularly, the time required for ionization electrons to reach the anode wires [Sau77][Boc].

The operational procedure of the drift chamber is quite similar to that of the proportional counter in producing avalanches via gas ionization by incident charged particles. However, the main difference is that the collecting signals are from the avalanches themselves [Gru96]. For small drift fields the energy distribution of the electrons is the thermal energy distribution and the average thermal energy of the electrons becomes

constant [Alt06]. For this reason, the drift velocity follows the following relation:

$$v_d \propto \frac{E}{N} \tag{2.7}$$

where, N is the number of electrons and E is the electric field. Applying the ideal gas law $pV = NkT$, we obtain:

$$v_d \propto \frac{ET}{p} \tag{2.8}$$

where T is the temperature and p is the pressure.

According to equation 2.8, for constant pressure, temperature and electric field the drift velocity is constant. To summarize, the drift velocity in the drift chamber (also in the TPC) is constant because the drift fields are small.

2.3.5 Time Projection Chamber (TPC)

The Time Projection Chamber (TPC) is a cylindrical multi-wire proportional chamber [Gru96] and was developed in 1970 by D.R. Nygren. It consists of a gas filled volume divided into two halves separated by the central electrode. If a charged particle passes through the gas volume, it will ionize the atoms of the gas around its trajectory. A homogeneous external electric field is applied between the two endplates of the TPC. The created electrons will drift to the anode due to the external electric field. Before they can be detected by the readout system they have to travel through an amplification stage, where they are multiplied by a large factor (gas gain). The main characteristics of the TPC are:

-Only gas inside the active area, no constructional elements.

-Very long drift distance and constant drift velocity.

-The track points can be recorded in 3D.

-The particle flavor is defined by the energy loss ($\frac{dE}{dx}$).

In order to suppress the diffusion perpendicular to the electric field, a magnetic field (parallel to the drift direction) is utilized.

2.4 Gas Electron Multiplier (GEM)

The Gas Electron Multiplier (GEM) is a proven amplification method, the first prototype was developed by F. Sauli at CERN, 1997 (for more details see chapter 5). It consists of a very thin sheet of two metal layers separated by an insulator layer [Sau12]. The tiny holes are made in a regular matrix on the GEM sheet (Figure 2.4a). A voltage difference of $200 - 400$ V is applied between the two metal layers which generates an

electric field with focusing point inside the GEM holes (Figure 2.4b). Accordingly, if an electron enters any hole, it creates an avalanche with amplification factor of 100-1000. The number of created electrons is large enough to generate a current which is easily detected by electronics. One can use a series of many GEMs that provides additional amplification stages.

There are many possible applications for the GEMs such as, radiation detection [JM07], medical imaging [Sau07], astrophysics [AL07] and high energy physics.

The advantages of the GEM are;

-High resolution time and position can be achieved.

-Ability for high radiation rate.

-Flexible and can compile with many readout systems.

-Low costs.

(A)

(B)
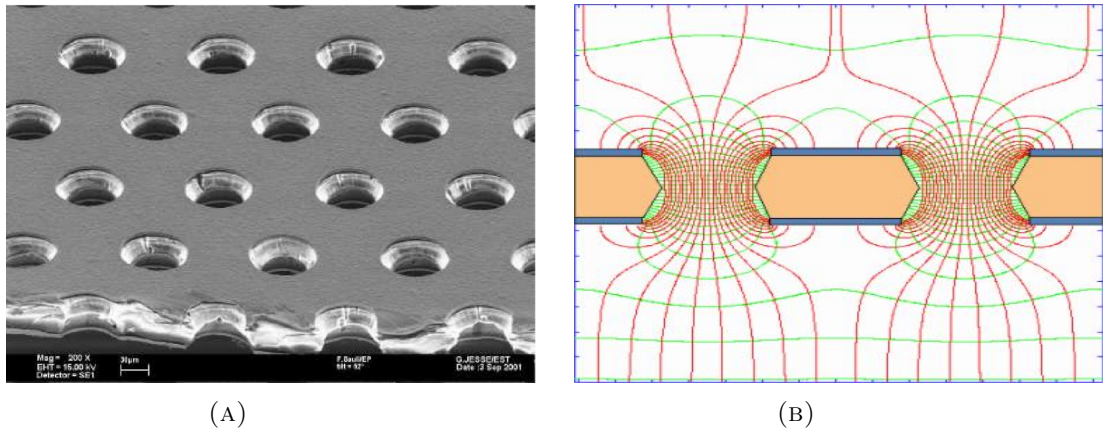
FIGURE 2.4: The gas electron multiplier (GEM) (A) is a microscopic image of a GEM (B) is the electric field distribution lines inside the GEM holes [Sau12].

Chapter 3

Experimental setup

In this chapter, the discussion focuses on the setup of the lab at Siegen University which consists of two parts. The first one is the test chamber or the small chamber (which is the main theme of this thesis), the second part is the prototype of the Time Projection Chamber (TPC).

3.1 Test chamber

The test chamber is a small gas-filled drift detector which is used to check and test the response and the performance of the GEMs, Figure 3.1. Its structure permits to use not only one GEM but also two or three GEMs at the same time. Particularly, in this thesis I used one GEM and combinations between two GEMs. The scheme of the arrangement of the GEMs is shown in Figure 3.2. It is important to realize, that the distance between the cathode and the nearest GEM is called the drift gap at which the drift field is generated. Additionally, the distance between the readout system and the closest GEM is called the induction gap for producing the induction field. In case of using two -or more- GEMs, the distance between the GEMs is called the transfer gap.

3.2 TPC prototype

The time projection chamber (TPC) prototype at Siegen University lab is shown in Figure 3.3. It consists of 2 lids and a central cylindrical body with diameter of 240 mm and a total length of 400 mm. The whole body of the TPC is fixed on a movable aluminum holder which enables the user to move the chamber in x and y directions.

(A) (B)
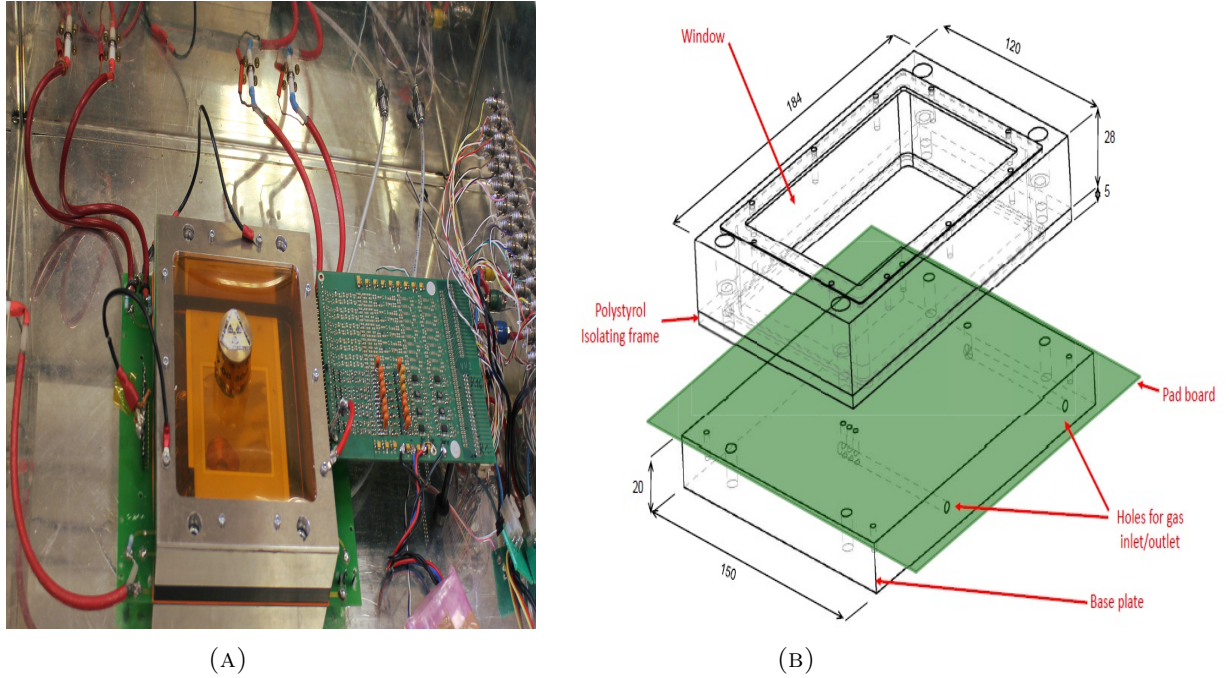
FIGURE 3.1: The test chamber st the University of Siegen, (A) is a real image of the test chamber and (B) is a drawing of the test chamber [Gau08].

(A) (B)
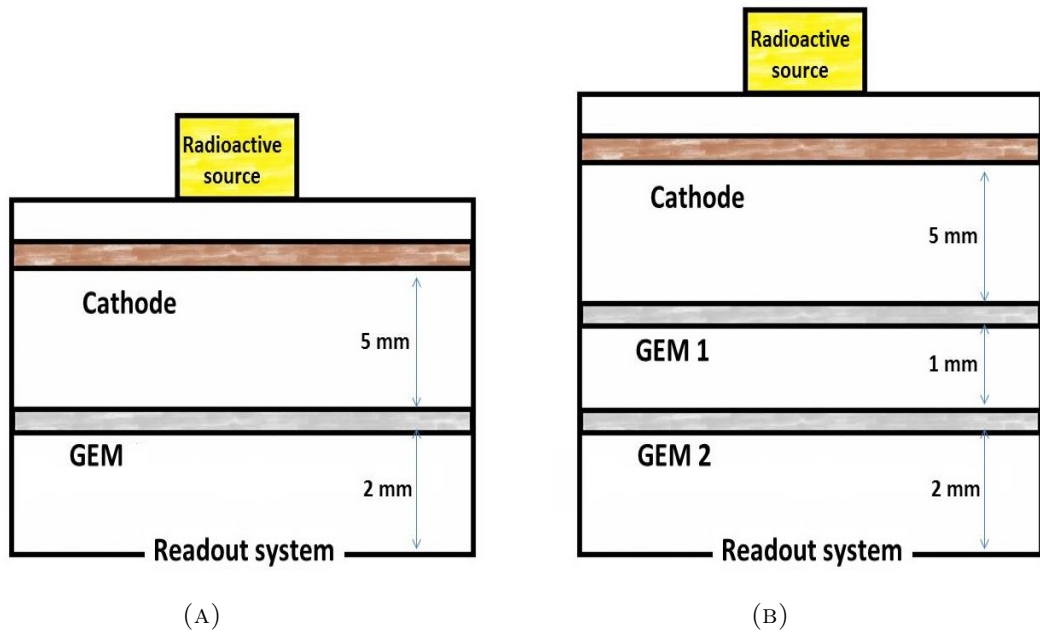
FIGURE 3.2: A scheme of the arrangement of the GEMs inside the test chamber, (A) in case of using one GEM and (B) for 2 GEMs.

The overlook of the TPC prototype is shown in Figure 3.4. A gas mixture flows inside the TPC from four gas inlet connectors on the endcap lid. In addition, there are two gas outlet connectors on the cathode lid in order to insure the homogeneity of the gas inside the chamber.
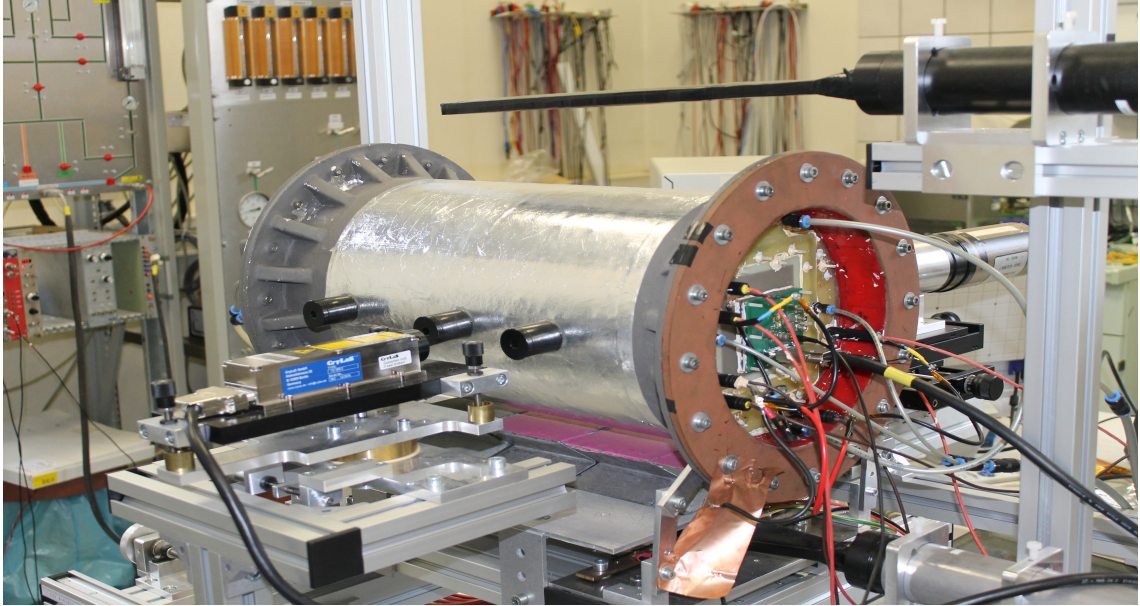
FIGURE 3.3: The overlook of the TPC prototype at Siegen University.
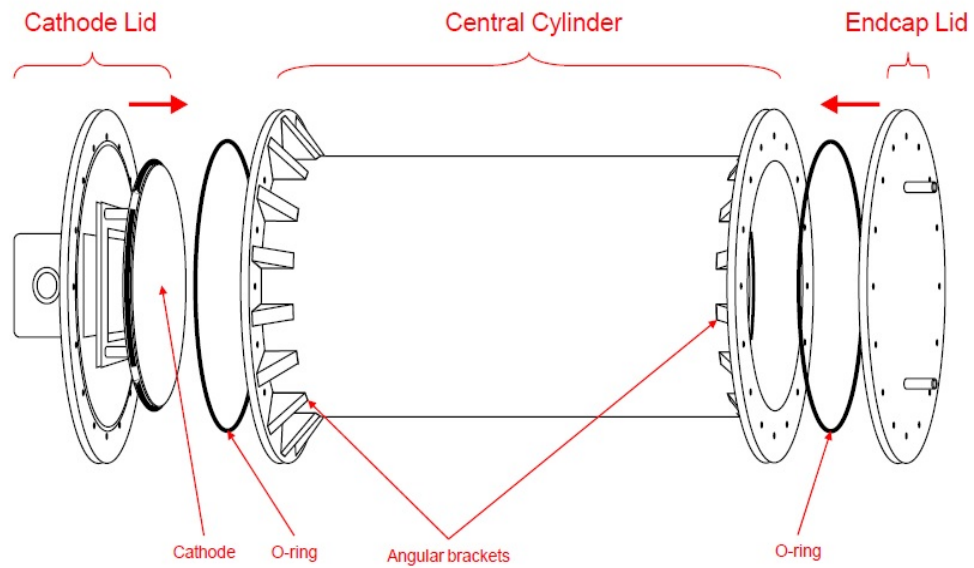
FIGURE 3.4: The geometrical drawing of the TPC prototype at Siegen University [Gau08].

3.3   High Voltage System (HVS)

The HVS is an integration of many components (e.g. power supplies, current meters and high voltage cables) that function to provide the GEMs with the required voltage difference and set the drift field inside the chamber.

3.3.1   HVS of the test chamber

The test chamber HVS is shown in Figure 3.5. It consists of up to seven power supplies. The number of the used supplies depends on the number of the used GEMs. They can be adjusted manually to reach the required voltage. Also, the user can use the HVS of the TPC to run the test chamber by generating a ramp files for two GEMs, see appendix B.

FIGURE 3.5: The HVS for the test chamber.

3.3.2   HVS of the TPC

Similarly, the HVS for TPC contains seven supplies (for 3 GEMs) in addition to seven current meters (Figure 3.6). The function of these current meters is to detect the current at each GEM and make sure it does not exceed the current limit. Users can define the current limits for the HVS by the HVS Lab-View program, see appendix B. The HVS is protected by an automatic-shutting-down function which stops the whole system automatically if the detected current exceeds the limit.

3.4   Gas system

The gas system is the unit for mixing the different gases to achieve the required gas mixture. Generally, this system can mix four kinds of gases together. In fact, for our
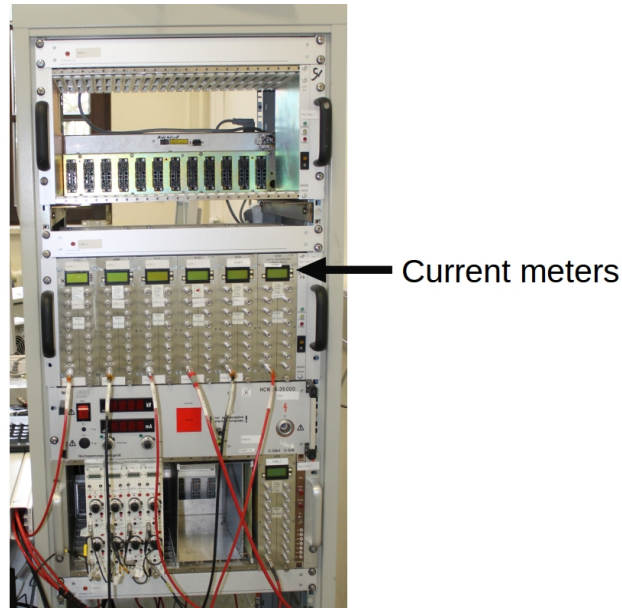
FIGURE 3.6: The HVS for the TPC.

experiment we use Argon-Carbondioxide mixture with different ratios (e.g. $90-10\%$, $80-20\%$ and $70-30\%$). The gas system is provided with a monitoring system which enables the user to monitor the mixing quality, the pressure and temperature of the gas. The procedure of gas system's setup and configurations is explained in Appendix A.

3.5 The Readout system

3.5.1 For test chamber

The test chamber readout system is a pad-readout which collects the electrons generated inside the chamber [Sha14]. The collected signal on each pad is sent to the Multi-Channel Analyzer (MCA) by a charge-sensitive amplifier. In other words, each pad is connected to a charge-sensitive channel at the preamplifier which is the first point in the amplification stage (for more details see chapter 4). The pad numbers corresponding to the charge-sensitive preamplifier channels are shown in Figure 3.7.

3.5.2 For TPC

The readout system for the time projection chamber consists of two main parts namely, the TimePix Chip and FPGA card. They are connected by the intermediate board, for more details see Appendix B and TOS manual [JK].
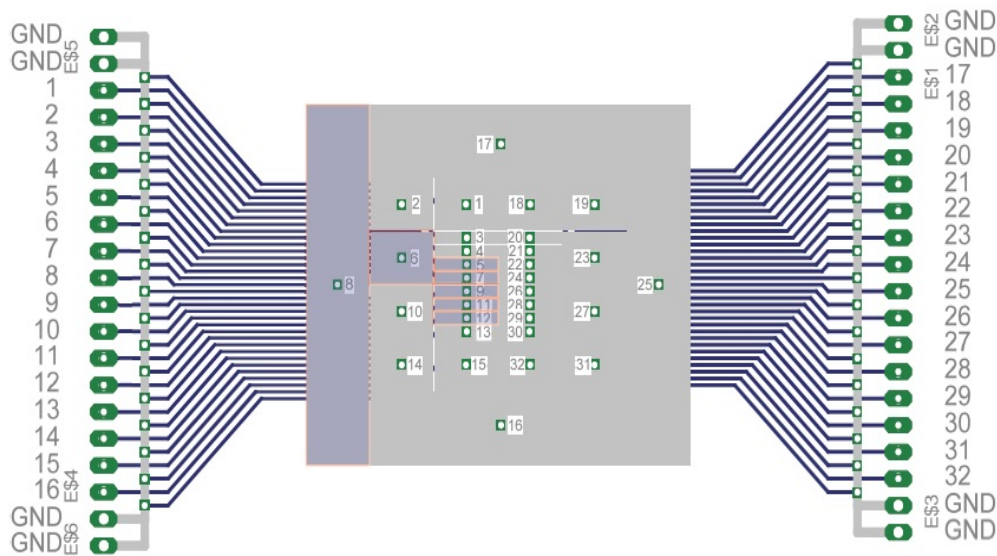
FIGURE 3.7: The pad readout system and the related charge-sensitive preamplifier channel .

3.5.2.1 TimePixChip

The development of the Timepix chip is based on the Medipix2 chip [CERb]. It is a Silicon board with 256 x 256 square pixels representing an active area of 2 cm^2. Each pixel has its own electrical circuit to detect and process data created from the detector [Kö11].

3.5.2.2 FPGA card

The FPGA card is the bridge of the data from the detector to the PC (Figure 3.8). It controls the type of data passed to the PC. Also, it can store the data on its removable flash memory. The passage for the data can be adjusted by the S1 switches on the FPGA board, Figure 3.9 shows the used configuration.

3.6 The radioactive sources

There are many different available radioactive sources in Siegen lab. Usually, we use ^{55}Fe for test chamber and UV-laser for TPC. The characteristics of the collimated Iron-55 radioactive source are list in Table 3.1.

FIGURE 3.8: The FPGA card (Model: Virtex-6 ML605).

FIGURE 3.9: The used FPGA card's pins configuration.

3.6.1 Iron-55 spectrum

^{55}Fe is an X-rays emitter with an energy of 5.89 keV. If the Argon gas is exposed to the ^{55}Fe, the photons (X-rays) will be absorbed via the photoelectric effect [Gau08]. This produces electrons with kinetic energy depending on the difference between the incident photon's energy and the binding energy. In addition, the created vacancy can be filled by Auger electron. The characteristic X-ray photon for the Argon (the used gas in our experiment) has an energy lower than the binding energy. Thus, it escapes from the detector due to the re-absorbing

Type decay	X-rays
Maximum energy	X-ray = 5.89 keV
	$K_{alpha} = 5.19$ keV and $K_{beta} = 6.49$ keV
Half life	2.7 years

TABLE 3.1: Iron-55 characteristics.

For this reason, the recorded spectrum of the used radioactive source (^{55}Fe), is shown in Figure 3.10, has two peaks. The higher peak includes the X-rays= 5.89 keV and the lower peak is for argon escape with energy = 3.89 keV.
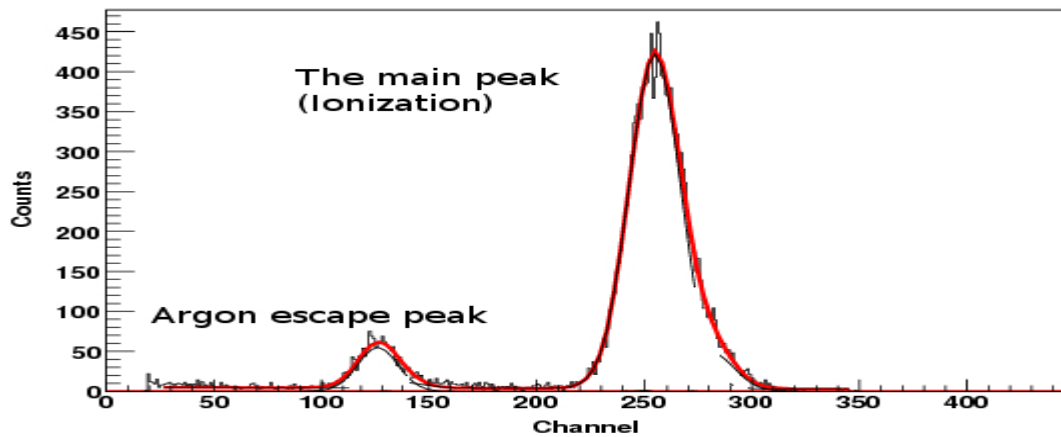
FIGURE 3.10: Iron-55 spectrum with Argon

Note:
For better view about the test chamber, watch the video about the procedure of the small chamber under name (Test chamber in one minute). The download link is (http://www.4shared.com/video/O_DBRpfLba/Test_chamber_in_one_minute_.html)

Chapter 4

Calibration of the MCA

According to The Automotion system and Instrumentation Dictionary [N/A03], calibration means "a test during which known values of measurand are applied to the transducer and corresponding output readings are recorded under specified conditions". Moreover, calibration is considered to be the connection between the measured data and the required results. As an illustration, by calibration, the channel number in the MCA can be converted to the electrical charge reaching the readout system. For this reason, one important task in our experiment is the calibration of the Multi-Channel Analyzer (MCA). To achieve the calibration a special system has been designed, as following:

4.1 Arrangement of the calibration System

Generally speaking, the main idea is to send specific pulses (which represent the charge) to the amplification stage and then monitoring the produced signal on the MCA. Consequently, the channel number can be converted into electrical charge. An external pulser is used to generate the required pulses, Figure 4.1 shows the setup of the calibration circuit and Figure 4.2 represents the connection circuit between the pulser and the preamplifier.
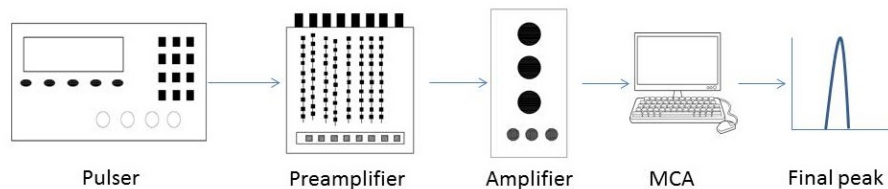
FIGURE 4.1: Scheme of the calibration circuit
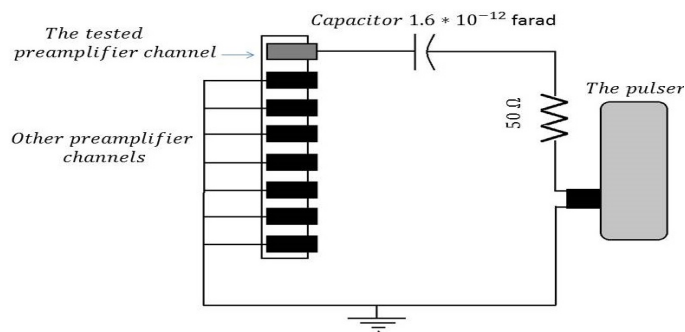
FIGURE 4.2: The connection circuit between the pulser and the pre-amplifier.

The signal from the pulser goes through the amplification stage that consists of the preamplifier and the main amplifier which -in turn- sends the signal to the MCA for digitalization stage. Finally, the MCA generates the final output as counts versus channel number.

4.1.1 The pulser

As mentioned before, the first point in the calibration circuit is the pulser that generates the signal to calibrate the MCA. This section provides the information about the pulser used in the calibration. Table 4.1 lists the main parameters for the generated pulses used to execute this process. As it shown in Figure 4.2, we use a capacitor to connect the pulser with the pre-amplifier. This capacitor is used as an integrator for the circuit and to stabilize the power.

Frequency	1000 Hz
Offset	Zero
Pulse width	100 μs

TABLE 4.1: The parameters of the generated pulses for the MCA calibration

Figure 4.3 shows the shape of generated pulse by the external pulser, Figure 4.3a is the pulse taken directly from the pulser (for magnitude 20 mV, as an example) for time scale of 500 μs per unit length of the oscilloscope which represents a bunch of the generated peaks. In addition, for time scale of 20 μs per unit length of the oscilloscope (which represents one single peak) is shown in Figure 4.3b.

4.1.2 The pre-amplifier

The pre-amplifier is the first station in the amplification process and the second point in the calibration process. In this section, two pre-amplifier channels were investigated to

(A)   (B)
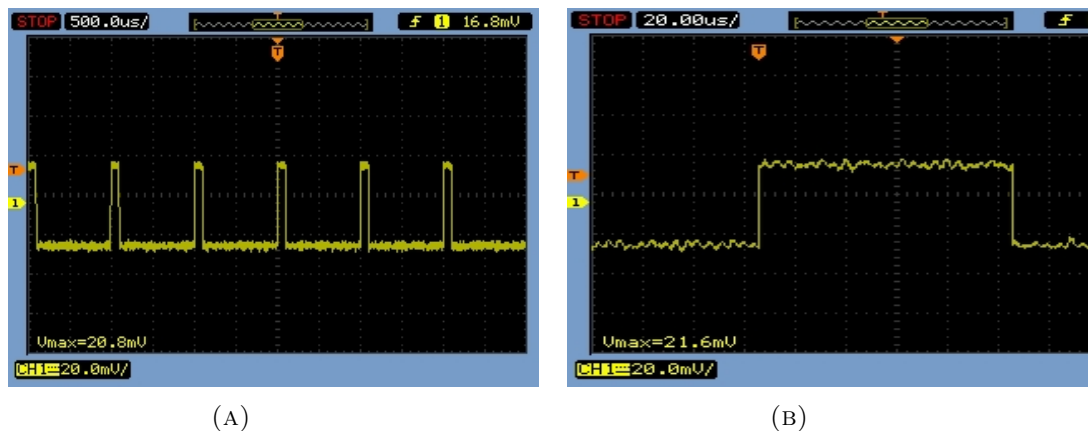
FIGURE 4.3: The shape of the peak directly from the pulser.

observe and decide which one will be used in the calibration and the experiment. The inspected pre-amplifier channels are number **six** and **eight**, because they are correlated with the largest parts in the readout board, for more details see section 3.5.1.

Figure 4.4 shows the form of the produced signals for the two selected pre-amplifier channels. Figures 4.4a and 4.4c display one edge of the signal (time scale = 5 μs) for preamplifier channels six and eight, respectively. While, Figures 4.4b and 4.4d display the whole shape of the signal (time scale = 200 μs). As there is no significant difference between both channels, **channel eight** was chosen for conducting the experiment. The signal after the pre-amplifier comparing with the original one from the pulser is shown in Figure 4.5. One can see, the signal after the pre-amplifier contains positive and negative peaks which are produced from the charging and discharging of the used capacitance. After accomplishment of this stage in the path of our calibration signal, the following station to be considered is the main amplifier.

4.1.3 The main amplifier

The second juncture in the amplification process is the main amplifier which plays the main role in shaping and amplifying the outcome signal- Figure 4.6. There are many parameters to be configured in the main amplifier, for instance the fine gain, the pulse mode, the peaking time and the main gain. In the following part we discuss the effects of two parameters (the main gain and the peaking time) on the shape and the amplitude of our peaks. The rest of the parameters are fixed to values which are correlated with the used model of the MCA. As the main gain and the peaking time are the most important parameters for forming the final spectrum, we investigate the following parameters for the main gain = 50 & 100 & 200 and peaking time = 3 & 8 μs. The results for the calibration with various parameters are given in section 4.2. Figure 4.6 shows the shape of the original pulse from the pulse generator (the yellow peak) and after the main

(A)

(B)

(C)

(D)
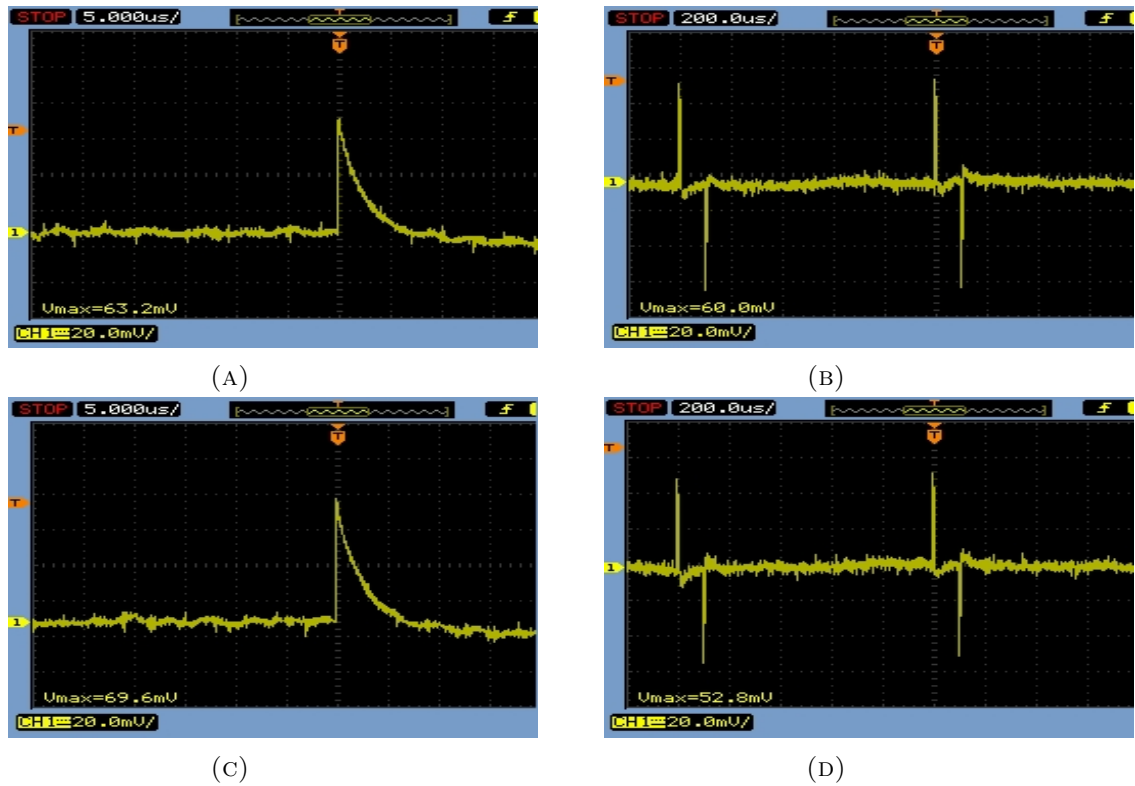
FIGURE 4.4: The shape of the peaks from pre-amplifier channels ; (A & B) Channel number 6 for time scale = 5 & 200 μs, respectively. (C & D) Channel number 8 for time scale = 5 & 200 μs. (The original signal is generated by the pulser with amplitude of 20 mV)

(A)

(B)
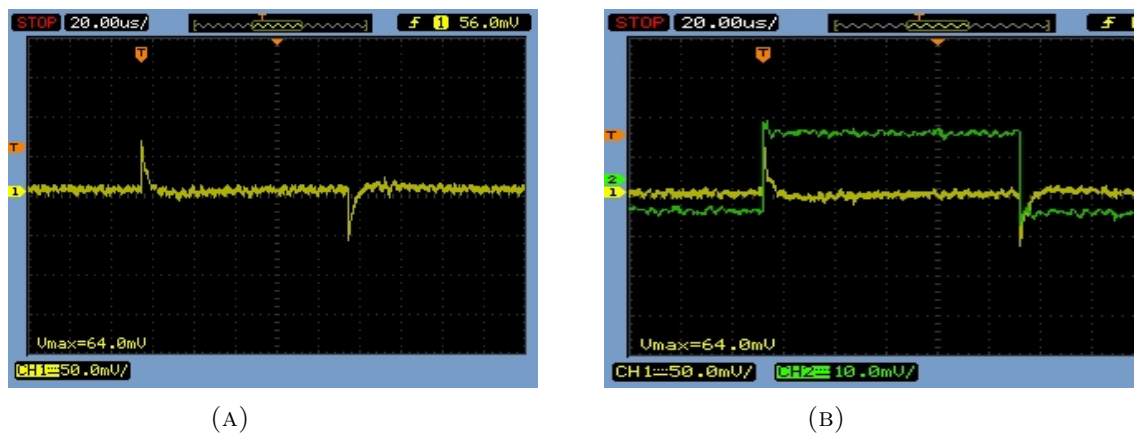
FIGURE 4.5: (A)The shape of the peak after the pre-amplifier using channel 8. (B) The combination between the peak from the pulser - the green peak- and the peak after pre-amplifier - the yellow one. (The original signal is generated by the pulser with amplitude of 20 mV. The positive and the negative peaks are related to the charging and discharging of the capacitor)

amplifier (the green peak). Thus, the calibration system is ready and the next step is to generate the relation to connect the channel number of the MCA with the corresponding charge.

FIGURE 4.6: Combination between the pulser peaks (the yellow peak) and the same peak after main amplifier (green one).

4.2 Calibration of the MCA

In this part, we generate a simple relation between the channel number of the MCA and the related charge. This procedure can be done for each parameter on the main amplifier as the following:

1. Setup the specific parameters for the main amplifier that need to be calibrated.

2. Connect the pulser to the pre-amplifier.

3. Operate the pulser and increase the amplitude of the generated peak.

4. Scan and save the main peak position on the MCA for each amplitude.

5. Fit the main peak position vs the applied voltage, this fitting is linear and the equation of the straight line is the relation between the voltage and the channel number on the MCA.

4.2.1 Peaking time 3 μs

As mentioned before, the investigation is done for two parameters, the main gain and the peaking time. First, for peaking time 3 μs for the main gain with values 50, 100 and 200 are investigated. The spectrum for each voltage was measured for 3 minutes. That means, 180000 pulses per each voltage (the used frequency is 1000 Hz).

Figures 4.7, 4.8 and 4.9 display the MCA spectra for different pulse amplitudes for main gain 50, 100 and 200, respectively. In each spectrum, there are two peaks. The peak on the right side represents the raising edge for the original peak. The second is for the falling edge. This peak should be neglected. Table 4.2 gives the positions of the main peak for each applied voltage. The fitting of these values gives the relation between the voltage and the channel number on the MCA. Figures 4.10, 4.11 and 4.12 show the linear fitting. Equations 4.1, 4.2 and 4.3 are the final relations between voltage and channel number for main gain 50, 100 and 200, respectively. These relations will be used later to estimate the gas gain of the system. As it was expected, the channel number on the MCA related to each voltage is proportional to the value of the main gain of the main amplifier. Consequently, the slope of the linear fitting changes with constant factor depending on the value of the main gain. From the Gaussian fitting of the spectra, we extracted the width of each peak which changes accordingly with the main gain. Table 4.3 lists the values for peak width related to the voltage.

$$\text{Voltage (mV)} = -0.057 \pm 0.188 + (0.019 \pm 1.2 * 10^{-4}) * \text{channel number (mV)} \quad (4.1)$$

$$\text{Voltage (mV)} = 0.05 \pm 0.012 + (0.0087 \pm 4.5 * 10^{-6}) * \text{channel number (mV)} \quad (4.2)$$

$$\text{Voltage (mV)} = 0.04 \pm 0.074 + (0.00431 \pm 1.6 * 10^{-5}) * \text{channel number (mV)} \quad (4.3)$$

Voltage (mV)	Peak position (MCA)		
—	Main gain 50	Main gain 100	Main gain 200
5	247.1 ± 0.18	567.87 ± 0.780	1160.8 ± 0.40
10		1146.90 ± 0.083	2305.5 ± 0.14
15	761.67 ± 0.055	1718.49 ± 0.089	3448.7 ± 0.13
20		2292.64 ± 0.088	4657.8 ± 0.16
25	1278.91 ± 0.054	5794.9 ± 0.16	5794.9 ± 0.16
30		3441.47 ± 0.090	6946.2 ± 0.29
35	1797.18 ± 0.052	4017.01 ± 0.092	
45	2316.20 ± 0.052		

TABLE 4.2: The peak position in the MCA related to each applied voltage from the pulser for peaking time 3 μs

Voltage (mV)	Peak width		
—	Main gain 50	Main gain 100	Main gain 200
5	27.6 ± 0.52	70.8 ± 0.12	121.4 ± 0.20
10		69.6 ± 0.13	139.3 ± 0.21
15	31.97 ± 0.087	69.4 ± 0.14	129.8 ± 0.23
20		68.8 ± 0.13	178.8 ± 0.29
25	31.2 ± 0.12	70.1 ± 0.12	230.9 ± 0.25
30		68.0 ± 0.14	198.6 ± 0.79
35	31.93 ± 0.082	67.5 ± 0.14	
45	32.05 ± 0.089		

TABLE 4.3: The peak width related to each applied voltage from the pulser for peaking time 3 μs

(A)

(B)

(C)

(D)
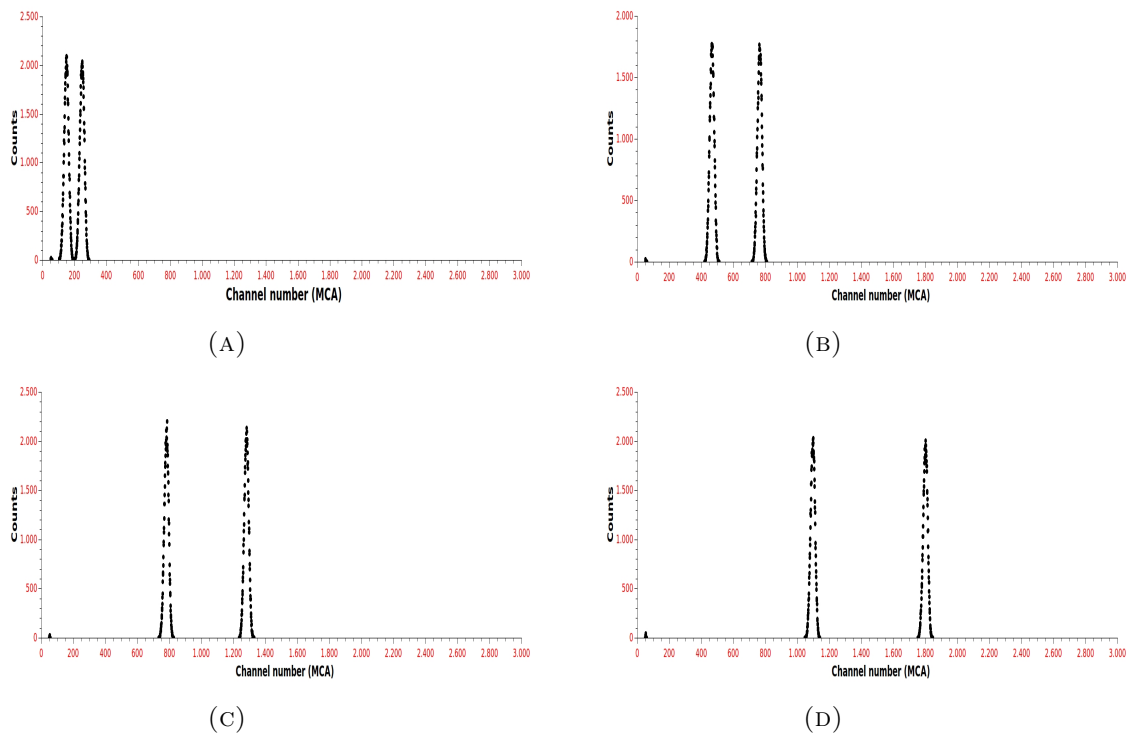
FIGURE 4.7: The distribution of the measured channel number with the MCA for main gain 50. Peaking time 3 μs and pulse amplitude; (A)5 mV. (B)15 mV. (C)25 mV. (D)35 mV.
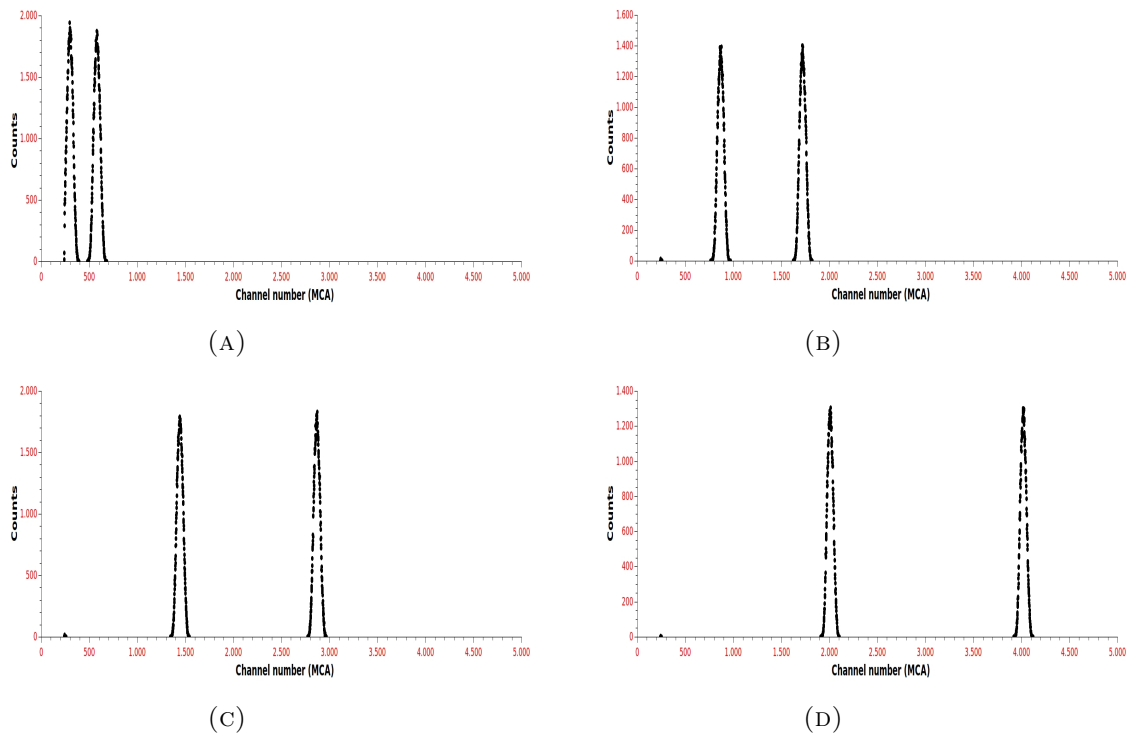
FIGURE 4.8: The distribution of the measured channel number with the MCA for main gain 100. Peaking time 3 μs and pulse amplitude; (A)5 mV. (B)15 mV. (C)25 mV. (D)35 mV.
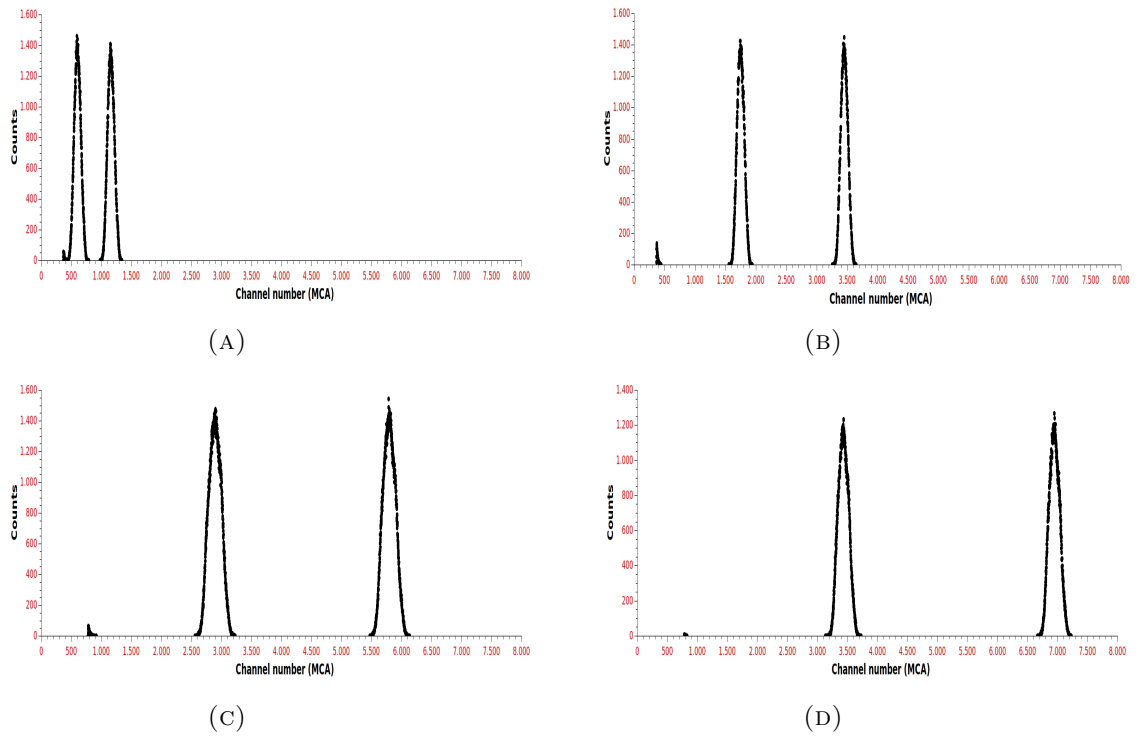
FIGURE 4.9: The distribution of the measured channel number with the MCA for main gain 200. Peaking time 3 μs and pulse amplitude; (A)5 mV. (B)15 mV. (C)25 mV. (D)35 mV.

Equation	y = a + b*x		
Adj. R-Square	0,99983		
		Value	Standard Error
A	Intercept	-0,05726	0,18829
A	Slope	0,01951	1,27652E-4
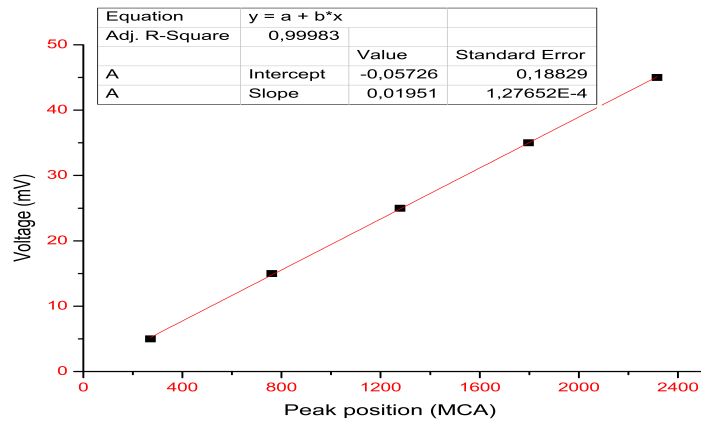
FIGURE 4.10: The linear fitting for pulser applied voltage vs main peak position on the MCA for main gain 50 and peaking time 3 μs.

Equation	y = a + b*x		
Adj. R-Square	1		
		Value	Standard Error
C	Intercept	0,051	0,01164
C	Slope	0,0087	4,53847E-6
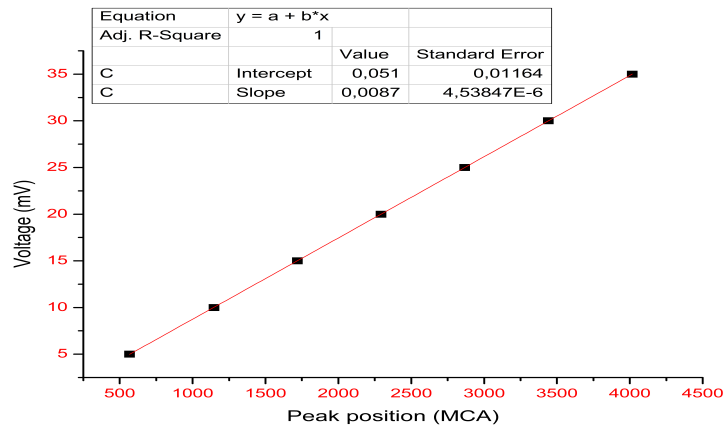
FIGURE 4.11: The linear fitting for pulser applied voltage vs main peak position on the MCA for main gain 100 and peaking time 3 μs.

Equation	y = a + b*x		
Adj. R-Square	0,99993		
		Value	Standard Error
C	Intercept	0,0395	0,07365
C	Slope	0,00431	1,63295E-5
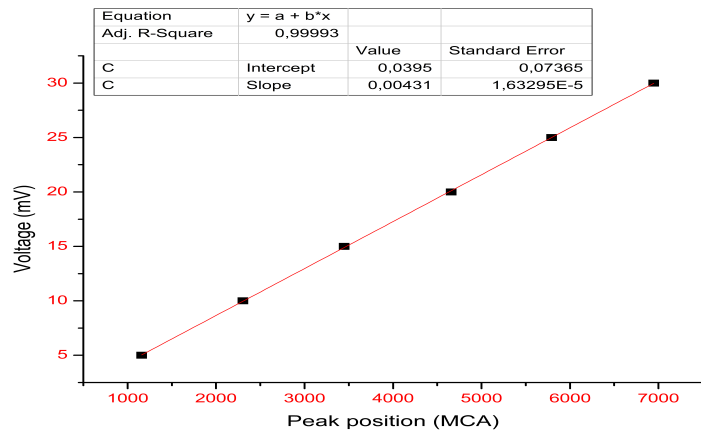
FIGURE 4.12: The linear fitting for pulser applied voltage vs main peak position on the MCA for main gain 200 and peaking time 3 μs.

4.2.2   Peaking time 8 μs

In the same technique as for peaking time 3 μs we execute the calibration for peaking time 8 μs. This can be established via setting the peaking time to be 8 μs and changing the gain for main amplifier. Table 4.4 lists the peak positions related to the voltage for main gain 50, 100 and 200. Figures 4.13, 4.15 and 4.16 display the spectra of the MCA for each main gain. Figure 4.14 shows the linear fitting for main gain 50. One can see, when we switched to main gain 100 and 200, peaking time 8 μs shows many strange features like triple peaks or many entries with nearly zero amplitude (see Figures 4.15 and 4.16). For this reason, this setting was excluded from the experiment and peaking time 3 μs should be used.

Voltage (mV)	Peak position (MCA)		
—	Main gain 50	Main gain 100	Main gain 200
5	130.29 ± 0.023	238.24 ± 0.061	506.2 ± 0.15
15	424.41 ± 0.009	748.0 ± 0.17	1483.7 ± 0.78
25	719.34 ± 0.024	1288.25 ± 0.041	2500 ± 2
30		1548.71 ± 0.033	2975.1 ± 0.13
35	1012.21 ± 0.027	4017.01 ± 0.092	
45	1306.43 ± 0.029	2063.15 ± 0.05	3915.0 ± 0.11

TABLE 4.4: The peak position in the MCA related to each applied voltage from the pulser for peaking time 8μs
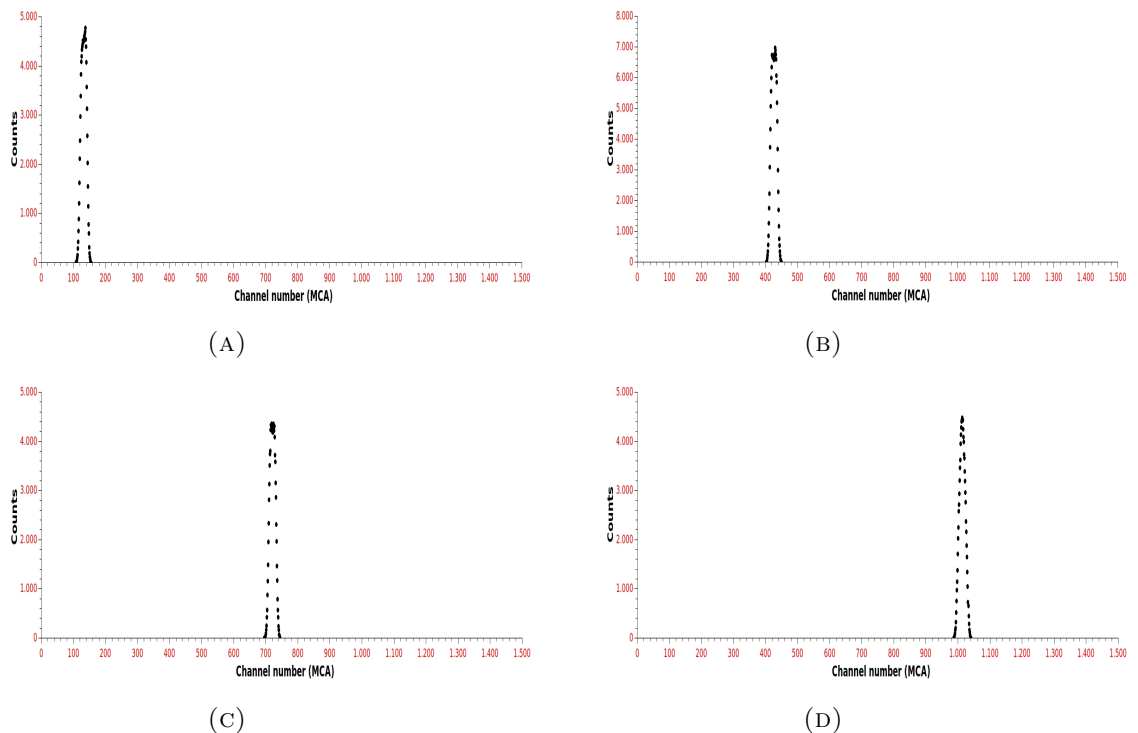
FIGURE 4.13: The distribution of the measured channel number with the MCA for main gain 50 and peaking time 8 μs; (A)5 mV. (B)15 mV. (C)25 mV. (D)35 mV.
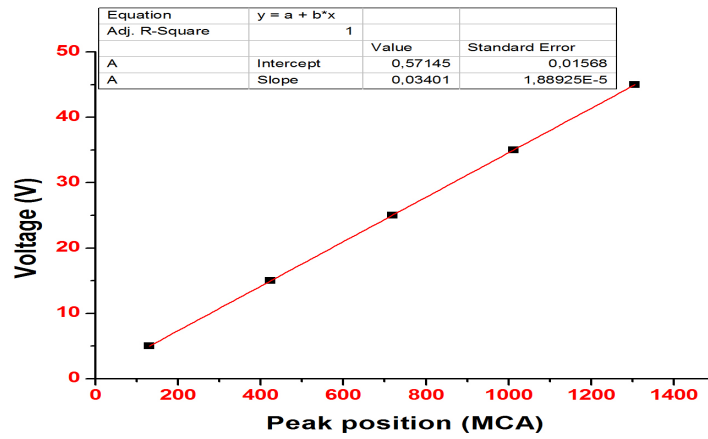
FIGURE 4.14: The linear fitting for pulser applied voltage vs main peak position on the MCA for main gain 50 and peaking time 8 μs.

(A)

(B)

(C)

(D)
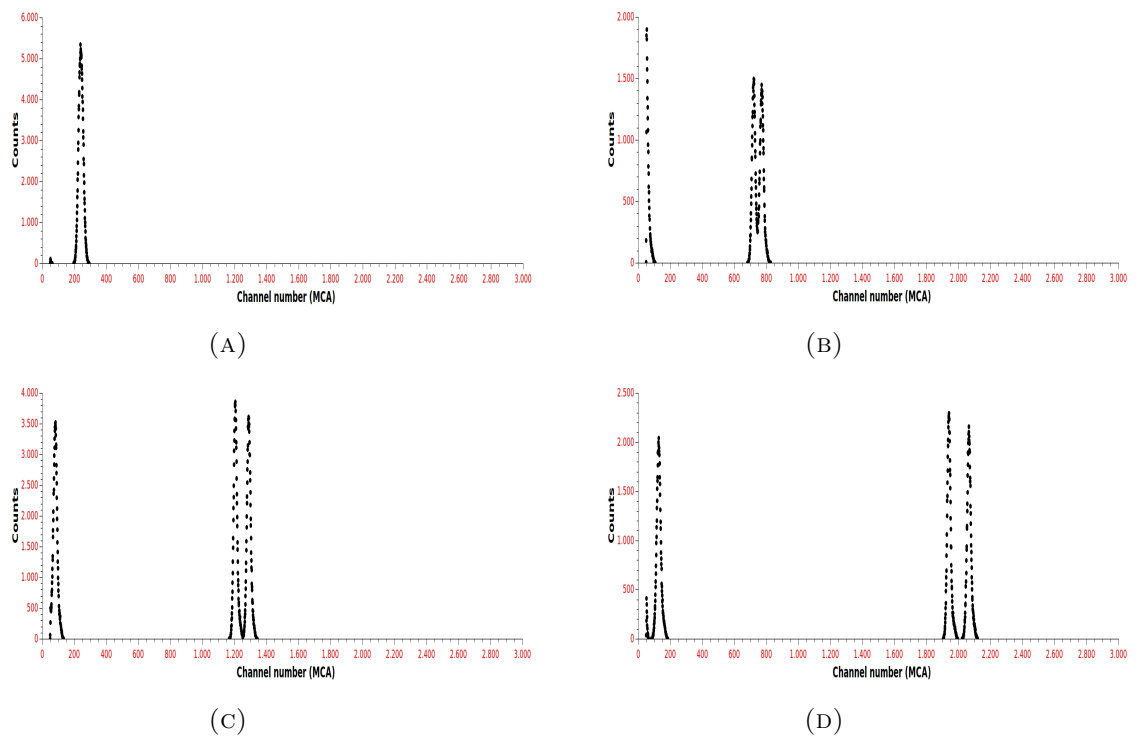
FIGURE 4.15: The distribution of the measured channel number with the MCA for main gain 100 and peaking time 8 μs; (A)5 mV. (B)15 mV. (C)25 mV. (D)40 mV.
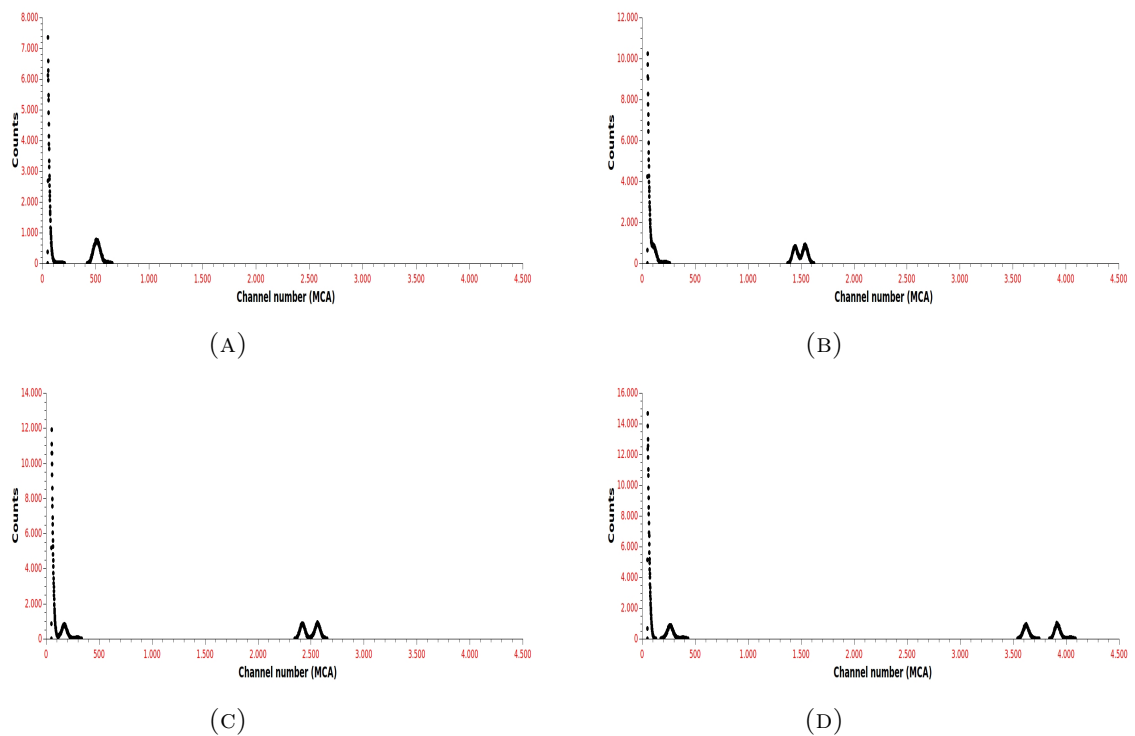
FIGURE 4.16: The distribution of the measured channel number with the MCA for main gain 200 and peaking time 8 μs ; (A)5 mV. (B)15 mV. (C)25 mV. (D)40 mV.

4.3   Gas gain calculation

The following lines show the methodology to calculate the gas gain for the system. First, we go through the theoretical calculations. Starting with the master equation for the gas gain- equation (4.4).

$$G_g = \frac{N}{n} \tag{4.4}$$

Where,

N : number of the electron after the gas amplification inside the GEMs.

n : number of primary electrons produced by the radioactive source.

When using a radioactive source, e.g. ^{55}Fe, the number of primary electrons is given by the following formula:

$$n = \frac{E_s}{E_i} \tag{4.5}$$

Where,

E_s : *the energy of the radioactive source,* $E_{Fe_{55}} = 5.89\ keV$.

E_i : *the ionization energy of the gas.*

In our experiment we use a mixture of $Ar - CO_2; 80 - 20\%$. According to this ratio we find $E_i = 15.363$ eV , where $E_{Ar} = 15.7596$ eV and $E_{CO_2} = 13.777$ eV,

$$n = 383 \text{ electrons} \tag{4.6}$$

Calculation of electrons after amplification stage:

$$Q = Ne^- = CV \tag{4.7}$$

Where,

Q : *the charge (coulomb).*

N : *number of electrons.*

e^- : *electron charge,* $1.6 * 10^{-19}$ *(coulomb).*

C : *the capacitance (farad).*

V : *the voltage (volt).*

For the used capacitance of $1 * 10^{-12}$ farad, the charge produced from the pulse of the pulse generator is given by the following formula:

$$Q(\text{coulomb}) = 10^{-12}(\text{farad}) * \text{V (volt)} = 10^{-15}(\text{farad}) * \text{V (millivolt)} \tag{4.8}$$

Thereupon, the relation between the charge and the channel number for each main gain can be derived from equation 4.8. That can be executed by substituting equations 4.1, 4,2 and 4.3 (which represent the relation between the voltage and the channel number) in equation 4.8 as following:

4.3.1 Main gain 50

Compiling equations 4.1 with 4.8 in order to find the desired relation for main gain 50. Equation 4.9 represents the relation between the charge and the channel number in the MCA for main gain 50.

$$Q(coulomb) = 10^{-15}(f).(mV)(-0.057 \pm 0.188 + (0.019 \pm 0.00012) * \text{channel number}) \tag{4.9}$$

In the following part we used a measured data from a setup using two GEMs - as an example- to show the procedure to reach the value of the gas gain. Figure 4.17 shows

the spectrum before and after the calibration (A and B respectively) for applied voltage on both GEMs of 340 V. In figures both the main peak and the escape Argon peak are clearly visible.

After the Gaussian fitting for spectrum in Figure 4.17b, the related charge for the main peak is $(1.37 * 10^{-14} \pm 3.3 * 10^{-18})$ coulomb.
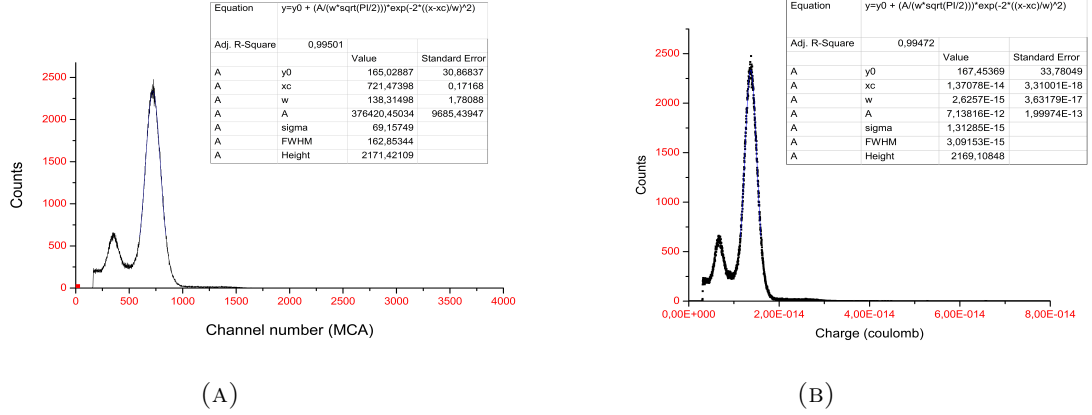
FIGURE 4.17: Test data for calibration process- these measurements were taken for random gas mixture for main gain 50 with two GEMs. A) the spectrum as counts vs channel number. B) the spectrum as counts vs Charge.

Hence, from equation 4.7 the number of electrons after the gas amplification inside the GEMs (for applied voltage difference on the two GEMs is 340 V) can be calculated as following;

$$N = \frac{1.37 * 10^{-14} \pm 3.3 * 10^{-18}}{1.6 * 10^{-19}} \tag{4.10}$$

Using equation 4.10 in equation 4.4, the gas gain for applied voltage difference 340 V can be found;

$$G = \frac{\frac{1.37*10^{-14} \pm 3.3*10^{-18}}{1.6*10^{-19}}}{383} = 223.52 \pm 0.053 \tag{4.11}$$

Equation 4.11 is the actual value of the gas gain of our system in case of 340 V is the applied voltage. The same manner was done for different voltages. Table 4.5 lists the values for each gas gain associated to a given GEMs voltage difference.

As the gas gain of the GEM is exponentially related with the voltage difference on the GEM [Sau12], the exponential fitting for the gas gain was executed (Figure 4.18). The equation of the exponential fitting is $f(x) = \exp{(p_0 + p_1 * x)}$. From this fitting, we extracted the parameters of the fitting where p_0 is the constant and p_1 is the slope. Hence, the relation 4.12 shows the exponential relation between the gas gain and the

Voltage (V)	Gas gain
340	223.52 ± 0.053
345	296.10 ± 0.048
350	402.54 ± 0.084
355	491.7 ± 0.22
360	700.5 ± 0.16
365	819.8 ± 0.21

TABLE 4.5: Gas gain for each GEMs voltage difference for main gain 50
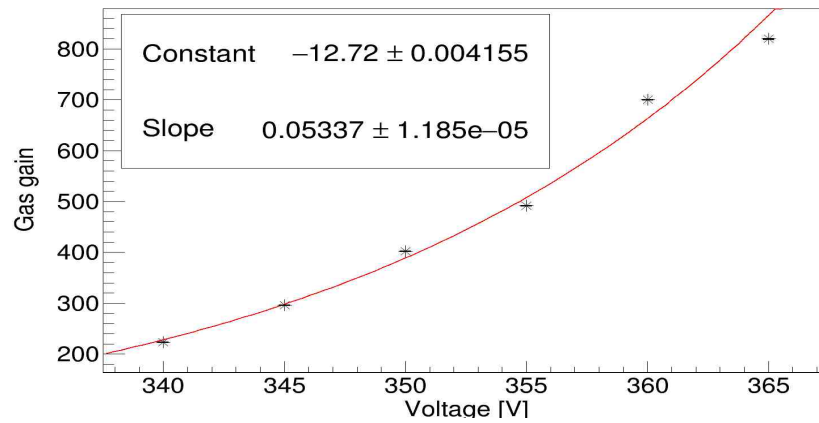
FIGURE 4.18: Gas gain vs GEMs voltage.

applied voltage:

$$\text{The gas gain} \; = \; \exp((-12.72 \pm 0.004) + (0.05337 \pm 1.185 * 10^{-5}) * \text{voltage}) \quad (4.12)$$

> ✎ **Important note:**
> The gas gain is a characteristic of the GEMs and it must be independent of the gain chosen at the main amplifier.

4.3.2 Main gain 100

Substituting in equations 4.2 with 4.8 gives equation 4.13 which represent the relation between the charge and the channel number in case of main gain 100. Then, the same procedure as for main gain 50 is used and the gas gain is calculated. Table 4.6 lists the values for gas gain and Figure 4.19 is the exponential fitting. Equation 4.14 gives the relation between the gas gain and the applied voltage for this main gain.

$$Q(coulomb) = 10^{-15}(f).(mV)(-0.05 \pm 0.011 + (0.0087 \pm 4.5 * 10^{-6} * \text{channel number}))$$
$$(4.13)$$

Voltage (V)	Gas gain
340	237.4 ± 0.16
345	278.46 ± 0.07
350	354.4 ± 0.25
355	479.6 ± 0.25
360	599.0 ± 0.28
365	734.7 ± 0.35

TABLE 4.6: Gas gain for each GEMs voltage difference for main gain 100
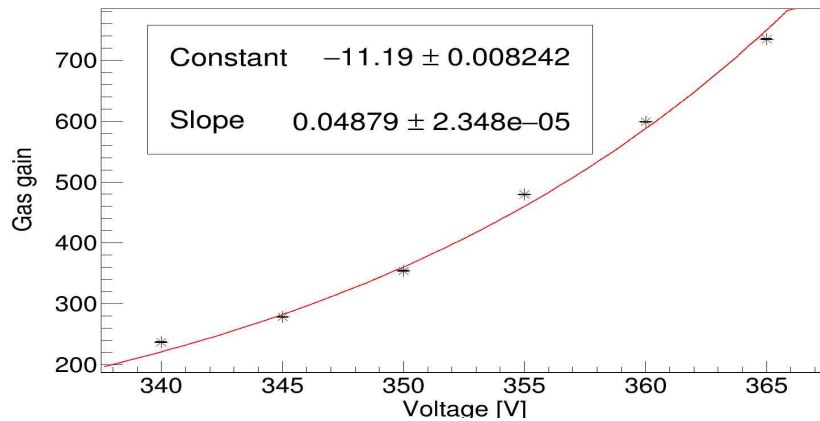
FIGURE 4.19: Gas gain vs GEMs voltage for main gain 100.

$$\text{The gas gain} \ = \ \exp((-11.19 \pm 0.0082) + (0.04879 \pm 2.348 * 10^{-5}) * \text{voltage}) \quad (4.14)$$

4.3.3 Main gain 200

In the same manner, equation 4.15 is the relation between the charge and the channel number for main gain 200. Table 4.7 shows the gas gain values for each applied voltage and Figure 4.20 is the exponential fitting. Equation 4.16 is the relation between the gas gain and the applied voltage.

$$Q(coulomb) = 10^{-15}(f).(mV)(0.03 \pm 0.073 + (0.00431 \pm 1.63 * 10^{-5} * \text{channel number})) \quad (4.15)$$

Voltage (V)	Gas gain
340	238.4 ± 0.12
345	306.6 ± 0.15
350	371.7 ± 0.26
355	490.6 ± 0.31

TABLE 4.7: Gas gain for each GEMs voltage difference for main gain 200
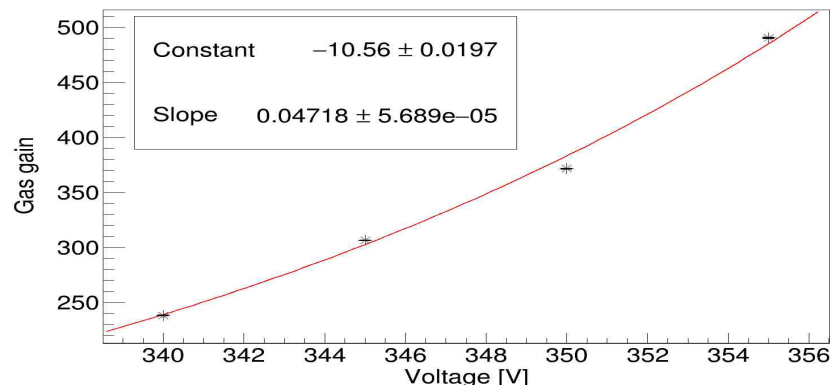
FIGURE 4.20: Gas gain vs GEMs voltage for main gain 200.

$$\text{The gas gain} \; = \; \exp((-10.56 \pm 0.0197) + (0.04718 \pm 5.689 * 10^{-5}) * \text{voltage}) \quad (4.16)$$

As can be seen, the relation between the gas gain and the applied voltage for main gain 50 (equation 4.12) shows slight fluctuation comparing with the ones for main gains 100 and 200 (equations 4.14 and 4.16). Thus, the main gain 50 is excluded from the experiment. On the other hand, the main gain 200 produced signals which exceed the MCA range. For this reason, main gain 200 was eliminated.

4.4   The chosen configuration and the final setup

Table 4.8 and Figure 4.21 give the decided configurations and the final setup for the system used in the experiment.

Gas mixture	$Ar - CO_2; 80 - 20\%$
Radioactive source	^{55}Fe
Fields	
Drift field	50 V/mm
Transfer field	200 V/mm
Induction field	300 V/mm
Pre-amplifier channel	number 8
Main amplifier	
Main gain	100
Peaking time	3 μs
Fine gain	0.7
MCA mode	Pulse Height Analyzer (PHA)

TABLE 4.8: The configurations for the system
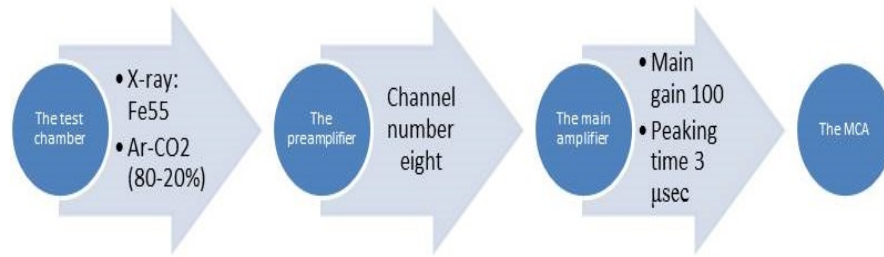
FIGURE 4.21: The final setup .

Chapter 5

GEMs investigation

Many developments have been done to boost the performance of the GEMs in order to achieve the required stability and electrical spark resistance, which are the vital parameters that have to be dealt with. The used materials of metal layers and the insulators, the thickness of the GEM and the diameter of the holes are the main influential parameters of the GEM.

This chapter shows a comparison between two kind of GEMs with different materials and different geometries:

- CERN GEM (was developed by Fabio Sauli at CERN).

- Ceramic GEM (was developed by Siegen University with cooperation of KOA company).

The technique of changing the applied GEM voltages and measuring the gas gain for each value of these voltages provides a clear overview about the behavior of the GEMs[1]. To point out, by using the test chamber (section 3.1) and radioactive source the gas gain for single CERN GEM, combination between two CERN GEMs, single ceramic GEM, combination between two ceramic GEMs and combination between CERN and ceramic GEM was measured. The idea of using the combination of ceramic and CERN GEMs is to distinguish the correlation between them. In next sections we discuss -in details- the results for each mentioned setup.

---

[1] All these measurements are taken according to the chosen system configuration mentioned in section (4.4).

5.1   CERN GEM

CERN GEM is an assured method to achieve the amplification for detection process in gas detector [Sau12]. Table 5.1 and Figure 5.1 show the specifications for CERN GEMs.

Conductor	copper
Insulator	Kapton
Size	50 mm x 50 mm
Holes shape	Conical from both entry sides
Copper holes diameter	70 micrometer
Kapton holes inner diameter	50 micrometer
Thickness	50 micrometer

TABLE 5.1: The specifications the of CERN GEM
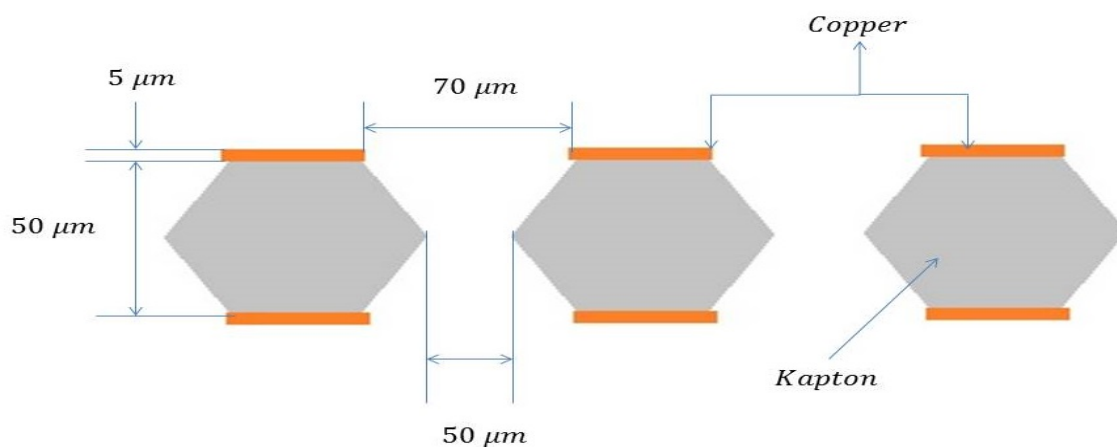
FIGURE 5.1: The specifications of the CERN GEM

In the next few pages the performance of the CERN GEMs is discussed. A single GEM and a combination between two have been tested as following:

5.1.1   One CERN GEM

The first step in our investigation is to use a single CERN GEM. Under the chosen configurations (see section 4.4), a single GEM is exposed to the radioactive source as well as the applied GEM voltage is changed. This procedure was done for two different CERN GEMs. Changing the voltage difference between the top and bottom of the GEM changes the gas gain and consequently changes the main peak position of our spectrum in the MCA. Tables 5.2 and 5.3 show the values of the main peak position and the actual gas gain related to the applied voltage for two different GEMs. The MCA peaks for the first and the second GEMs are shown in Figures 5.2 and 5.3. Figure 5.4 displays the exponential relationship between the gas gain and the applied voltages for both used

GEMs. From the equation for the exponential fitting, we extracted the relation between the gas gain and the applied voltage on the first single CERN GEM:

$$\text{The gas gain} \ = \ \exp((-7.7 \pm 0.13) + (0.0279 \pm 0.00037) * \text{voltage})$$

and for the second CERN GEM:

$$\text{The gas gain} \ = \ \exp((-7.93 \pm 0.018) + (0.02832 \pm 5.1 * 10^{-5}) * \text{voltage})$$

Overall, the first detectable spectrum was measured for voltage different 350 V for each GEM. Also one can see the gas gain for both GEMs is roughly the same. The uncertainties given in the table are the statistical uncertainties from the fitting only and do not contain any systematic contribution. The measurements for the two GEMs were performed on the same day with a constant temperature in the room.

(A)

(B)

(C)
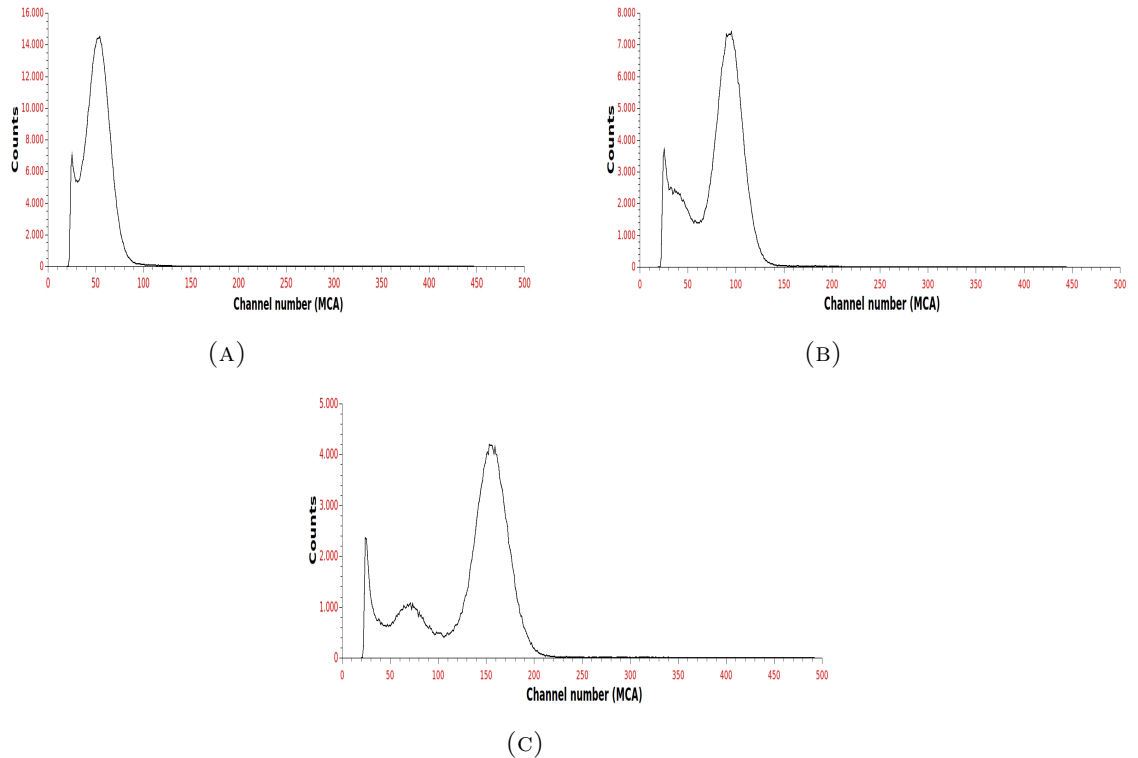
FIGURE 5.2: The MCA distributions for the first single CERN GEM. (A) the voltage difference = 350 V. (B) the voltage difference = 370 V. (C) the voltage difference = 390 V.

(A)

(B)

(C)
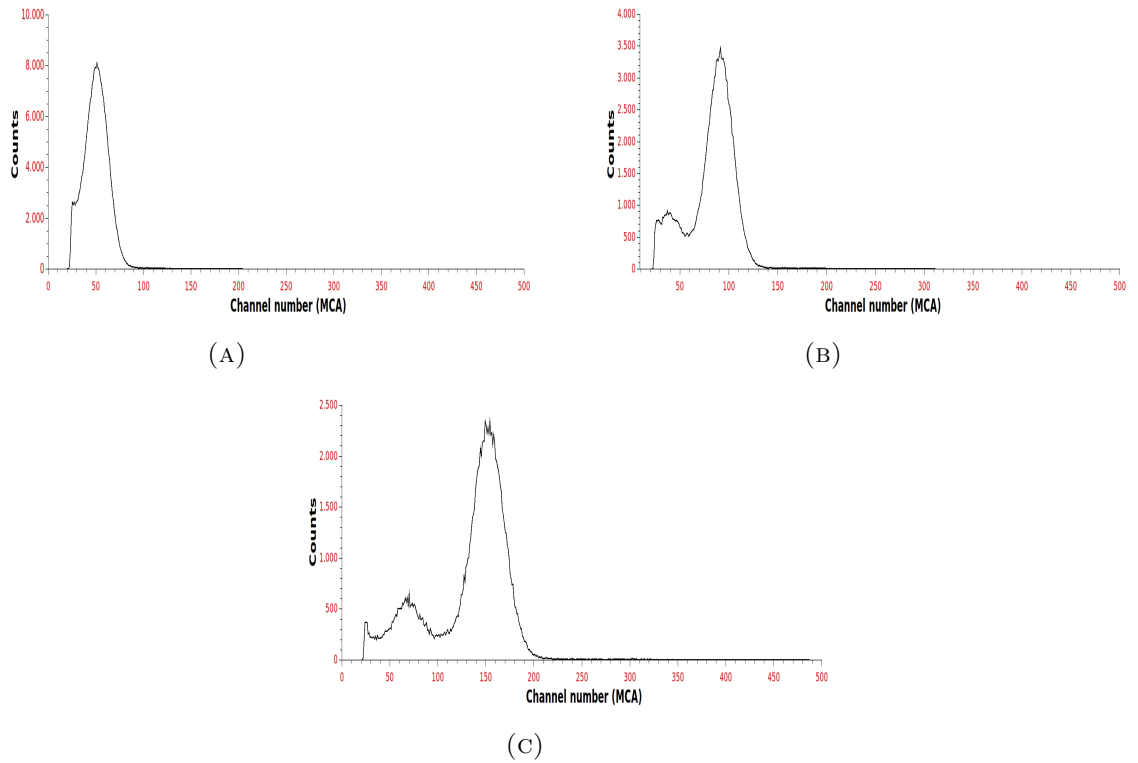
FIGURE 5.3: The MCA distributions for the second single CERN GEM. (A) the voltage difference = 350 V. (B) the voltage difference = 370 V. (C) the voltage difference = 390 V.

Voltage (V)	Peak position (MCA)	Gas gain
350	52.20 ± 0.05	7.420 ± 0.007
360	69.7 ± 0.4	9.75 ± 0.056
370	96.0 ± 0.29	13.44 ± 0.04
380	122.8 ± 0.25	17.19 ± 0.035
390	158.0 ± 0.4	22.40 ± 0.056

TABLE 5.2: The peak position and the actual gas gain for the first single CERN GEM related to each applied voltage

Voltage (V)	Peak position (MCA)	Gas gain
350	50.7 ± 0.05	7.14 ± 0.007
360	69.9 ± 0.12	9.75 ± 0.016
370	93.9 ± 0.36	13.10 ± 0.05
380	122.2 ± 0.25	17.10 ± 0.035
390	154.3 ± 0.35	21.70 ± 0.049

TABLE 5.3: The peak position and the actual gas gain for the second single CERN GEM related to each applied voltage
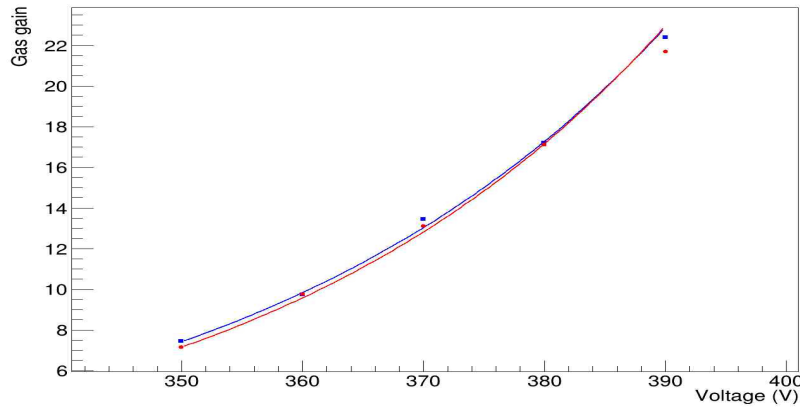
FIGURE 5.4: The gas gain for the used two CERN GEMs vs the applied voltage. The blue points represent the first GEM and the red points are for the second one.

5.1.2 Two CERN GEMs

In the second step, the combination between two CERN GEMs (Figure 5.5) is used. Figure 5.6 presents the recorded spectrum for different applied voltages and Table 5.4 shows the main peak position of the spectrum and the gas gain for each applied voltage difference. The voltage difference was the same for both GEMs. Figure 5.7 displays the exponential fitting. From the equation for the exponential fitting, we extracted the relation between the gas gain and the applied voltage on the two GEMs:

$$\text{The gas gain } = \text{ exp}((-12.24 \pm 0.0078) + (0.04745 \pm 2.13 * 10^{-5}) * \text{voltage})$$

In the next part, the gas gain for each individual GEM in the combination was estimated. The main goal is to investigate the behavior of a single GEM in case of using a combination of more than one GEM. Equation 5.1 is a simple relation to estimate the gas gain for a single GEM in case of using a combination between two **similar** GEMs. This equation can only be used when both GEMs in the combination contribute in the same way to the total gas gain.

$$\text{Gas gain}_{\text{single GEM}} = \sqrt{\text{gas gain}_{\text{two GEMs}}} \tag{5.1}$$

Table 5.5 lists the estimated gas gain for single GEM related to the applied voltage. Figure 5.8 displays the exponential fitting for the estimated gas gain. Figure 5.9 presents a comparison between the gas gain for both cases; the black points represent the estimated gas gain for a single GEM in case of using a combination between two CERN GEMs, the red points and the green represent the actual gas gain for the first and the second GEM, respectively.

Compared to the previous measurements, the CERN GEMs gave higher gas amplification in case of using combination of two GEMs than using single GEM. The difference is around $6 - 11\%$. The reason of this behavior is not clear yet and it is still under the investigation.
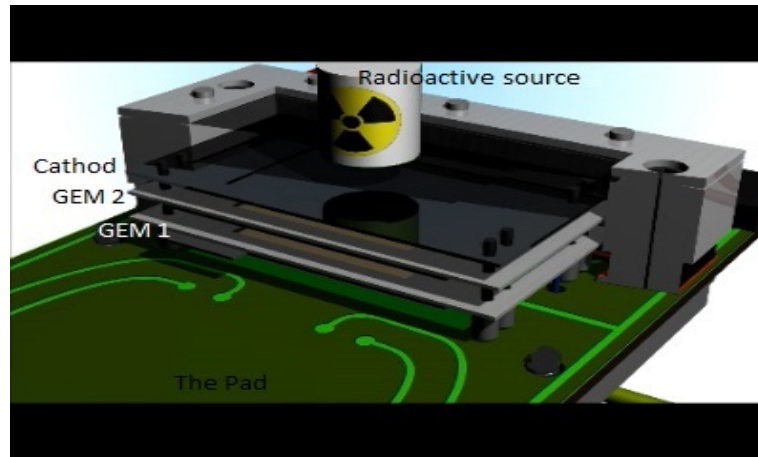
FIGURE 5.5: Setup of the test chamber

(A)

(B)

(C)
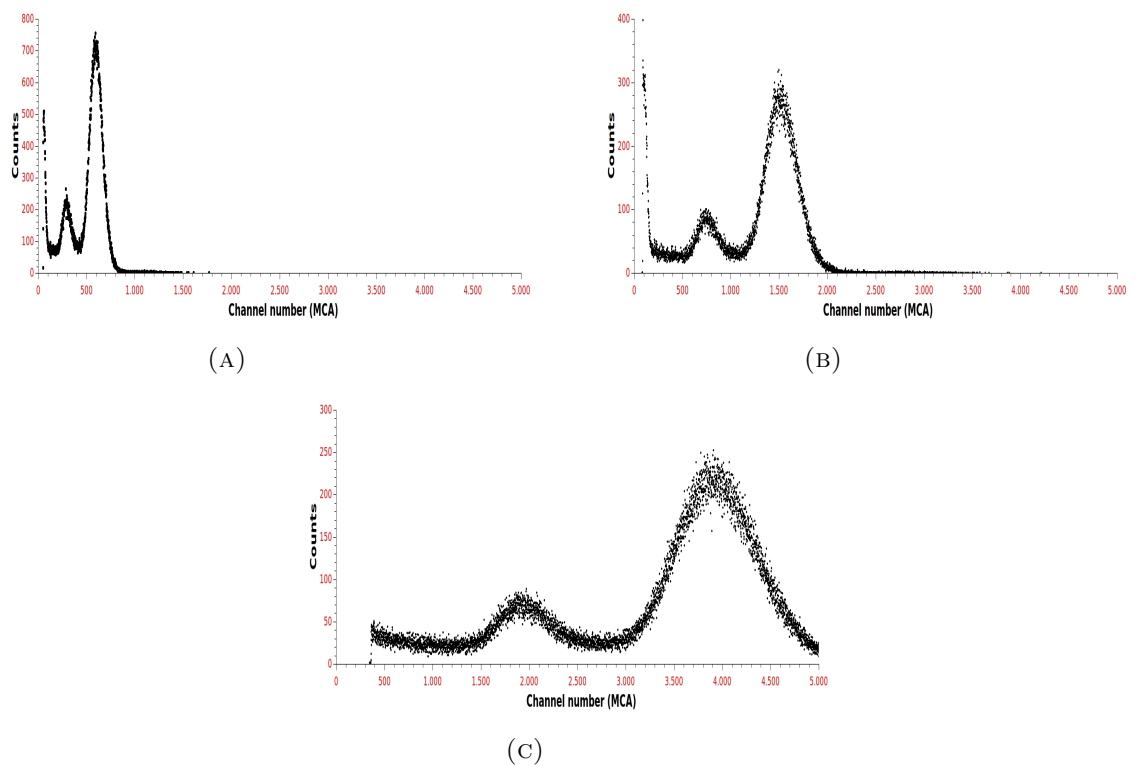
FIGURE 5.6: The MCA distributions for two CERN GEMs; (A) the voltage difference applied on each GEM = 350 V. (B) the voltage difference applied on each GEM = 370 V. (C) the voltage difference applied on each GEM = 390 V.

Voltage (V)	Peak position (MCA)	Gas gain
350	591.2 ± 0.35	82.74 ± 0.044
360	907.2 ± 0.55	126.98 ± 0.077
370	1516 ± 2	212.2 ± 0.28
380	2441 ± 1.9	341.7 ± 0.26
390	3909 ± 3.4	547.2 ± 0.42

TABLE 5.4: The peak position in the MCA and the gas gain for the combination of two CERN GEMs related to each applied voltage on the GEMs
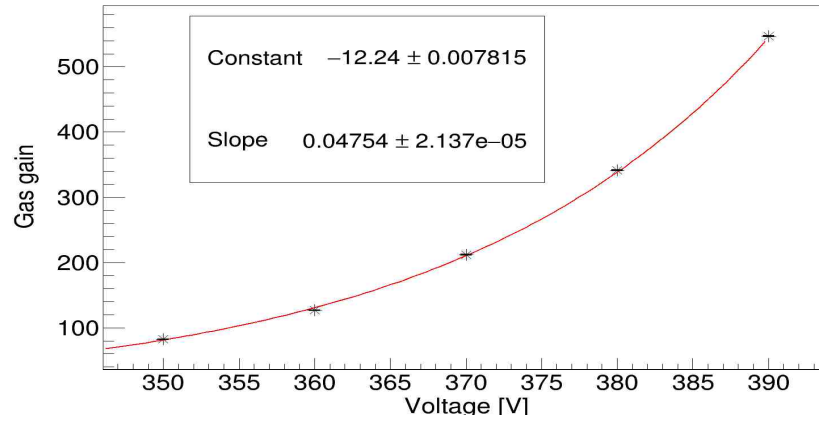
FIGURE 5.7: The gas gain for two CERN GEMs vs the applied voltage

Voltage (V)	Estimated gas gain for a single GEM
350	9.0 ± 0.20
360	11.2 ± 0.27
370	14.5 ± 0.52
380	18.4 ± 0.50
390	23.3 ± 0.64

TABLE 5.5: The estimated gas gain for single CERN GEM related to each applied voltage
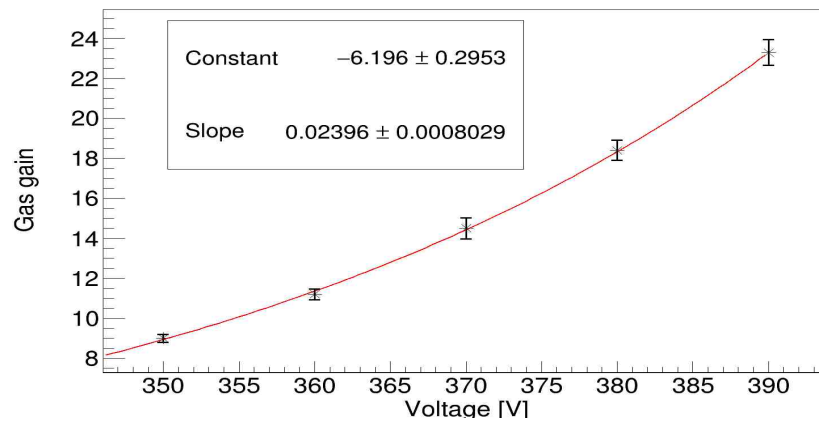
FIGURE 5.8: The estimated gas gain for a single CERN GEM vs the applied voltage
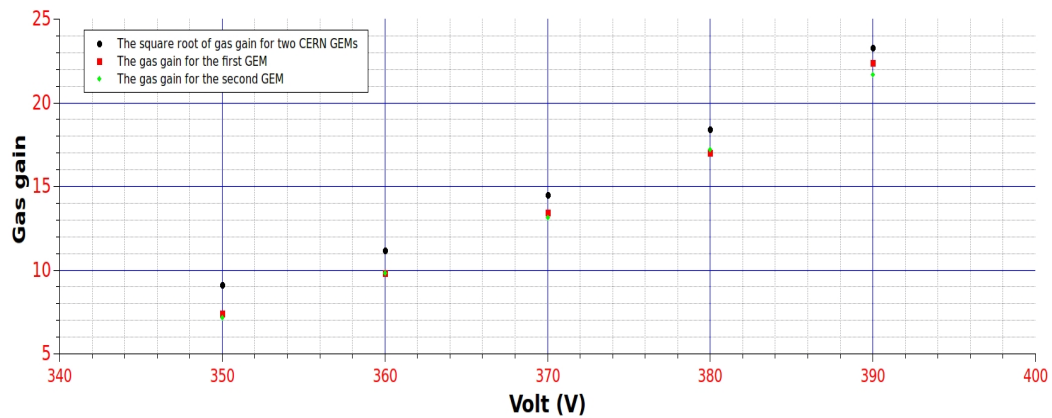
FIGURE 5.9: The estimated and actual gas gain for a single CERN GEM

5.2 The ceramics GEMs

A ceramic GEM is a new aspect for gaseous amplification process. The vital reason to use these GEMs is due to the characteristics of the ceramic material. The heat capacity, hardness and the resistance against the electrical sparks nominate the ceramic GEM to be the reliable technique to reach the required results. Table 5.6, Figure 5.10 and Figure 5.11 show the parameters and the geometry of the ceramic GEMs. Figure 5.12 shows a microscopic picture for one of the holes in the ceramic GEMs. In the next part, the performance of the ceramic GEMs is investigated. By following the same procedure, the actual gas gain for a single ceramic GEM is measured. Then, a combination of two ceramic GEMs is examined and the single ceramic GEM gas gain is estimated.

Size	90 mm x 90 mm
Thickness	0.12 mm
Conductor	Silver and two layers (Nickel and Gold)
Insulator	The ceramic
Holes shape	Cylindrical
Holes diameter	200 μm
Distance between holes	180 μm
Ceramic body	Glass-Alumina composite

TABLE 5.6: Ceramic GEMs specifications
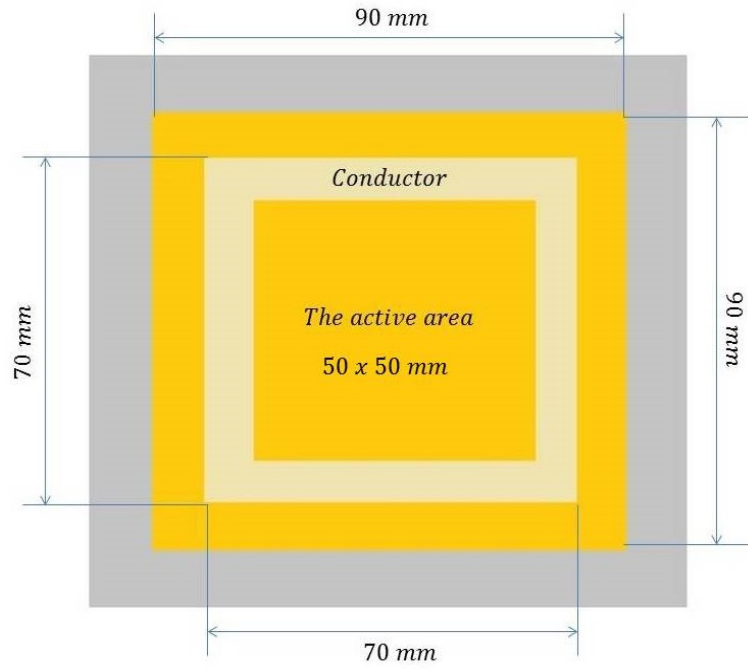
FIGURE 5.10: The Geometry of the ceramic GEM
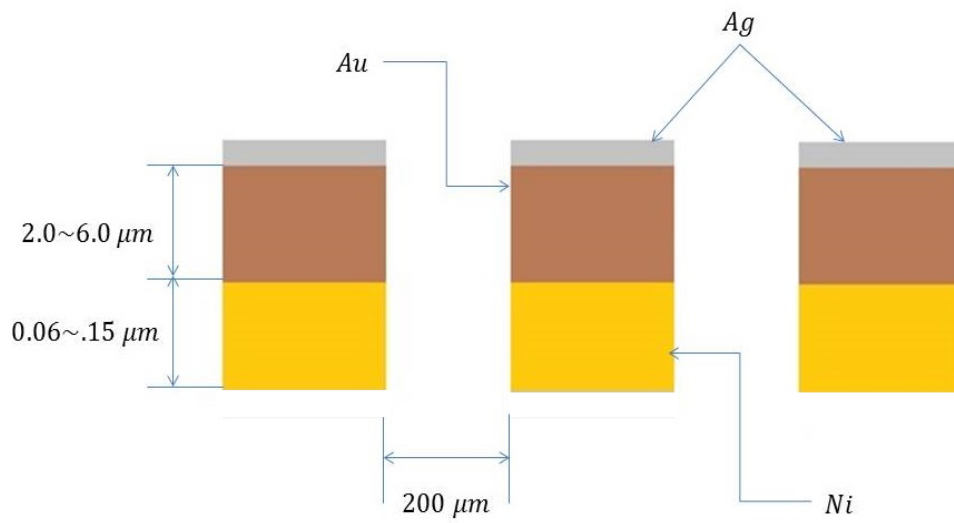
FIGURE 5.11: The layer of the conductor material
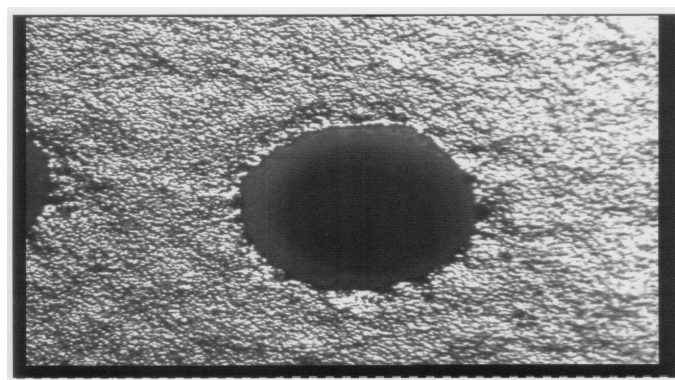
FIGURE 5.12: Microscopic picture for a ceramic GEM's hole

5.2.1 One Ceramic GEM

The ceramic was glued first to a plastic and then to a ceramic frames, as shown in Figure 5.13. This Geometry of layers was designed to fit the geometry of the test chamber. Also, the usage of two frames increases the strength of the ceramic GEM.
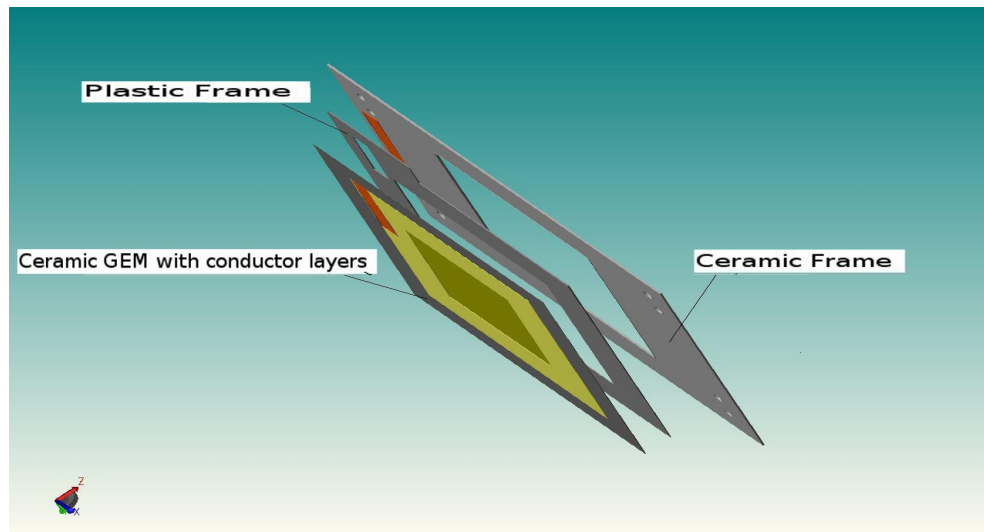
FIGURE 5.13: The geometry of the layers

The next step is to investigate the demeanor for a single ceramic GEM individually. By applying the same procedure, a single ceramic GEM is exposed to the source and the applied voltage is changed. Figure 5.14 displays the MCA peaks for different applied voltages[2]. Table 5.7 lists the main peak position and the actual gas gain related to the applied voltage on a single ceramic GEM. Figure 5.15 is the exponential fitting for the actual gas gain. The relation between the gas gain and the applied voltage on a single ceramic GEM is:

$$\text{The gas gain} \ = \ \exp((-10.35 \pm 0.023) + (0.02111 \pm 3.776 * 10^{-5}) * \text{voltage})$$

Compared to the CERN GEMs one can see that due to the larger thickness a larger voltage difference is needed to reach the same gas gain.

---

[2] The first peak was expected to appear for voltage difference around 700 V, since the thickness of the ceramic GEM is twice as long as that of a CERN GEM. The first peak appeared around voltage difference = 580 V, which gives a good sign and motivation to consider this new aspect.

(A)

(B)

(C)
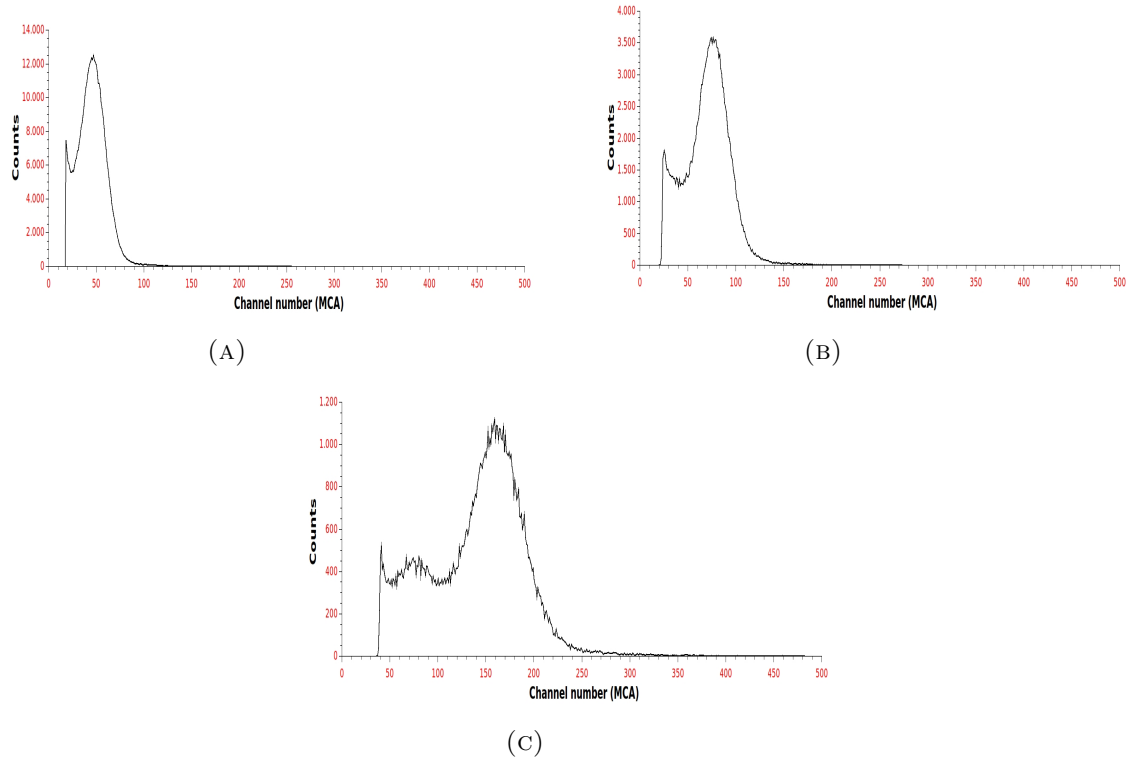
FIGURE 5.14: The MCA distributions for a single ceramic GEM ; (A) the voltage difference = 580 V. (B) the voltage difference = 600 V. (C) the voltage difference = 640 V.

Voltage (V)	Peak position (MCA)	Gas gain
580	46.54 ± 0.086	6.51 ± 0.012
590	60.2 ± 0.15	8.42 ± 0.021
600	75.8 ± 0.29	10.61 ± 0.026
610	92.7 ± 0.13	12.97 ± 0.018
620	112.1 ± 0.16	15.69 ± 0.022
630	135.6 ± 0.22	18.98 ± 0.030
640	161.2 ± 0.32	22.56 ± 0.044

TABLE 5.7: The main peak position and the actual gas gain related to each applied voltage for a single ceramic GEM
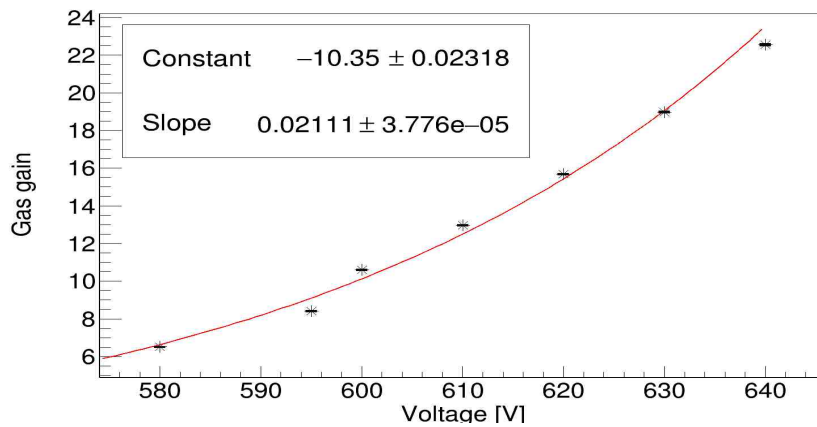
FIGURE 5.15: The actual gas gain for a single ceramic GEM vs the applied voltage

5.2.2 Two Ceramic GEMs

For the same experimental configurations, a stack of two ceramic GEMs is exposed to our source and the applied voltage on the GEMs is changed. Figure 5.16 shows the MCA distribution for different applied voltages and Table 5.8 lists the main peak position and the gas gain for each applied voltage . Figures 5.17 show the exponential relationship between the applied voltages versus the ceramic gas gain for each voltage difference on the ceramic GEMs, respectively. The relation between the gas gain and the applied voltage on two ceramic GEMs is:

$$\text{The gas gain } = \exp((-18.51 \pm 0.02126) + (0.03834 \pm 3.701 * 10^{-5}) * \text{voltage})$$

Then, the data from the ceramic combination is used to estimate the gas gain for a single ceramic GEM. From equation 5.1, the estimated gas gain for a single ceramic GEM is calculated. The values of estimated gas gains are listed in Table 5.8. Figure 5.18 represents the exponential relationship between the estimated gas gain for a single ceramic GEM and the related applied voltage.

Furthermore, Figure 5.19 shows the comparison between the estimated gas gain for a single ceramic GEM (black points) and the actual gas gain for single ceramic GEM (red points).

For the CERN GEMs a good agreement between the results from the measurements with a single and two GEMs is found. In this case the results from the two GEMs give slightly lower results than those of the single GEM.

In brief, comparing the relation between the gas gain and the applied voltage for CERN and ceramic GEMs. One can observe that in case of using a single GEM the exponential

relation of CERN GEM is better than the one of the ceramic. However, for two GEMs, the ceramic GEMs give a smother exponential curve than CERN GEMs.

(A)

(B)

(C)
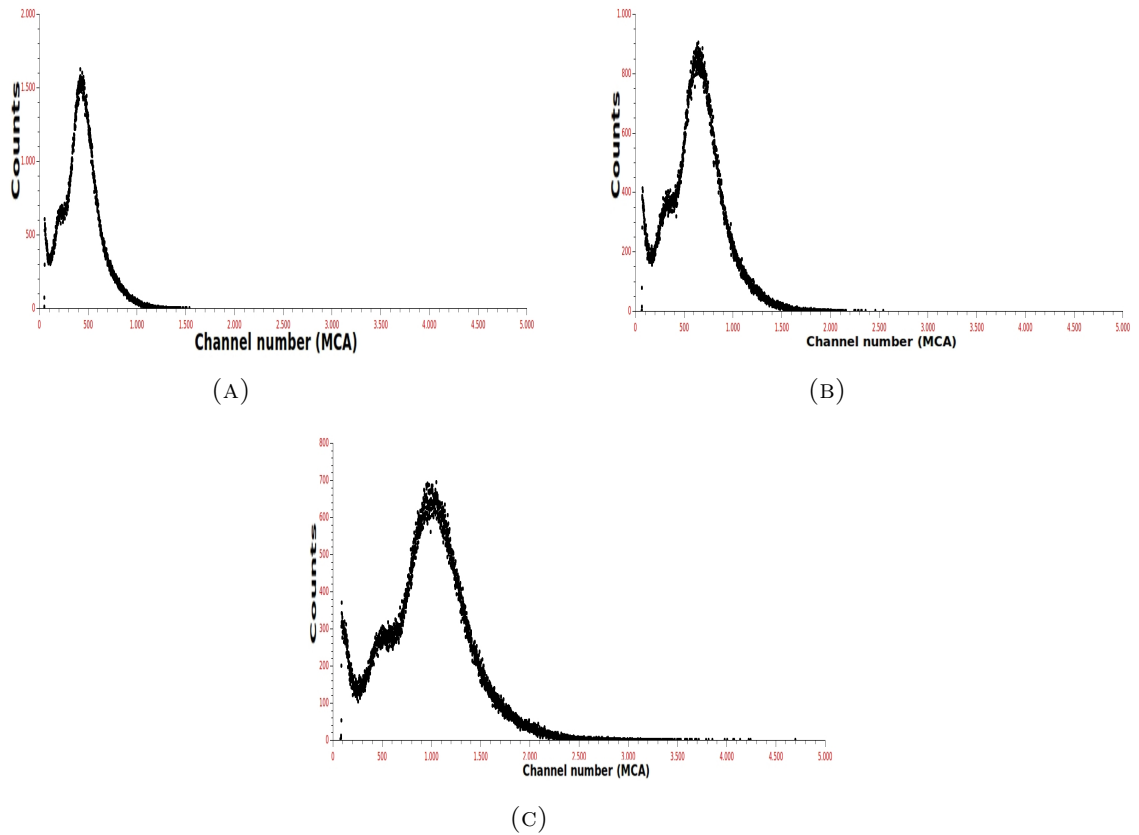
FIGURE 5.16: The MCA distributions for two ceramic GEMs ; (A) the voltage difference applied on each ceramic GEM = 590 V. (B) the voltage difference applied on each ceramic GEM = 600 V. (C) the voltage difference applied on each ceramic GEM = 610 V.
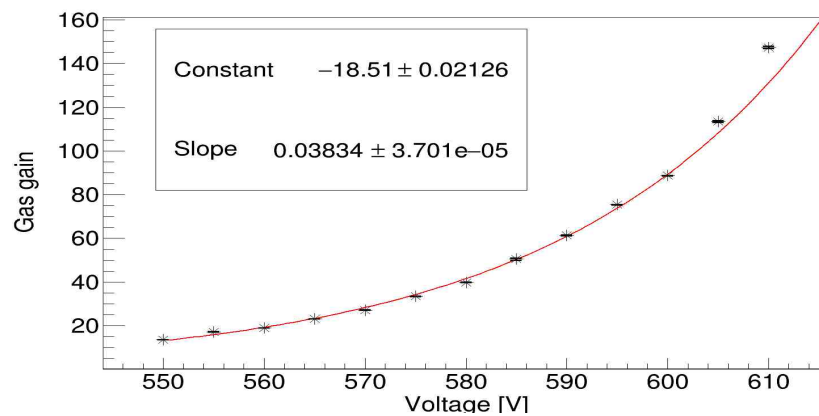
FIGURE 5.17: The ceramic gas gain for each applied voltage on the ceramic GEMs

Voltage (V)	Peak position (MCA)	Gas gain	Estimated gas gain for a single GEM
550	97.3 ± 0.18	13.62 ± 0.02	3.6 ± 0.14
555	122.7 ± 0.41	17.17 ± 0.057	4.1 ± 0.23
560	135.6 ± 0.26	18.98 ± 0.036	4.3 ± 0.18
565	165.3 ± 0.32	23.14 ± 0.044	4.8 ± 0.20
570	193.9 ± 0.35	27.14 ± 0.049	5.2 ± 0.22
575	238.8 ± 0.51	33.43 ± 0.071	5.7 ± 0.26
580	284.5 ± 0.62	39.83 ± 0.086	6.3 ± 0.29
585	361 ± 3.6	50.5 ± 0.50	7.1 ± 0.70
590	439 ± 1.4	61.4 ± 0.19	7.8 ± 0.43
595	539 ± 1.1	75.4 ± 0.15	8.6 ± 0.38
600	634 ± 1.2	88.7 ± 0.16	9.4 ± 0.40
605	811 ± 3.4	113.5 ± 0.47	10.6 ± 0.68
610	1053 ± 3.8	147.4 ± 0.53	12.1 ± 0.72

TABLE 5.8: The peak position in the MCA related to each applied voltage on the GEMs
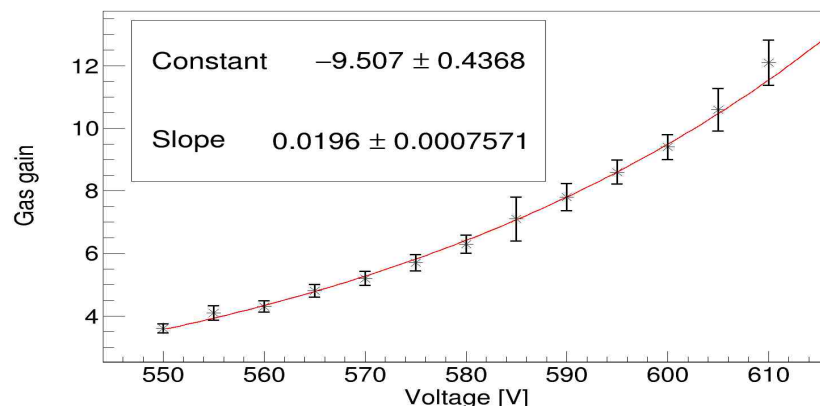
FIGURE 5.18: The estimated gas gain for single ceramic GEM related to each applied voltage
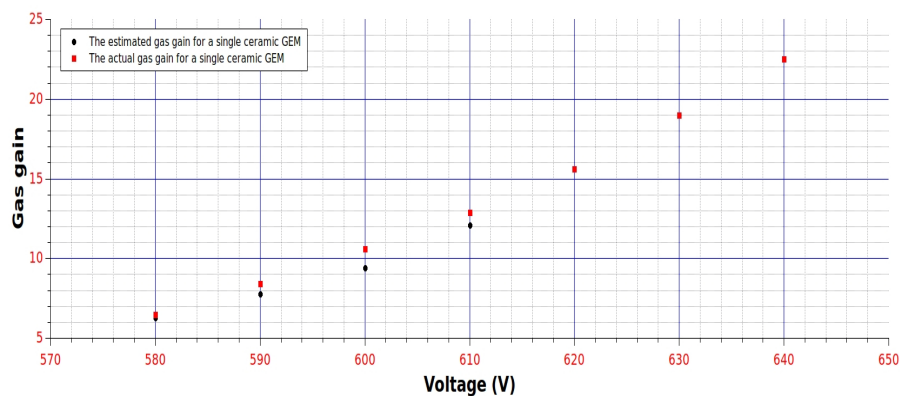
FIGURE 5.19: The estimated and actual gas gain for a single ceramic GEM

5.3 CERN and Ceramic combination

Thus, a combination between one CERN GEM and one ceramic GEM is used. There are two prospects, the first is ceramic GEM on top (Figure 5.20) and the second is CERN GEM on top (Figure 5.21). The experimental procedure is as following:

- Choose one of the two GEMs arrangements.

- Expose the combination to the source.

- Apply a fixed voltage on one of these GEMs and change the applied voltage on the another GEM. That means, the GEM with fixed voltage generates a fixed gas gain while the another GEM generates different gas gains related to the applied voltages.

- Use the previous data to determine the gas gain related to the fixed applied voltage voltage.

- Measure the gas gain for the combination and calculate the gas gain for the GEM with the variable applied voltage- see below.

- For the same arrangement, change the fixed applied voltage to be the variable one and the variable to be the fixed.

- Measure the gas gain for the new case.

- Reconstruct your setup to the second GEMs arrangement.

- Execute the same procedure.
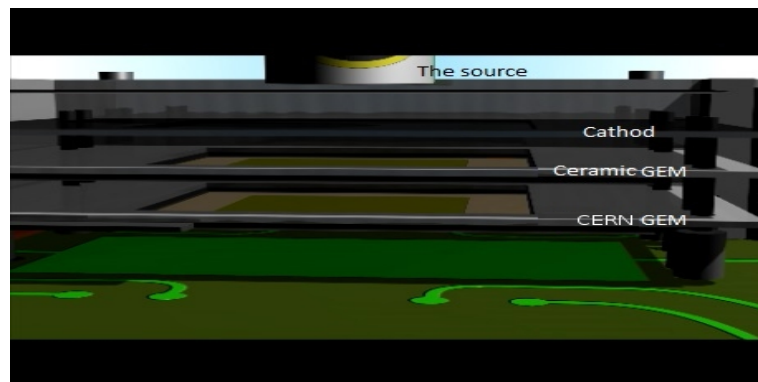
FIGURE 5.20: The arrangement of the GEMs in case of ceramic one on top

In the following part, we discuss how to calculate the gas gain for a single GEM in case of combination between two different GEMs. Equations 5.2 and 5.3 are the relations between the total gas gain for the combination and the gas gain for each single
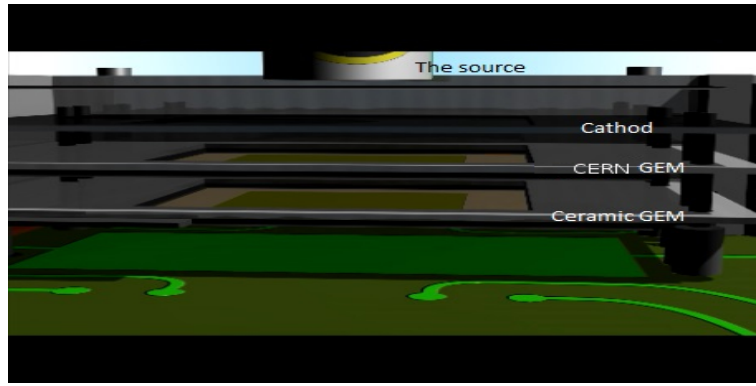
FIGURE 5.21: The arrangement of the GEMs in case of CERN one on top

GEM. Where, the total gas gain is the output of the combination of the two GEMs and (gas gain$_\text{bottom/top GEM}$) is substituted for the GEM with fixed applied voltage from its previous results. Then the gas gain for the second GEM is estimated.

$$\text{Gas gain}_\text{top GEM} = \frac{\text{the total gas gain}}{\text{Gas gain}_\text{bottom GEM}} \tag{5.2}$$

$$\text{Gas gain}_\text{bottom GEM} = \frac{\text{the total gas gain}}{\text{Gas gain}_\text{top GEM}} \tag{5.3}$$

5.3.1 Ceramic GEM on top

The arrangement with ceramic GEM on the top (Figure 5.20) is used.The first step is to fix the voltage on the CERN GEM and vary it on the ceramic one. Consequently, the performance for the ceramic GEM in this combination can be examined. Then, the opposite manner is repeated.

5.3.1.1 Fixed voltage on the CERN GEM

The voltage difference on the CERN GEM is fixed during the experiment in order to generate a constant gas gain (in this case V$_\text{CERN}$ = 350 V). The variation of the applied voltage on the ceramic spawns a shifting in the main peak position thats means changing in the gas gain for the system. Figure 5.22 displays examples for the MCA spectra for different applied voltages on the ceramic GEM. Table 5.9 gives the values for the main peak position and the total gas gain of the combination related to applied voltage on the ceramic GEM. Also, Figure 5.23 shows the exponential fitting for the total gas gain vs. the applied voltage on the ceramic GEM. The exponential relation between the

estimated gas gain for the ceramic GEM and the applied voltage is as following:

The estimated gas gain $= \exp((-7.85 \pm 0.04742) + (0.01767 \pm 8.423 * 10^{-5}) * \text{voltage})$

Accordingly, the gas gain for the ceramic GEM is estimated by using equation 5.2. As measured in section 5.1.1, the gas gain related to voltage difference 350 V on the CERN GEM (we used the second CERN GEM in this combination) is:

$$\text{Gas gain}_{\text{CERN}}^{350 \, \text{V}} = 7.14 \pm 0.007$$

Table 5.9 lists the value for the estimated gas gain for the ceramic GEM in case of combination between one CERN GEM (with fixed voltage) and one ceramic GEM (with variable voltage). As shown in Figure 5.24, the estimated gas gain for the ceramic GEM (the blue points) and the fixed gas gain for CERN GEM (red points). .

(A)

(B)

(C)
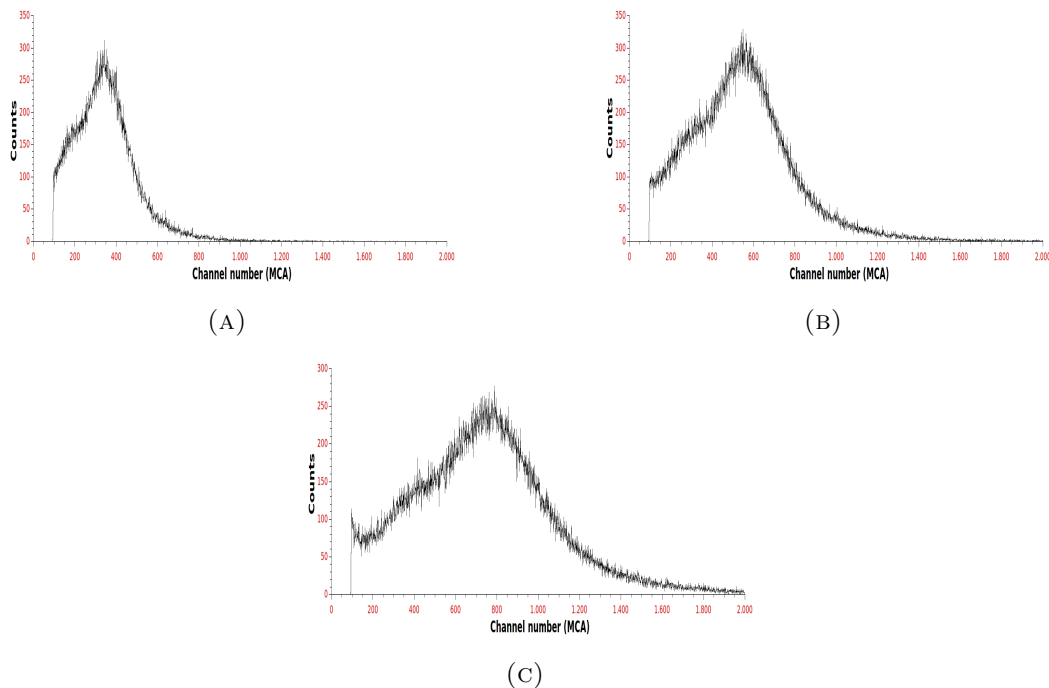
FIGURE 5.22: The MCA distributions for combination between one ceramic GEM and one CERN GEM- the constant applied voltage on the CERN GEM for all cases = 350 V ; (A) the voltage difference applied on the ceramic GEM = 550 V. (B) the voltage difference applied on the ceramic GEM = 580 V. (C) the voltage difference applied on the ceramic GEM = 600 V.

Voltage (V)	Peak position (MCA)	Total gas gain	Estimated gas gain for the ceramic GEM
550	330 ± 4.8	46.2 ± 0.59	6.4 ± 0.14
560	395 ± 2.5	55.3 ± 0.34	7.74 ± 0.18
570	481 ± 2.0	67.34 ± 0.31	9.43 ± 0.22
580	448 ± 2.1	74.0 ± 0.32	10.94 ± 0.29
590	652 ± 3.7	91.28 ± 0.50	12.78 ± 0.43
600	773 ± 4.1	108.22 ± 0.53	15.15 ± 0.40

TABLE 5.9: The peak position in the MCA, the total gas gain and the estimated ceramic gas gain related to each applied voltage on the ceramic GEM - with CERN voltage = 350 V
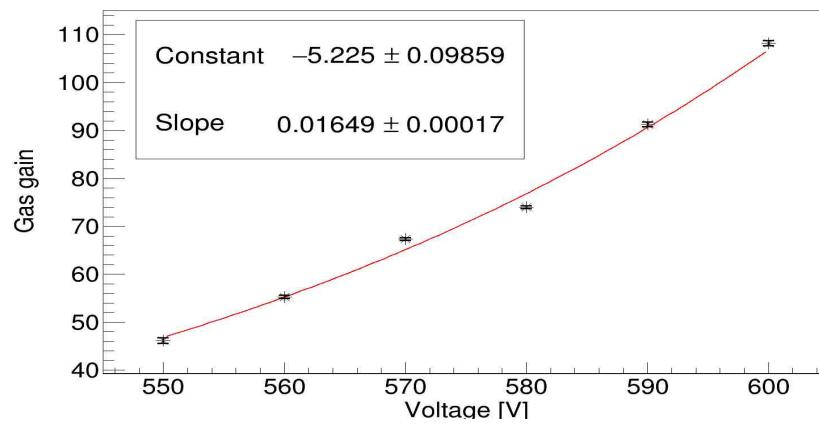
FIGURE 5.23: The exponential relation between the total gas gain for the combination and the applied voltage on the ceramic GEM
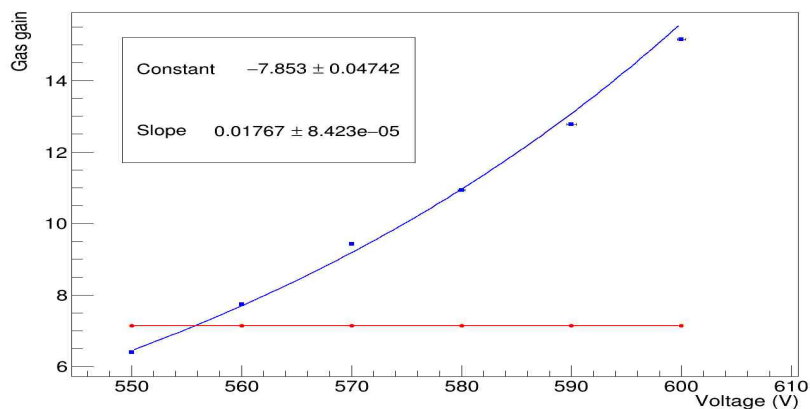
FIGURE 5.24: The relation between the estimated gas gain for the ceramic GEM and the applied voltage on it (the blue line). The red line represents the fixed gas gain for the CERN GEM related to applied voltage =350 V

5.3.1.2 Fixed voltage on the ceramic GEM

Furthermore, the applied voltage on the ceramic GEM is fixed to be 580 V and changing the applied voltage on the CERN GEM. Figures 5.25 and 5.26 show the MCA spectra and the total gas gain for different applied voltages, respectively. Table 5.10 lists the values for the MCA main peak position, the total gas gain and the estimated gas gain for the CERN GEM vs the applied voltage on it.

(A)

(B)

(C)
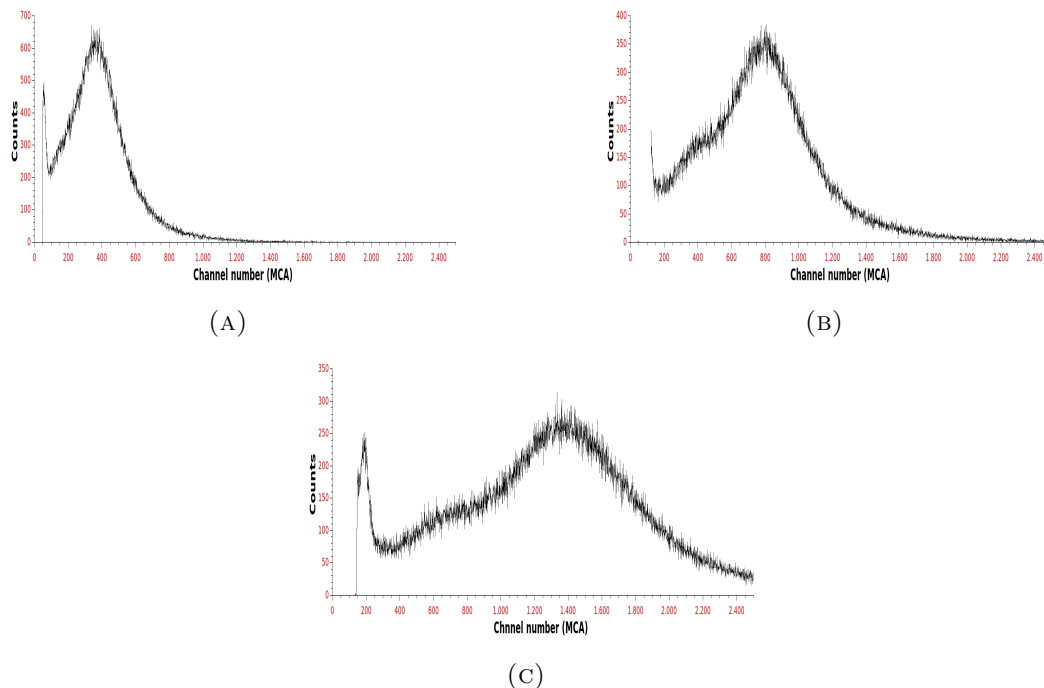
FIGURE 5.25: The MCA distributions for combination between one ceramic GEM and one CERN GEM- the fixed applied voltage on the ceramic GEM for all cases = 580 V ; (A) the voltage difference applied on the CERN GEM = 350 V. (B) the voltage difference applied on the CERN GEM = 370 V. (C) the voltage difference applied on the CERN GEM = 390 V.

Voltage (V)	Peak position (MCA)	Total gas gain	Estimated gas gain for the CERN GEM
350	358 ± 2.4	50.4 ± 0.33	7.7 ± 0.05
360	600 ± 4.1	84.0 ± 0.57	12.9 ± 0.08
370	789 ± 2.6	110.4 ± 0.36	16.9 ± 0.05
380	1054 ± 3.5	147.5 ± 0.49	22.5 ± 0.07
390	1379 ± 3.5	193.0 ± 0.49	29.6 ± 0.07

TABLE 5.10: The main peak position in the MCA and the total gas gain for the combination related to each applied voltage on the ceramic GEM - with fixed ceramic voltage = 580 V

Similarly, using equation 5.3 to estimate the gas gain for the CERN GEM in this combination. From section 5.2 the gas gain for the single ceramic GEM related to voltage

difference 580 V is:

$$\text{Gas gain}^{580\text{ V}}_{\text{Ceramic}} = 6.51 \pm 0.012V$$

Figure 5.27 displays the estimated gas gain for the CERN (the blue line) and the fixed gas gain for the ceramic GEM related to 580 V (the red line). The exponential relation between the estimated gas gain for CERN GEM and the applied voltage is:

The estimated gas gain $= \exp((-9.967 \pm 0.005186) + (0.03453 \pm 1.402 * 10^{-5}) * \text{voltage})$
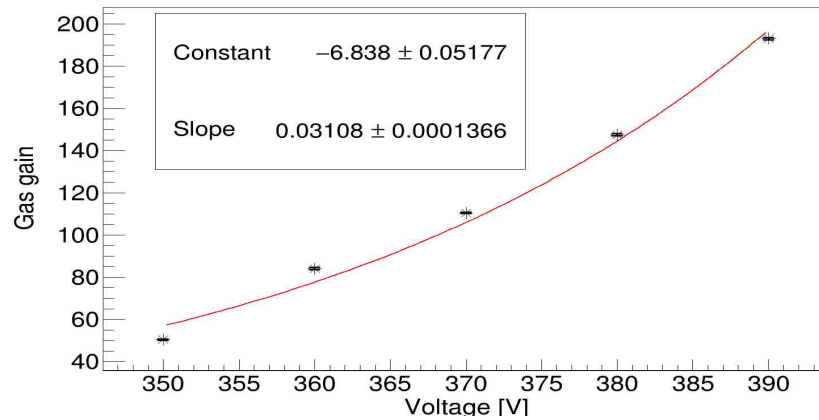
FIGURE 5.26: The exponential relation between the total gas gain for the combination and the applied voltage on the CERN GEM
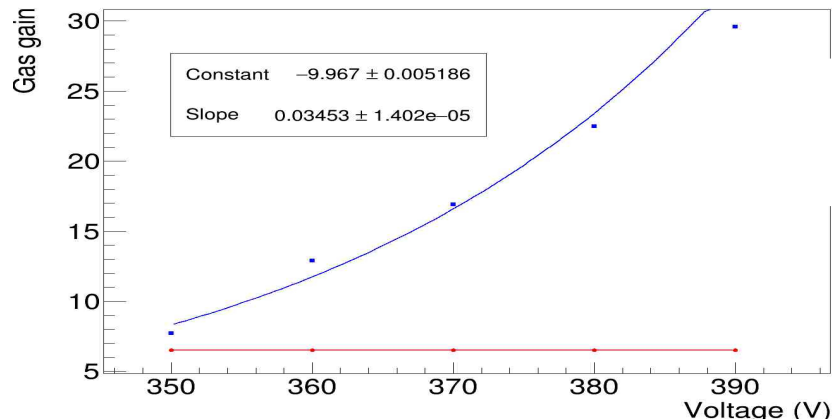
FIGURE 5.27: The relation between the estimated gas gain for the CERN GEM and the applied voltage on it (the blue line). The red line represents the fixed gas gain for the ceramic GEM related to applied voltage =580 V

5.3.2 CERN GEM on top

Likewise, the second GEMs arrangement is used (Figure 5.21) for two cases; fixed voltage on CERN GEM with variable voltage on the ceramic one then the opposite procedure.

5.3.2.1   Fixed voltage on the CERN GEM

Here, the CERN GEM voltage is fixed to be 350 V and expose our system to the radioactive source. Figure 5.28 displays the different MCA distributions for different applied voltage on the ceramic GEM. Figures 5.29 and 5.30 show the exponential relation for the total gas gain and the estimated gas gain, respectively. The exponential relation between the estimated gas gain for the ceramic GEM and the applied voltage is:

The estimated gas gain $= \exp((-7.18 \pm 0.05543) + (0.01707 \pm 9.847 * 10^{-5}) * \text{voltage})$

Table 5.11 lists the peak position, the total gas gain and the estimated gas gain for each applied voltage.

(A)

(B)

(C)
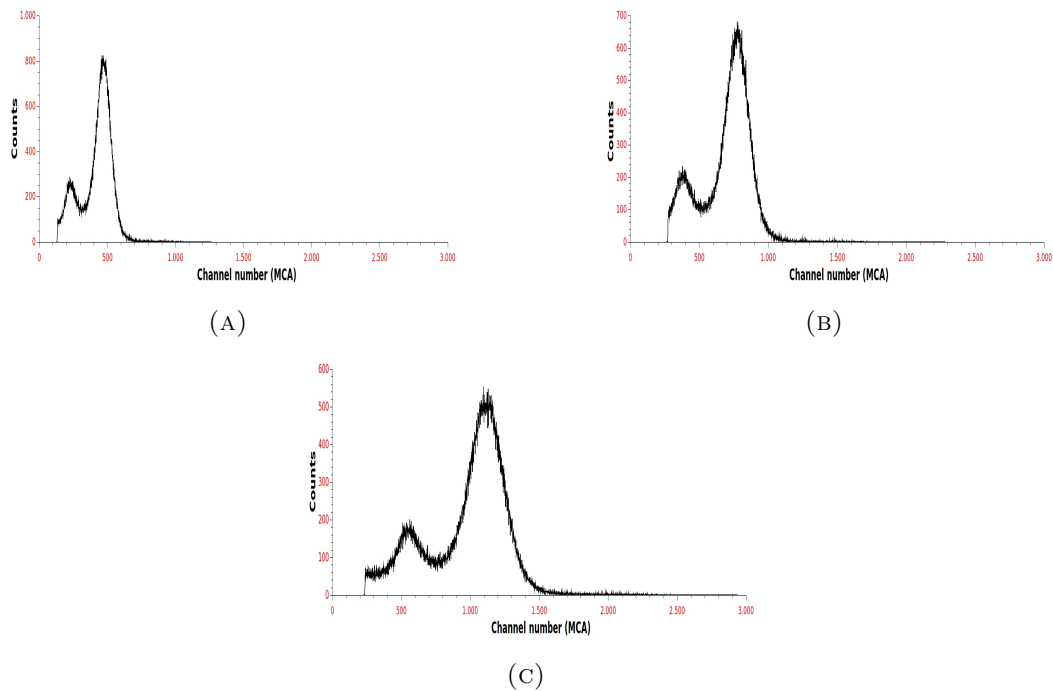
FIGURE 5.28: The MCA distributions for combination between one ceramic GEM and one CERN GEM- the fixed applied voltage on the CERN GEM for all cases = 350 V ; (A) the voltage difference applied on the CERN GEM = 550 V. (B) the voltage difference applied on the CERN GEM = 580 V. (C) the voltage difference applied on the CERN GEM = 600 V.

Voltage (V)	Peak position (MCA)	Total gas gain	Estimated gas gain for the ceramic GEM
550	471.4 ± 0.51	65.58 ± 0.07	9.18 ± 0.04
560	550.8 ± 0.46	76.56 ± 0.06	10.7 ± 0.9
570	660.3 ± 0.25	91.78 ± 0.03	12.8 ± 0.89
580	775.7 ± 0.78	107.8 ± 0.1	15 ± 1.2
590	945.9 ± 0.93	131.4 ± 0.12	18.4 ± 0.63
600	1116 ± 1.3	155.1 ± 0.18	21.7 ± 0.35

TABLE 5.11: The peak position in the MCA, the total gas gain and the estimated ceramic gas gain related to each applied voltage on the ceramic GEM - with CERN voltage = 350 V
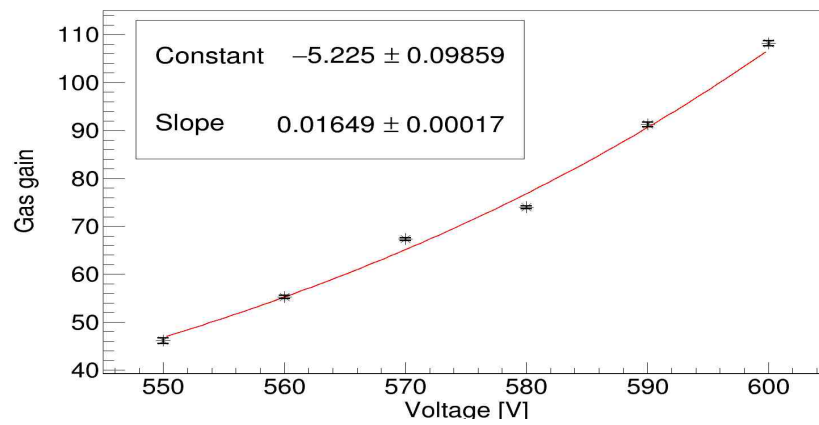
FIGURE 5.29: The relation between the total gas gain for the combination and the applied voltage on the ceramic GEM
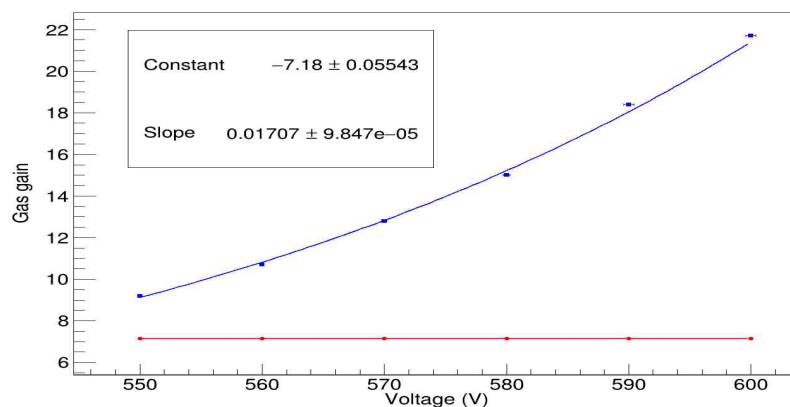
FIGURE 5.30: The relation between the estimated gas gain for the ceramic GEM and the applied voltage on it (the blue line). The red line represents the fixed gas gain for the CERN GEM =350 V

5.3.2.2 Fixed voltage on the ceramic GEM

In like manner, fixing the applied ceramic GEM (580 V) and changing the applied voltage on the CERN GEM. Figure 5.31 shows the MCA spectra for many different voltages. Figures 5.32 and 5.33 show the total gas gain and the estimated gas gain, respectively. Table 5.12 lists all these values. The exponential relation between the estimated gas gain for the CERN GEM and the applied voltage is:

$$\text{The gas gain} \ = \ \exp((-4.582 \pm 0.02126) + (0.0213 \pm 4.961 * 10^{-5}) * \text{voltage})$$

(A)

(B)

(C)
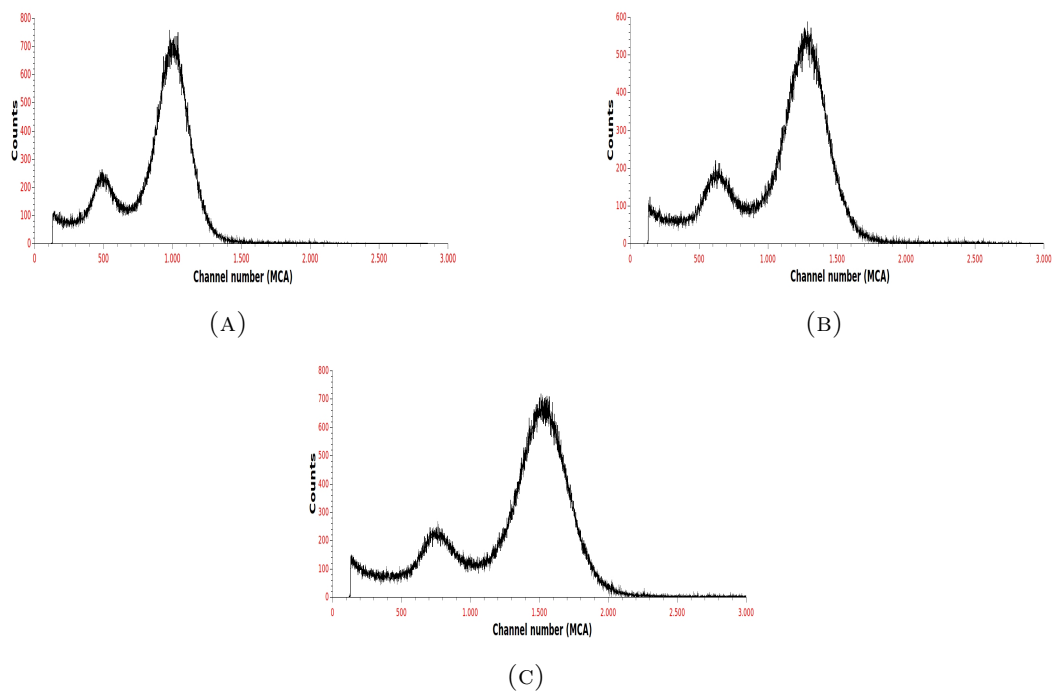
FIGURE 5.31: The MCA distributions for combination between one ceramic GEM and one CERN GEM- the fixed applied voltage on the ceramic GEM for all cases = 580 V ; (A) the voltage difference applied on the CERN GEM = 360 V. (B) the voltage difference applied on the CERN GEM = 370 V. (C) the voltage difference applied on the CERN GEM = 380 V.

Voltage (V)	Peak position (MCA)	Total gas gain	Estimated gas gain for CERN GEM
360	1005.3 ± 0.79	139.7 ± 0.10	21.41 ± 0.01
370	1322 ± 2.7	183.7 ± 0.37	28.21 ± 0.05
380	1564 ± 2.7	217.3 ± 0.37	33.37 ± 0.05
390	1861 ± 3.6	285.6 ± 0.50	39.72 ± 0.07

TABLE 5.12: The main peak position in the MCA and the total gas gain for the combination related to each applied voltage on the ceramic GEM - with fixed ceramic voltage = 580 V
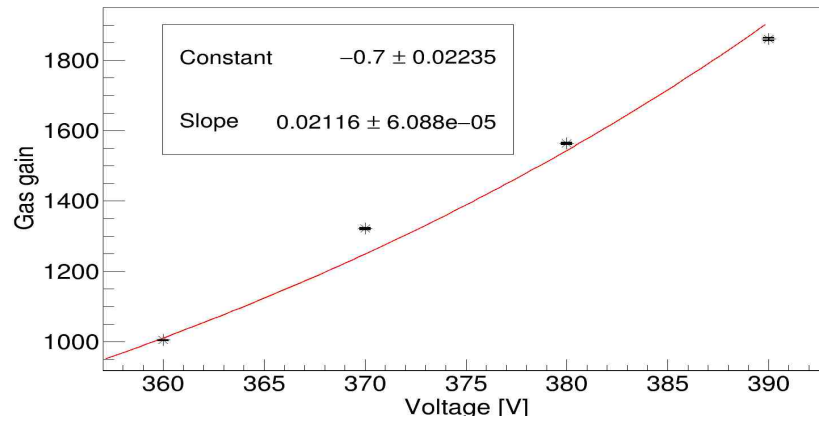
FIGURE 5.32: The relation between the total gas gain for the combination and the applied voltage on the CERN GEM
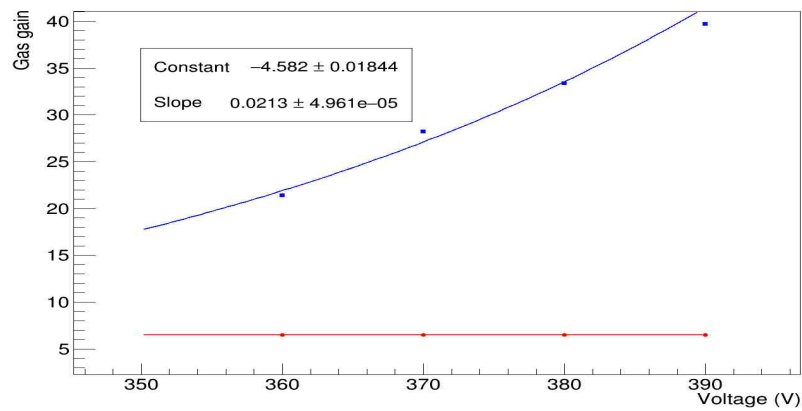
FIGURE 5.33: The relation between the estimated gas gain for the CERN GEM and the applied voltage on it (the blue line). The red line represents the fixed gas gain for the ceramic GEM related to applied voltage =580 V

5.4 Energy resolution

In brief, energy resolution is considered to be a measurement of monochromaticity of the detector. As an illustration, imagine a bunch particles have an energy E. They will be reconstructed with a different energy. This energy measured in the detector has a Gaussian distribution around the mean value $\bar{E}$. The value of the sigma parameter of the distribution is the gauge of the energy resolution. In other words, the smaller the sigma the higher the energy resolution and the bigger the sigma the lower the energy resolution. Oftenly, the full width at half maximum (FWHM) is preferred rather than the sigma. While, the distribution could be not only Gaussian but also Lorentzian or a mixture. Figure 5.34 shows the parameters of the Gaussian distribution. Energy resolution can be calculated as following;

$$\text{Energy resolution} = \frac{\text{ch}_2 - \text{ch}_1}{\text{ch}_0} = \frac{\text{FWHM}}{\text{ch}_0} \tag{5.4}$$

where ch_1 and ch_2 are the number channel at the half maximum count of the peak and ch_0 is the channel number of the maximum count of the peak.
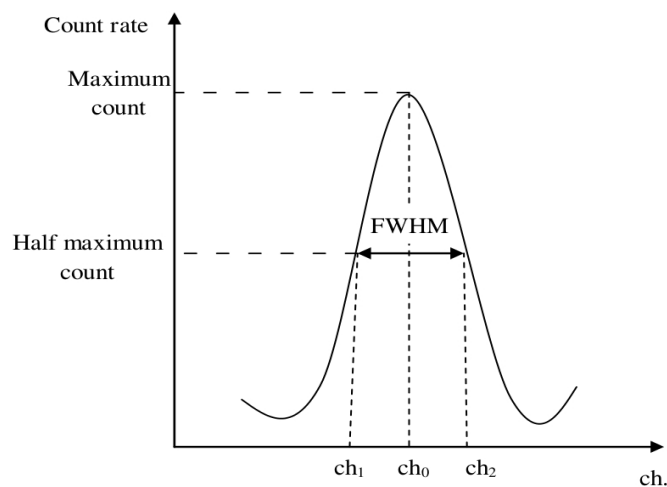
FIGURE 5.34: The gaussian distribution

Under those circumstances, we compare the energy resolution for all previous setups, i.e. for a single GEM, two GEMs of the same kind and combination of two different GEMs.

Single CERN GEM: Figure 5.35 displays the Gaussian fitting for the spectrum measured by a single CERN GEM for voltage difference 350 V (Figure 5.35a) and 390 V (Figure 5.35b). The attached table represents the parameters of this fitting, where (xc) is the channel number for the highest count. Table 5.13 lists the energy resolution and the

FWHM for different applied voltages and Figure 5.36 shows the energy resolution vs the voltage. The energy resolution decreases with increasing the voltage difference and consequently with increasing the gain.

Voltage (V)	FWHM	Energy resolution
350	23.4	46.2%
360	29.7	42.6 %
370	31.75	33%
380	35.04	28.5%
390	36.4	23.9 %

TABLE 5.13: The energy resolution and the FWHM vs the voltage for a single CERN GEM
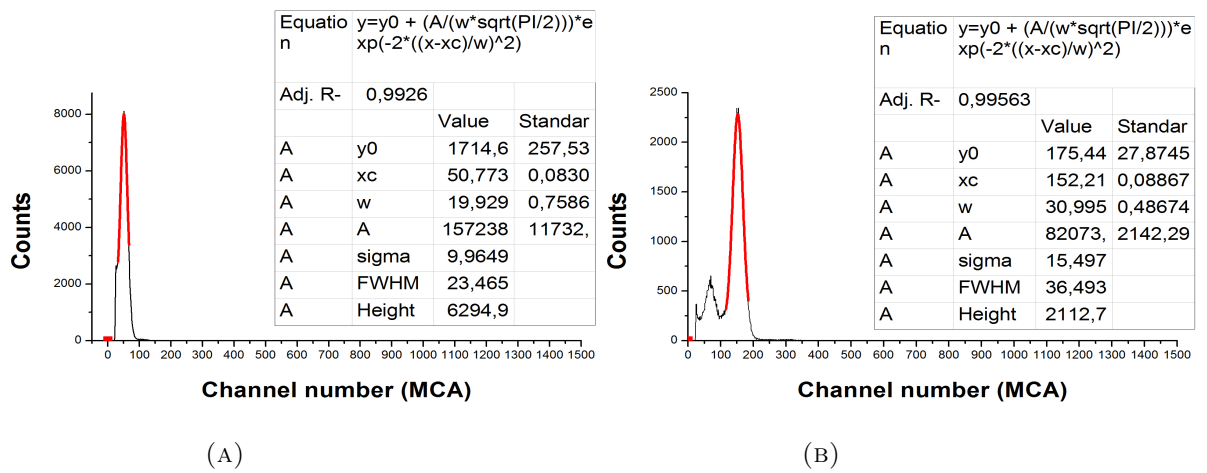
FIGURE 5.35: Gaussian fitting for a single CERN GEM, (A) for voltage difference 350 V and (B) for voltage difference 390 V.
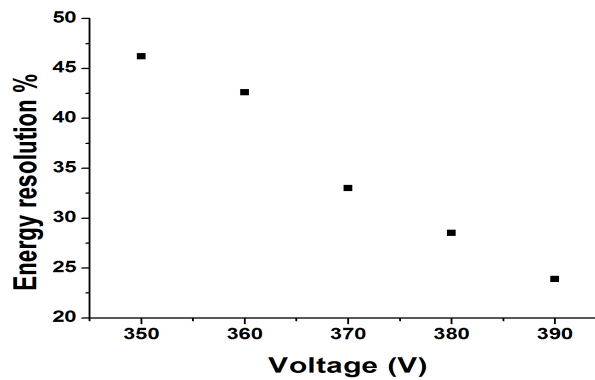
FIGURE 5.36: Energy resolution vs applied voltage for a single CERN GEM

Two CERN GEMs: Figure 5.37 displays the Gaussian fitting for the spectrum measured by two CERN GEMs for voltage difference 350 V and 390 V. Table 5.14 lists the energy resolution and the FWHM for different applied voltages. Figure 5.38 shows the energy resolution vs the voltage. In this case the energy resolution is stable and does not change anymore. Therefore the resolution is not dominated anymore by the number of the produced electrons.

Voltage (V)	FWHM	Energy resolution
350	143.9	24.1%
360	233.7	25.6 %
370	396.4	26.7%
380	626.4	25.6%
390	987.6	25.1 %

TABLE 5.14: The energy resolution and the FWHM vs the voltage for two CERN GEMs

(A) (B)
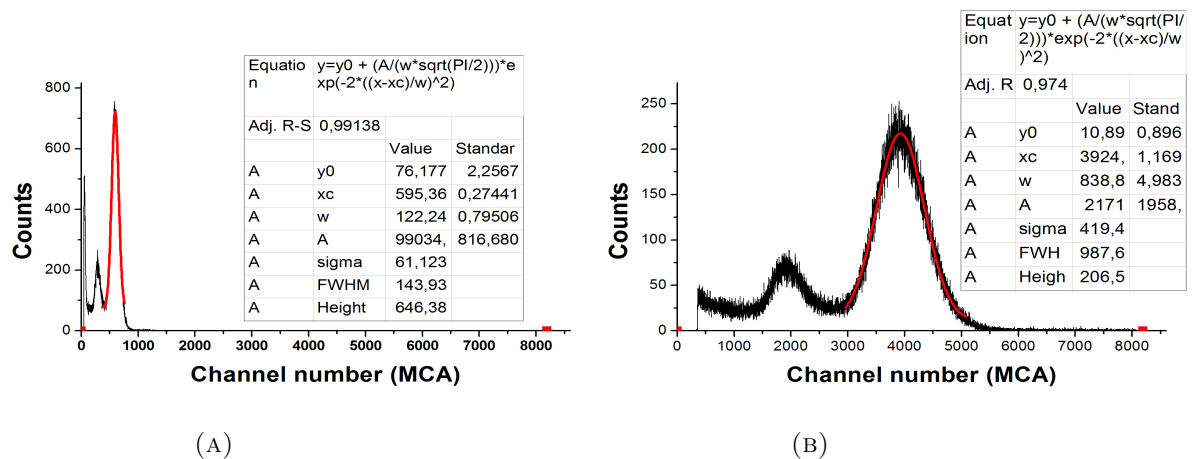
FIGURE 5.37: Gaussian fitting for two CERN GEM, (A) for voltage difference 350 V and (B) for voltage difference 390 V.
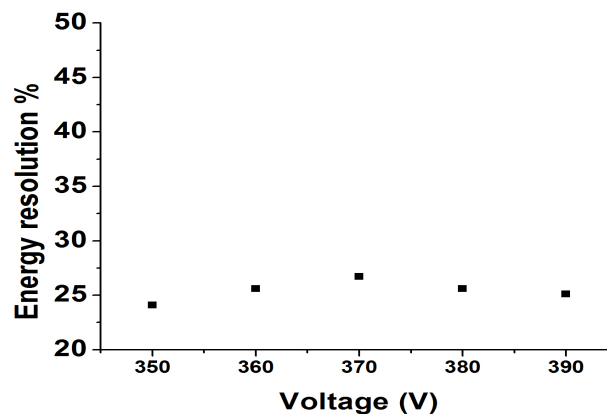
FIGURE 5.38: Energy resolution vs applied voltage for two CERN GEMs

Single ceramic GEM: Figure 5.39 shows the Gaussian fitting (the red curve) for the spectrum of a single ceramic GEM for applied voltages $580V$ (Figure 5.39a) and 640 (Figure 5.39b). Table 5.15 represents the FWHM and the energy resolution. Figure 5.40 displays the energy resolution vs the voltage . The resolution decreases with increasing gain, but becomes stable for voltages above 600 V.

Voltage (V)	FWHM	Energy resolution
580	20.7	45.1%
590	24.5	40.6 %
600	27.0	35.6%
610	35.3	34.8%
620	38.5	34.4%
630	46.7	34.4%
640	51.5	32.1 %

TABLE 5.15: The energy resolution and the FWHM vs the voltage for a single ceramic GEM

(A)

(B)
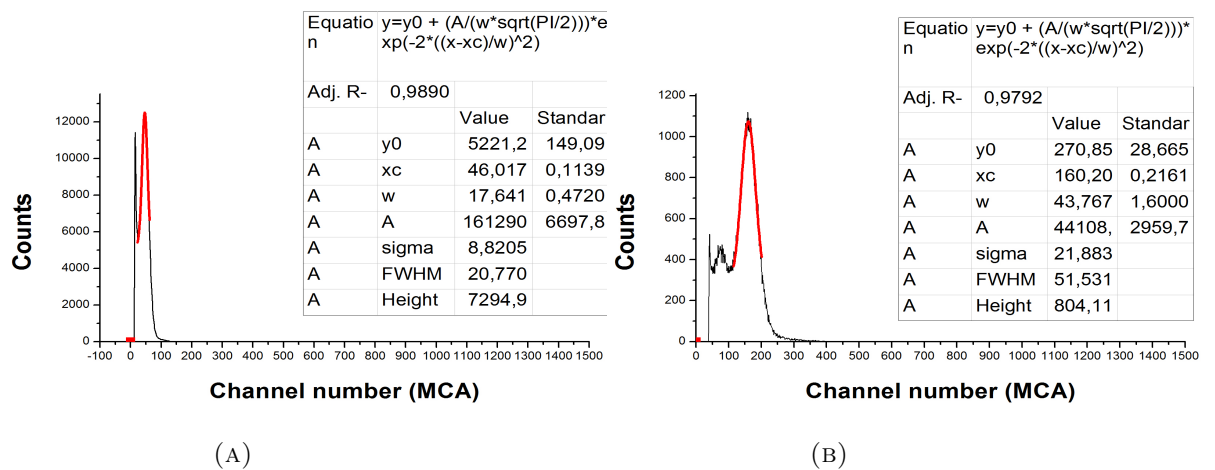
FIGURE 5.39: Gaussian fitting for a single ceramic GEM, (A) for voltage difference 580 V and (B) for voltage difference 640 V.
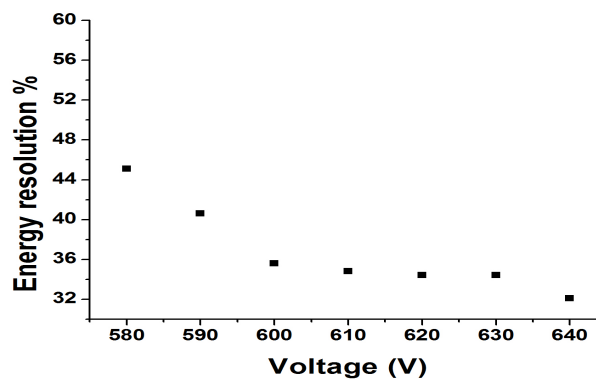
FIGURE 5.40: Energy resolution vs applied voltage for a single ceramic GEM

<u>Two ceramic GEMs:</u> Figure 5.41 is the Gaussian fitting and Figure 5.42 shows the energy resolution vs the voltage. Table 5.16 represents the values of the FWHM and the energy resolution for different voltages. The energy resolution is rather stable with respect to the applied voltage difference, but opposite to the case of the CERN GEMs, the resolution is worse in case of two GEMs than for one GEM.

Voltage (V)	FWHM	Energy resolution
575	131.3	54.9%
585	151.2	41.8 %
695	236.7	43.9%
600	343.2	54.1%
610	564.0	55.8 %

TABLE 5.16: The energy resolution and the FWHM vs the voltage for two ceramic GEMs
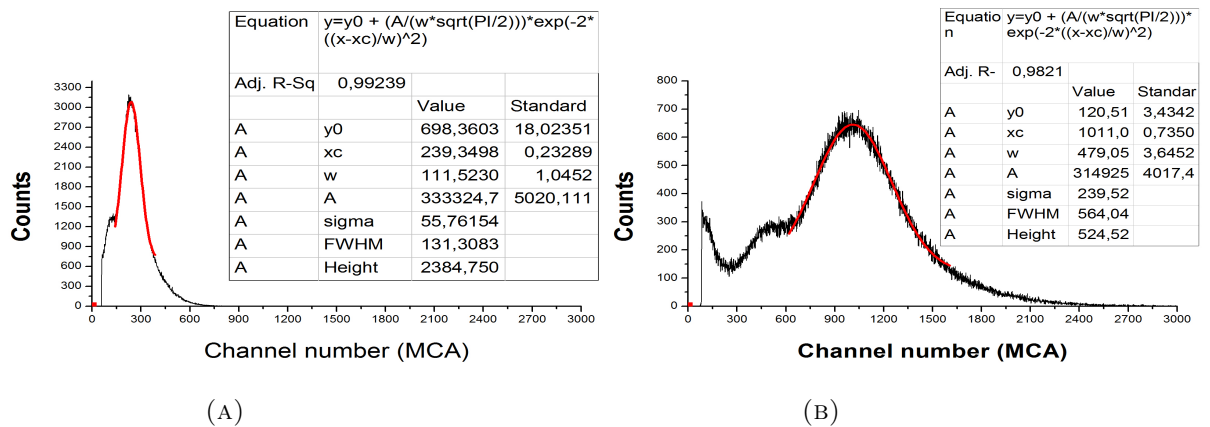
FIGURE 5.41: Gaussian fitting for two ceramic GEMs, (A) for voltage difference 575 V and (B) for voltage difference 610 V.
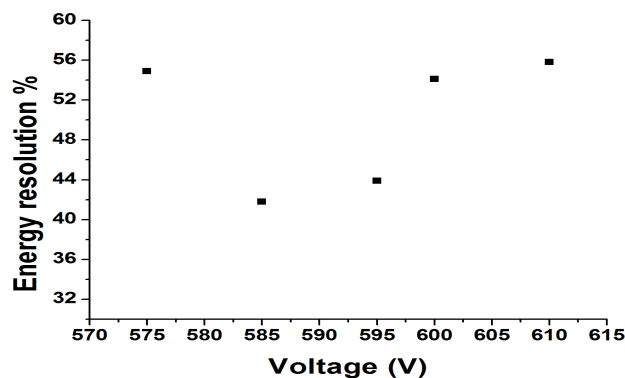
FIGURE 5.42: Energy resolution vs applied voltage for two ceramic GEMs

Ceramic on top: For combination between ceramic and CERN GEMs with ceramic GEM on top, the voltage on the CERN GEM is fixed to be 350 V. Table 5.17 shows the values of the FWHM and the energy resolution for each applied voltage on the ceramic GEM. Figures 5.43 and 5.44 display the Gaussian fitting and the energy resolution, respectively. Here the resolution is rather constant for all voltages except for two values at 570 V and 580 V, like in case of two ceramic GEMs, but are significantly larger.

Voltage (V)	FWHM	Energy resolution
550	229.2	67.5%
560	248.4	62.4 %
570	264.3	54.1%
580	365.4	81.6%
590	396.6	68.3 %
600	488.3	64.9 %

TABLE 5.17: The energy resolution and the FWHM vs the voltage for combination of ceramic and CERN GEMs (ceramic GEM on top)
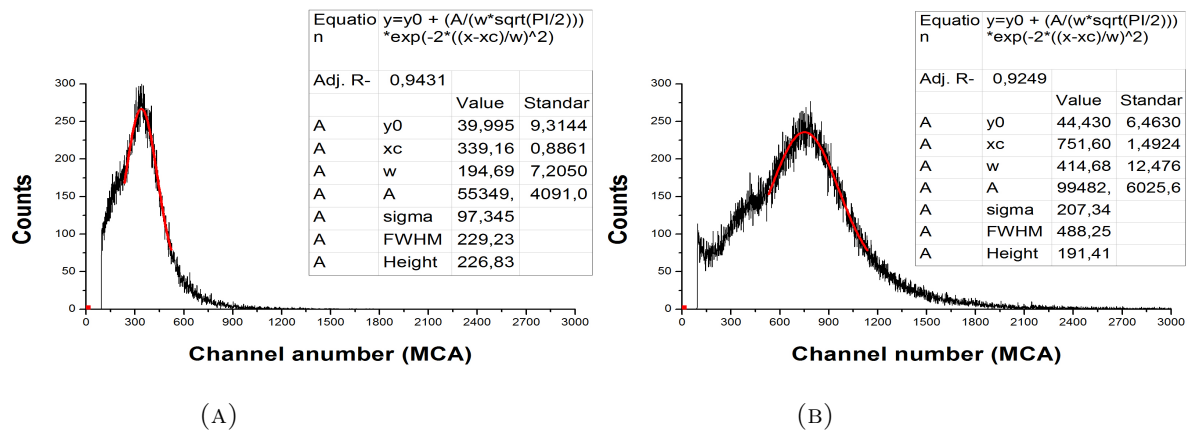
FIGURE 5.43: Gaussian fitting for combination between one ceramic GEM(on top) and CERN one(with fixed applied voltage =350V), (A) for voltage difference 550V and (B) for voltage difference 600V.
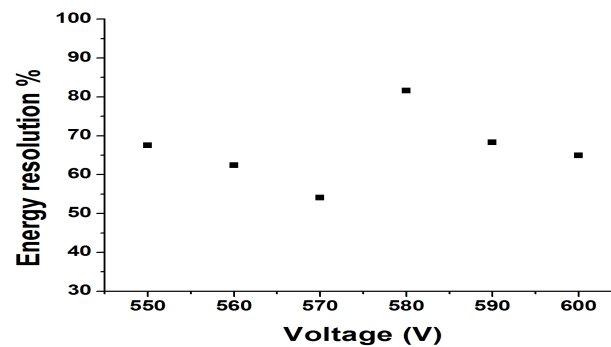
FIGURE 5.44: Energy resolution vs applied voltage for combination of ceramic and CERN GEMs (ceramic GEM on top)

CERN on top: The CERN GEM is on top with fixed voltage 350 V. Table 5.18 lists the values for the FWHM and the energy resolution. Figure 5.45 is the Gaussian fitting for different spectra and Figure 5.46 shows the energy resolution vs the voltage. Here the energy resolution is similar to that of two CERN GEMs. This leads to the assumption that the GEM on top is resonsible for the energy resolution.

Voltage (V)	FWHM	Energy resolution
550	132.3	28%
560	137.1	24.9 %
570	163.4	24.6%
580	178.8	22.9%
590	220.8	23.2 %
600	293.8	26.4 %

TABLE 5.18: The energy resolution and the FWHM vs the voltage for combination of ceramic and CERN GEMs (CERN GEM on top)

(A)

(B)
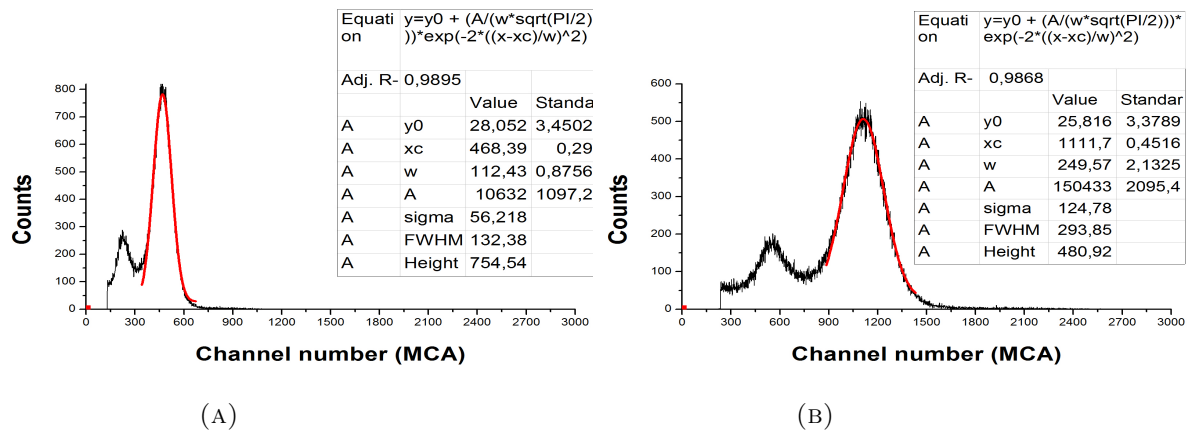
FIGURE 5.45: Gaussian fitting for combination between one ceramic GEM and CERN one(on top and with fixed applied voltage =350V), (A) for voltage difference 550V and (B) for voltage difference 600V.
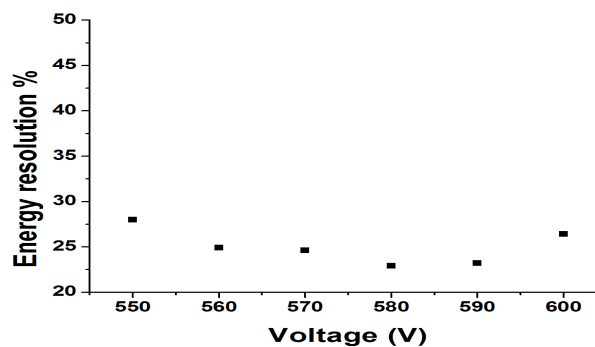
FIGURE 5.46: Energy resolution vs applied voltage for combination of ceramic and CERN GEMs (CERN GEM on top)

5.5 The active area

The active area or the opened area is the ratio between the area of the holes and the total area of the GEM. It can be calculated as following;

$$\text{The active area} = \frac{\text{Number of holes x hole area}}{\text{Total area}} \tag{5.5}$$

5.5.1 CERN GEM active area

As mentioned before, the diameter of the hole is 70 μm and the holes pitch is 140 μm. As shown in Figure 5.47, the number of holes can be calculated as following;

$$\text{Number of holes} = (\text{Number of holes per line})^2$$

$$(\text{Number of holes per line}) = \frac{\text{The line length}}{(\text{Hole diameter} + \text{distance between two holes})}$$

Finally, the active area or the opened area for CERN GEM = 19.6%.
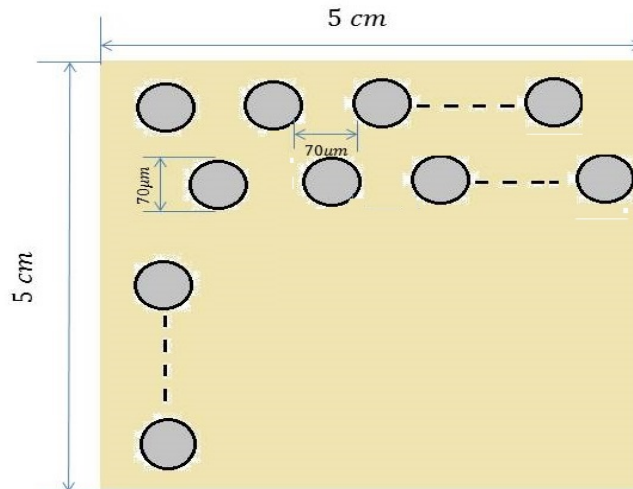
FIGURE 5.47: CERN GEM geometry

5.5.2 Ceramic GEM active area

The same previous procedure with respect to Figure 5.48, the diameter of the holes is 200 μm and the holes pitch is 360 μm. The active area for the ceramic GEM = 21.7%
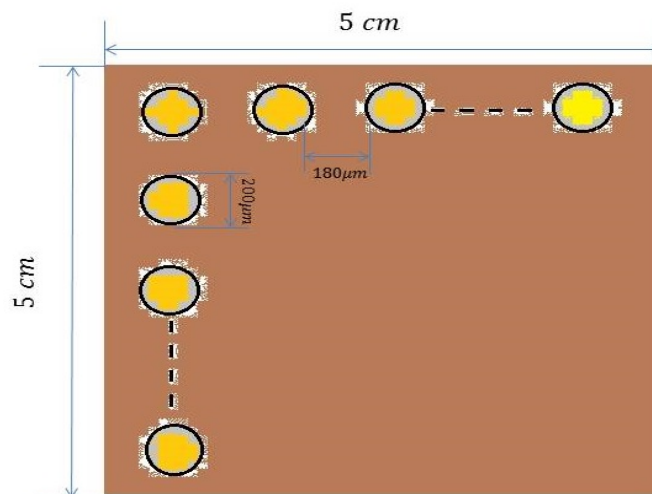
FIGURE 5.48: Ceramic GEM geometry

5.6 The range of the applied voltage and the electrical sparks

From the previous measurements, the range of the applied voltage for the CERN GEMs is from 350 V to 390 V. The first electrical spark was detected when the voltage exceed 400 V. For this reason, the maximum value was used for the measurements is 390 V. On the contrary, the range of the applied voltage for the ceramic GEMs is from 580 V to 640 V for a single GEM. The first electrical spark was detected for applied voltage 650 V. For two ceramic GEMs the range was from 550 V to 610 V. The maximum value was due to the limitations of our high voltage system.

5.7 CERN GEMs vs Ceramics GEMs

This section is the final comparison between the CERN GEM and the ceramic GEM. Table 5.19 presents the parameters summery of CERN GEMs and ceramic GEMs. Tables 5.20 and 5.21, show the final results for gas gain -for both kinds of the investigated GEMs- for many configurations. For both types of GEMs the gas gain per GEM was similar when using one or two GEMs of the same type. However, when using both types of GEMs in a setup the gain was larger when having the CERN GEM on the first amplification step.

The behavior of the energy resolution for both types of the GEMs is very different. The energy resolution improves with increasing the gas gain for the CERN GEMs and

reaches a minimum when using two CERN GEMs. On the other hand the energy resolution becomes worse, when using two ceramic GEMs instead of only one

	CERN GEM	Ceramic GEM
The developer	CERN	Siegen university and KOA company
Date of development	1998	2014
Size	50 mm x 50 mm	90 mm x 90 mm
Thickness	50 μm	120 μm
Condutor material	Copper	Silver, Nickel and Gold
Insulator material	Kapton	Ceramic
Shape of the holes	Conical	cylindrical
Holes diameter	70 μm for Cu and 50 μm for the Kapton	200 μm
Distance between holes	70 μm	180 μm
The opened area	19.6%	21.7%

TABLE 5.19: The summery of parameters for CERN and ceramic GEMs

GEM voltage (V)	Gas gain			
—	Single	square root	Ceramic on top	CERN on top
350	7.4	9.1	7.7	15.1
360	9.8	11.2	12.9	21.0
370	13.4	14.5	16.9	28.4
380	17.0	18.4	22.5	33.6
390	22.4	23.3	29.5	40.0

TABLE 5.20: The gas gain for CERN GEM for different configurations related to each applied voltage

GEM voltage (V)	Gas gain			
—	Single	square root	Ceramic on top	CERN on top
550	–	3.6	6.4	9.2
560	–	4.3	7.7	10.7
570	–	5.2	9.4	12,9
580	6.5	6.3	10.9	15.1
590	8.4	7.8	12.7	18.5
600	10.6	9.4	15.5	21.8
610	12.9	12.1	–	–

TABLE 5.21: The gas gain for Ceramic GEM for different configurations related to each applied voltage

Chapter 6

Conclusion

In this thesis the performance, the gas amplification and the energy resolution of the CERN GEMs and the new ceramic GEMs have been discussed. Using a small gas-filled chamber to achieve the gas amplification and Fe-55 radioactive source to produce the primary ionization. Single and combination of two GEMs have been investigated in order to compare the efficiency of the GEMs in both cases. In addition, the resistance of the GEMs against the electrical sparks has been taken into account. In other words, the maximum applied voltage difference that can be handled by the GEM without conducting electrical sparks.

During the experiment, the ceramic GEM has shown a sufficient stability and electrical sparks resistance with applied voltage difference range from 550 V (the first detected peak) to 630 V (the limits of our HVS). In comparison with CERN GEM, the applied voltage range was from 350 V to 400 V.

After data analysis for many GEMs arrangements it can be seen that, the best gas amplification and energy resolution were achieved by using a combination between CERN (close to the radioactive source) and ceramic GEMs (on top and close to the readout system).

All in all, the measurements taken from ceramic GEM nominate it to be a reliable candidate for high energy experiments.

Appendix A

Calculation of gas system

The following section shows the setup of the gas system and the mechanism to control the gas mixture percentage.

Figure A.1 and A.2 show the scheme of our gas system which contains two parts:

1. Gas mixturing unit - Figure A.1.

2. Gas monitoring unit - Figure A.2.

Flow control can be established - in the mixing unit- by using a mass flow controller. In our case, we use (MKS type 247 C four-channel readout) to reach the aimed gas mixture. In the following section, we discuss how to calculate the parameters for the mass controller. There are two main parameter one should consider:

1. Scaling Control Factor (SCF).

2. Setpoints.
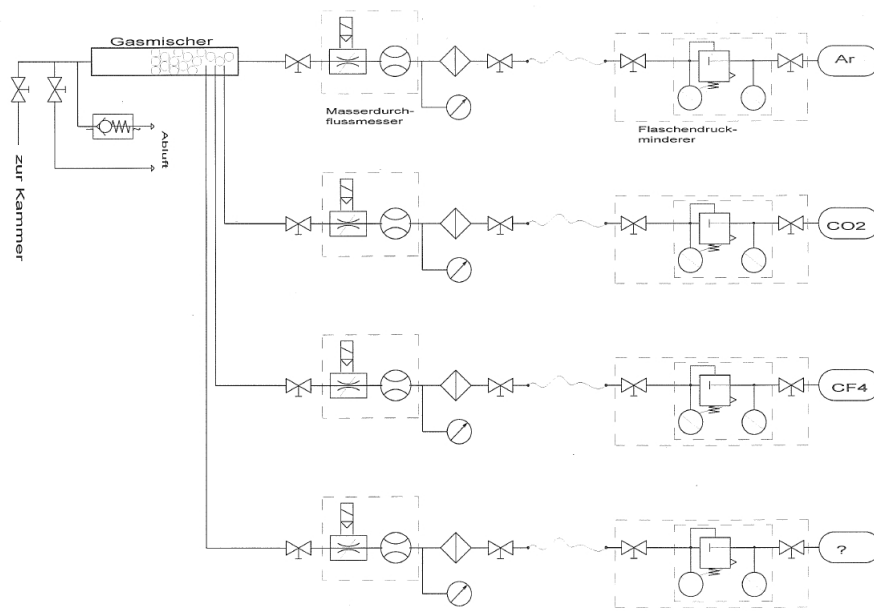
FIGURE A.1: Scheme of the gas mixing system
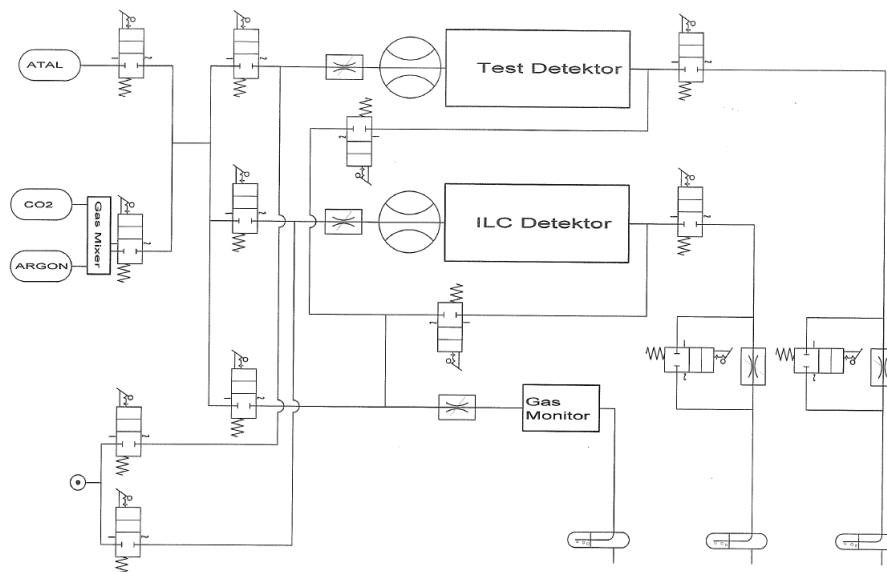
FIGURE A.2: Scheme of the gas monitoring system

Calculation of the Scaling Control Factor (SCF):

For each channel in the mass flow controller there is a scaling control potentiometer which should be configured according to the type of used gas. These potentiometers are located in the backside of the controller-Figure A.3.

The SCF is the product of gauge factor (scales the output of the channel to the full range) and the gas correction factor-(elucidates the ratio of flow rates of different gases which will produce the same output from the mass flow controller);

$$SCF = Gauge factor * Gas correction factor \qquad (A.1)$$

Flow range (sccm)	Gauge factor
1, 10, 100, 1000	100
2, 20, 200, 2000	200

TABLE A.1: Value of gauge factor for each range of the flow rate

Gas	Correction factor
Argon	1.39
Carbon Dioxide	0.70

TABLE A.2: Value of correction factor for each gas

In our case, we use the flow rate range = 1000. Finally, the SCF -for channel in which argon flows= 139 and SCF- for the channel in which carbon dioxide flows= 70.
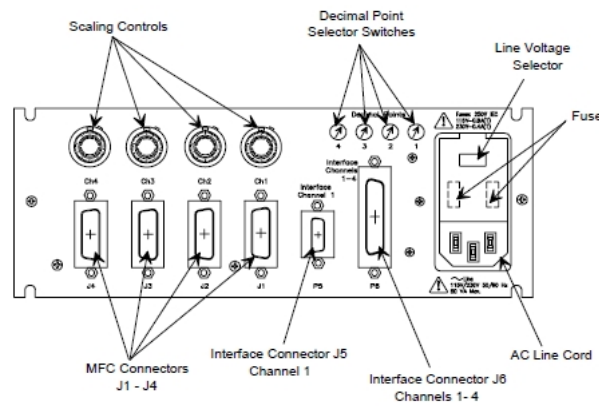
FIGURE A.3: Scheme of the backside panel of MKS device

Calculation of the Setpoints:

The flow rate is established by comparing the actual flow magnitude with the adjusted set point of the mass flow controller. The following section shows the techniques to calculate the set points according to two required gas mixtures- as an example.

Argon-Carbon Dioxide ; 80-20% :

Channel	Max flow rate (sccm)
1	500
2	50
3	15
4	15

TABLE A.3: The max flow rate for each channel in our mass flow controller according to the specifications of this model
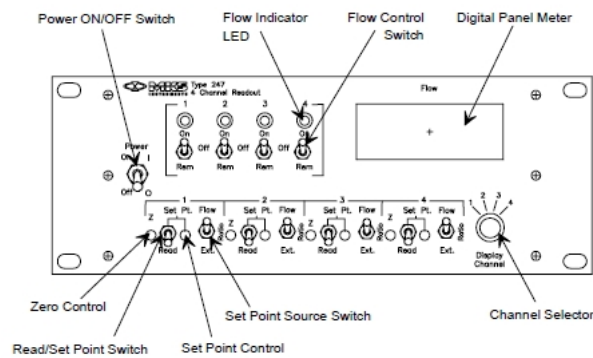
FIGURE A.4: Scheme of the frontside panal of MKS device

For simplicity, we set up channel 2 for Carbon-Dioxide (lower percentage) and channel 1 for Argon (higher percentage). Setting the channel 2 for the max flow rate (50 sccm) which represents th 20% of the final mixture. One can estimate the set point for channel one as following,

$$Setpoint(channel1) = (\frac{50}{20/100}) * (80/100) \tag{A.2}$$

Eventually, the estimated set points for (Ar-CO2 80-20%) shown in Table A.4,

Channel	The flowing gas	Set point (sccm)
1	Argon	200
2	Carbon-Dioxide	50
3	–	–
4	–	–

TABLE A.4: The set points for each channel for gas (Ar-CO2 80-20%)

Argon-Carbon Dioxide ; 90-10% :

The same produce for channel 2. The set point for channel 1 as following,

$$Setpoint(channel1) = (\frac{50}{10/100}) * (90/100) \tag{A.3}$$

The estimated set points for (Ar-CO2 90-10%) shown in Table A.5,

Channel	The flowing gas	Set point (sccm)
1	Argon	450
2	Carbon-Dioxide	50
3	–	–
4	–	–

TABLE A.5: The set points for each channel for gas (Ar-CO2 90-10%)

Appendix B

TPC manual

B.1 High Voltage system:

The high voltage system (HV sys) is the power supply for each part in TPC. It can be controlled by a LabView program which enables the user to set the required configurations for TPC.

FIGURE B.1: The LabView program shortcut for HV sys

The LabView program for HV sys is installed in the $Widows - PC$ and named as "HV−system". Figure B.1 shows the shortcut icon for this program and Figure B.2 displays the main window of it. As shown, the main window consists of three parts;
1) The tool bar.
2) The monitoring part, which monitors the status of the HV sys during the operation.
3) The controlling part, which enables the user to control the HV sys and upload the ramp file.

After running the program,it tells the steps to set the HV sys, as following;
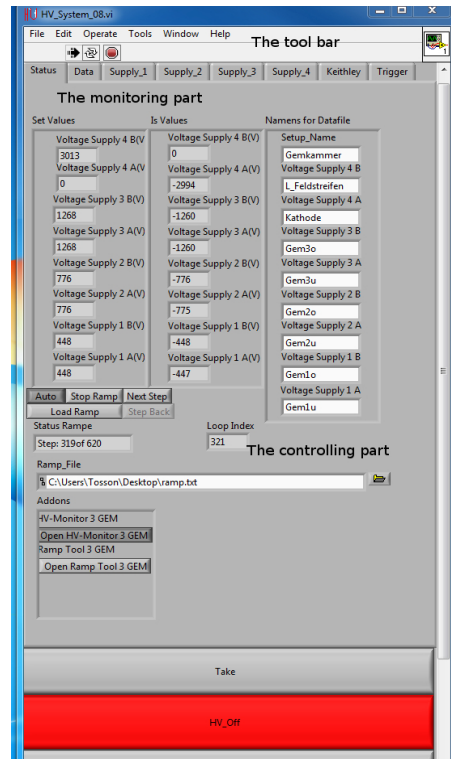
FIGURE B.2: The HV-LabView program main window

- To turn on the racks (Nim−crate−3 and Nim−crate−2).

- To remove the Lemo cable from the first HV supply.

- To set the limits for current meters. In our case, we use 30 μA.
  Note: the step is applied for seven current meters and it goes one after another, so
  be sure that you have done it seven times and all current meters are NOT blinking.

- To put the Lemo cable for the first HV supply again.

- To turn on the HV supplies.

- To turn on two external power supplies (Agilent and Kethley).

- Then, the system is ready.

While the initialization for HV sys has been done, the user needs to generate the ramp
file. The ramp file is a normal text file contains the information about the required

applied voltage on the GEMs, the induction field, the drift field and the transfer field. This file can be generated by using the ramp program which is an internal tool of the HV main program (it is called Ramp Tool 3 GEM and it is located at the controlling part in the HV main window- see Figures B.2 and B.3).
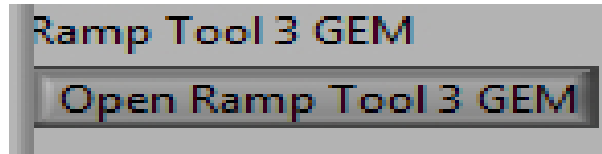
FIGURE B.3: Ramp tool button

The Ramp Tool 3 GEM program gives the user the ability to generate the required ramp file for running the HV sys. The user can enter the decided data in the main window of the Ramp Tool program- see Figure B.4.
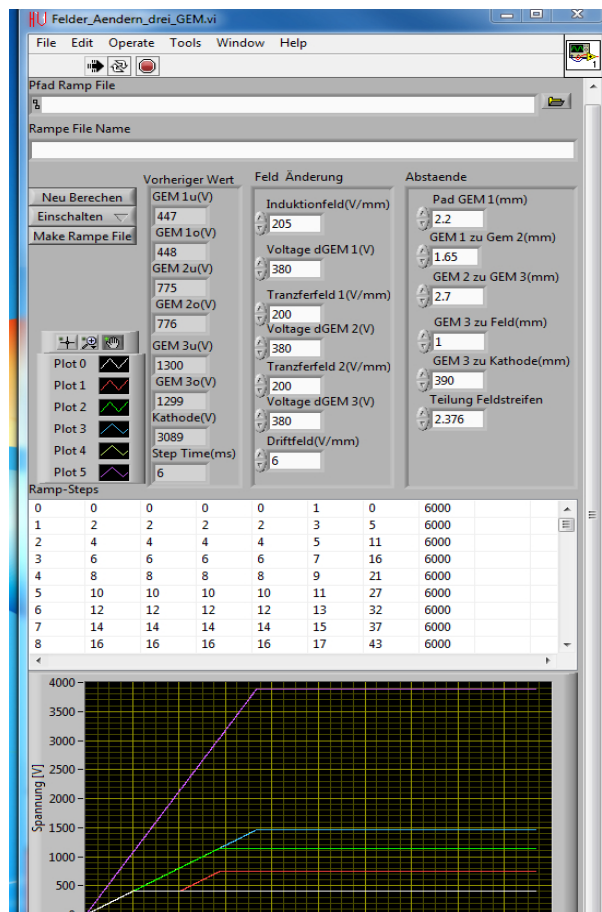
FIGURE B.4: The Ramp Tool program main window

The procedure is as following;

- Open the Ramp Tool GEM 3 program.

FIGURE B.5: The button for uploading the ramp file

- Enter the required values for each voltage and field.

- Save your ramp file as text file.

- Open the HV sys main window and upload your ramp file(by using uploading ramp button- see Figure B.5 and B.6).

- Load your ramp file (by using Load Ramp button- see Figure B.7).

- Press Take button and then HV-on button (Figure B.8).
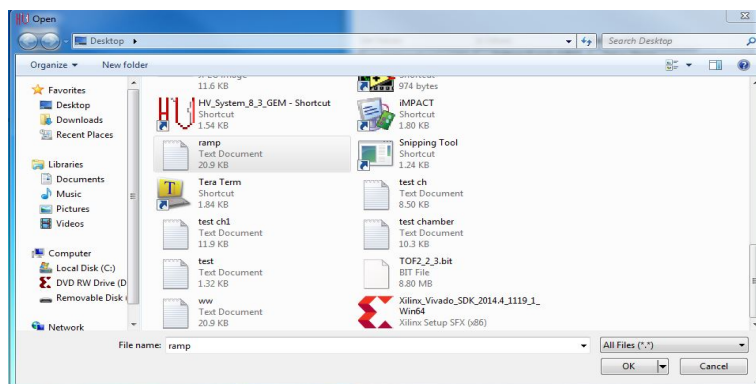
FIGURE B.6: The location window to choose your ramp file

FIGURE B.7: The button for uploading the ramp file
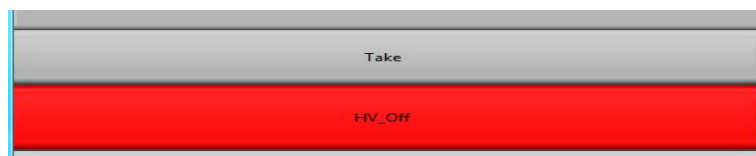
FIGURE B.8: HV-on button

Important notes:

1. Be sure that, the status of the control bins of the power supplies are at DAC position- see Figure B.9.

2. Check the monitoring part on the HV sys main window and be sure "Status Rampe", "Set value" and "Is value" are counting- see Figures B.10, B.11 and B.12.

FIGURE B.9: The control button of the power supply
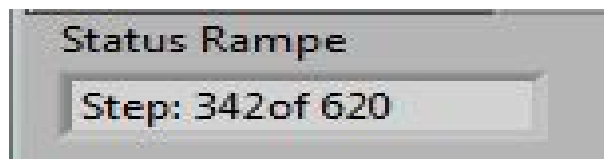
FIGURE B.10: The ramp status monitoring window
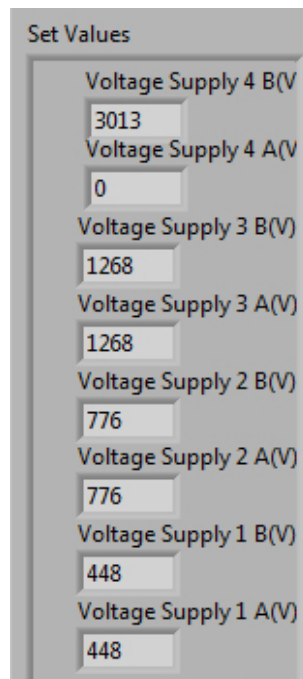
FIGURE B.11: Set value monitoring window
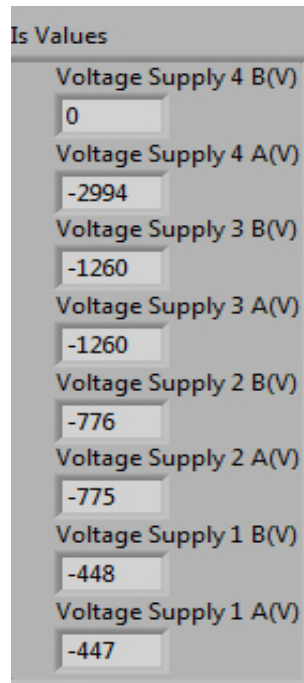
FIGURE B.12: Is value monitoring window

B.2   FPGA card

For more details about the FPGA card see section 3.5.2.2 and about configuration see the TOS- program user guide manual.

Must be remembered, the TPC user need interference program to upload the boundary condition configuration file. It is installed on the windows-PC under name "iMPACT" - Figure B.13. The configuration file is stored in the group cluster with ".bit" extension file with name "TOF2_2 _3.bit".

FIGURE B.13: The shortcut of the interference program for FPGA card

B.3   Laser system

Sometimes, the laser beam is used instead of the radioactive source. For specific conditions, the laser beam track can be monitored by the TPC. The laser system ables the TPC user to configure the laser beam as desired. This system consists of two main parts;

First, the laser system interference device (Figure B.14) which is connected to the windows-PC by an USB- cable. To point out, the laser system can be totally controlled by a special LabView-program installed in the window-PC. Figures B.15 and B.16 show the shortcut and the main window for this program, respectively. Take into consideration, the number of port (COM port) for the laser system USB-port should be entered. The repetition rate (frequency) of the beam can be easily adjusted from the main window. The on/off button in the -main window- is used to shoot and stop the beam.

FIGURE B.14: Laser system interference device

FIGURE B.15: Laser system program shortcut

Second, the beam generator is the tube from which the beam is shot -Figure B.17. The position of this tube can be adjusted to reach the required one.

🖊**Very important caution:**
Use the special glasses during working with the laser beam. This beam could damage your eyes.
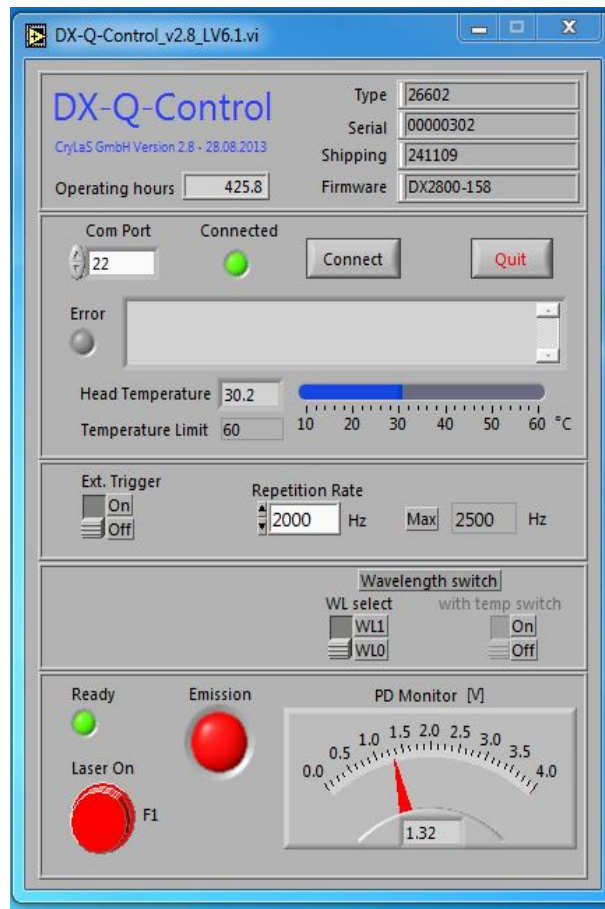
FIGURE B.16: Laser system program main window
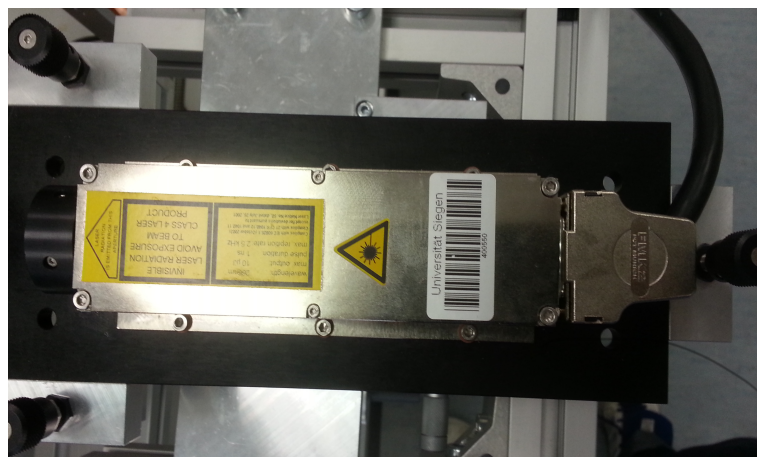
FIGURE B.17: Laser beam generator

Bibliography

[AAT04] P. Braun C. Garabatos A. Andronic, S. Biagi and G. Tsiledakis. Drift velocity and gain in argon- and xenon-based mixtures. *Nuclear Instruments and Methode in Physics Research.*, A 523, 2004.

[AL07] L. Buchmann S. Fox B. Fulton D. Gigliotti A.M. Laird, P. Amaudruz. Status of tactic: A detector for nuclear astrophysics. *Nuclear Instruments and Methode in Physics Research.*, A573, 2007.

[Alt06] G. Altenhofer. Development of a drift chamber for drift velocity monitoring in the cms barrel muon system, phd thesis. *Rheinisch-Westfälischen Technischen Ho chschule Aachen.*, 2006.

[Att09] D. Attie. Tpc review. *Nuclear Instruments and Methode in Physics Research.*, A598, 2009.

[Boc] Rudolf K. Bock. Drift chamber http://rkb.home.cern.ch/rkb/ph14pp/node50.html.

[CERa] CERN. The large hadron collider, home.web.cern.ch/topics/large-hadron-collider.

[CERb] CERN. The timepix chip, http://medipix.web.cern/medipix.

[Chu] G. Chui. Full documentation for the large hadron collider, http://www.symmetrymagazine.org/breaking/2008/08/25/free-online-full-documentation.

[Eme] Robert Emery. The linear accelerator (linac),http://rkb.home.cern.ch/rkb/ph14pp/node50.html.

[Fer86] R. Fernow. *Introduction to Experimental Particles Physics.* Cambridge University, 1986.

[Gau08] B. Gaur. First studies of prototype gem readout for a future ilc-tpc. master thesis. *Siegen University*, 2008.

[Gra] Paul Grannis. Technology benefits deriving from the international linear collider , http://www.linearcollider.org/ilc/why-do-we-need-the-ilc/technology-benefits.

[Gri08] D. Griffiths. *Introduction to Elementary Particles.* Wiley-VCH, 2008.

[gro] Jensen Graphic group. Industrial graphics and animation,http://www.jensen-graphics.com/6region.html.

[Gro12] ILD Concept Group. International large detector. 2012.

[Gru96] C. Grupen. *Particle Detectors.* Cambridge University, 1996.

[JK] M. Lupberger J. Kaminski. Manual for the timepix readout.

[JM07] N. Rhodes E. Schooneveld H. Natal da Luz J. Veloso J. Mir, R. Stephenson. Short induction gap gas electron multiplier (gem) for x-ray spectroscopy. *Nuclear Instruments and Methode in Physics Research.*, A573, 2007.

[Kle98] K. Kleinknecht. *Detectors for particle radiation.* Cambridge University, 1998.

[Kno89] G. F. Knoll. *Radiation Detection and Measurment.* John Wiley and Sons, Inc, 1989.

[Kö11] M. Köhli. Developing high resolution time projection chambers a gem and timepix approach. *University of Albert-Lugwigs, Germany*, 2011.

[N/A03] N/A. *Automation, Systems, and Instrumentation Dictionary (4th Edition).* ISA, 2003.

[Pet] Charlie Petit. Big international linear collider physics, https://ksj.mit.edu/tracker/2008/02/wired-news-big-international-linear-coll/.

[Sau77] F. Sauli. *Principles of Operation of Multiwire Proportional and Drift Chamber.* CERN, 1977.

[Sau07] F. Sauli. Imaging with the gas electron multiplier. *Nuclear Instruments and Methode in Physics Research.*, A580, 2007.

[Sau12] F. Sauli. Gas electron multiplier (gem) detectors: Princible of operation and applications. *RD51*, 2012.

[Sha14] S. Shahid. Development of a gem based time projection chamber prototype using a pixelized readout system, phd thesis. *Siegen University*, 2014.

[Tav10] S. Tavernier. *Experimental Techniques in Nuclear and Particle Physics.* Springer, 2010.

[Cel] CERN European Laboratory. Particle accelerators, http://www.cosmiclight.com/ofquasars/accelerators.html.

[Ens] European Nuclear Society. Ionization chamber, https://www.euronuclear.org/info/encyclopedia/i/ionizationchamber.htm.

[WB08] L. Rolandi W. Blum, W. Riegler. *Particle Detection with Drift Chambers.* Springer, 2008.

[WBR08] Werner Riegler Walter Blum and Luigi Rolandi. *Particle Detectionwith Drift Chambers.* Springer-Verlag Berlin Heidelberg, 2008.

[Wik] Wikipedia. $Largehadroncollider, https://en.wikipedia.org/wiki/large_hadron_collider$.

[XV] R. Cid X. Vidal. Circular accelerator, http://www.lhc-closer.es/1/3/2/0.